

编号: _____

陕西高等学校科学技术奖励推荐书

一、成果概况

成果名称		陕产矿物药矿物学特征及资源开发研究						
主要完成人		张丽倩; 刘养杰; 王成						
主要完成单位 (公章)		陕西国际商贸学院; 长安大学						
成果类型	A. 基础研究、应用基础研究 B. 技术开发、发明、推广 C. 软科学 D. 科普类成果 选 (A)		专业评审组	A. 数理力学 B. 电子信息 C. 化学化工 D. 环境科学	E. 机械 F. 轻工 G. 纺织 H. 工程建设	J. 动力电气 K. 地球科学 L. 材料科学 M. 农林畜牧	N. 生物技术 O. 医药卫生 P. 软科学 Q. 科普类 选 (O)	
	二级学科名称	药剂学		项目起止时间	2019-10-18 至 2020-10-18			
三级学科名称			总经费	10 万元				
任务来源及编号		地市(厅)级计划 17JK0945			评价形式	A. 鉴定 B. 评审 C. 验收 D. 专利 E. 检测 F. 引用评价 选 (A、F)		
已获奖励情况								
学校推荐意见 本成果属实, 人员排序无异议, 无知识产权纠纷, 同意推荐。						推荐等级 三等奖		
(公章) 年 月 日								

二、内容简介

提要：1、基础研究、应用基础研究类项目填写所属科学技术领域、主要研究内容、科学价值及同行引用评价情况；
2、技术开发、技术发明、技术推广类项目填写所属科学技术领域、主要技术内容、技术经济指标、促进行业科技进步作用及应用推广情况；
3、软科学类项目填写所属科学技术领域、主要研究内容、科学价值、社会效益及采纳情况。

1、所属科学技术领域

陕产矿物药矿物学特征及资源开发研究属于药学领域。

2、主要研究内容

(1) 陕产矿物药的矿物学肉眼鉴定特征研究

主要通过矿物学的肉眼鉴定，观察形态、光学性质、力学性质等，再与陕西省药材公司的样品进行对比分析。

(2) 矿物学地球化学分析测试

通过偏光显微镜、光谱半定量测试、X射线衍射技术(XRD)、红外光谱分析测试、差热分析等技术手段，将陕西省一些具有矿物药资源产地的样品与陕西省药材公司的矿物药进行对比测试，看化学成分差异、其中重金属及其它有害物质成分是否符合国家入药标准，从而判断作为矿物药资源开发利用的可行性。

(3) 初步药理研究

在对一些矿物学归类为一种矿物，但矿物药名称、药理不同，通过分析测试发现矿物药的成分、结构或其它矿物学特征差异，进行初步的药理差异与之相关度分析。

3、科学价值

通过对陕产矿物药资源的矿物学、药理等基础特征进行研究，对其矿物学特征与药用紧密结合起来，进行充分、合理地资源开发与利用，为人类健康贡献一份力量。

4、同行引用评价情况

项目成果得到了淄博市级非物质文化遗产重点保护示范基地淄博橘源血管病研究所桓台城区橘源堂中医诊所等的采用，评价良好。

三、项目详细内容

1. 立项背景

(提要：简明扼要地概述立项时国内外相关科学技术状况，主要技术经济指标，尚待解决的问题及立项目的)

矿物药指在中医药临床应用中可作为制作中成药或中药方剂的天然矿物或岩石，包括天然矿物、岩石、生物化石等，以矿物为主。矿物药在中药资源中占据重要地位，在传统中医药治疗中已有几千年的历史。传统研究记载历史如表 1。

表 1 中药典籍中矿物药所占比例

中药专著	药物种数	矿物药种数	矿物药所占比例
《神农本草》	365	46	12. 6%
《神农本草经集注》	730	73	10. 0%
《新修本草》	850	104	12. 2%
《证类本草》	1748	139	8. 0%
《本草拾遗》	447	106	23. 7%
《本草纲目》	1892	379	20. 0%
《中华人民共和国药典》(2010 版)	4567	24	0. 5%

文献查阅，国内矿物药研究虽数量不大，但具有明显的阶段性。矿物药电化学测试进行了梳理（张书胜等, 1997），本草考证、成分、鉴别方法等（王海波等, 2017）。综合前人研究，目前矿物药研究主要内容集中在鉴定方法、成分及临床应用，其次为药理、毒理、炮制、质量控制。其中矿物药的鉴定方法研究从传统的眼观、手摸、鼻闻、口尝、水试、火试等到红外、紫外、原子光谱、质谱、X 射线衍射、ICP-MS 等测试技术的应用，经历了经验判断到仪器、设备测试主导的过程，现代化测试手段对矿物药的成分，尤其是微量元素、重金属元素等种类、含量鉴别、测定具有重要促进作用（袁明洋等, 2014；黄必胜等, 2015；闫蔚, 2016；温海成, 2009；黄必胜等, 2013；雷咪, 2018；孙扬波, 2018）。临床应用多以某类元素或主要化学成分在临床的应用综述（陈生春, 1999；沈卫珍等, 2015；刘圣金等, 2016；刘圣金等, 2014；刘圣金等, 2019；陈晶晶等, 2014；沈卫珍等, 2014；王景云等, 1993）。成分和药理、毒理的综合研究多从药理出发，具有相同药理的不同种类矿物药的作用机理探究，毒理多与重金属等有害元素相关（张秀云, 2012；张晓敏, 2010；韩旭等, 2015；武世奎等, 2011；王晓烨等, 2017）。炮制多基于不同炮制工艺、方式下矿物药的质量控制（李向日, 2014；李伟东等, 2014；周灵君, 2012；刘圣金等, 2010, 2012, 2016；高金波, 2009；石典花等, 2015）。

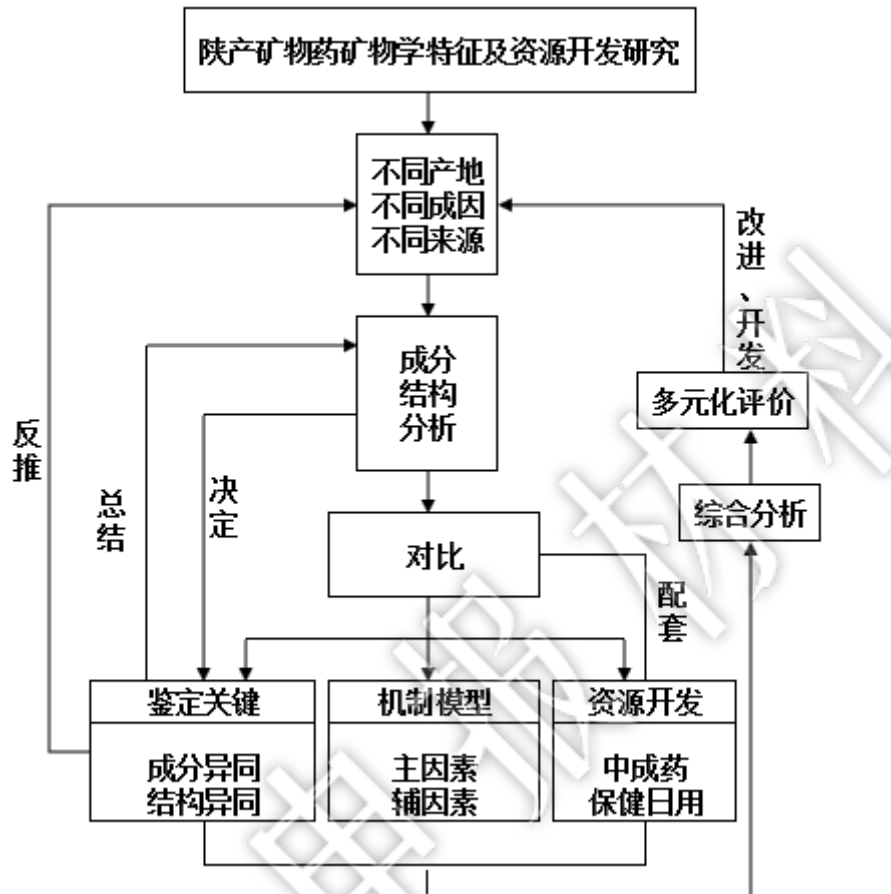
由于其研究涉及中医药学、地质学、药理学、化学等多个学科，而少有跨学科的学者相互渗透、配合研究，致使矿物药资源相关研究在国内近于止步不前，但是，调查发现，矿物药资源的开发与应用在韩国、日本等国家发展较快。如关于矿物药雄黄的研究表明，雄黄具有以下药用价值：抗肿瘤作用，能抑制移植性小鼠肉瘤 S-180 的生长，并对细胞有腐蚀作用；杀虫作用；水浸剂对金黄色葡萄球菌、结核杆菌、变形杆菌不同程度的抑制作用等。相反，肠道吸收后能引起吐、泻、眩晕、惊厥甚至慢性中毒，损害肝、肾，氧化成为我们俗称的砒霜。传统风俗中，部分地区端午节会喝“雄黄酒”饮品，作为解毒剂或杀虫药。

项目想尝试通过对雄黄矿物药资源的矿物学、药理等基础特征进行研究，对其矿物学特征与药用紧密结合起来，进行充分、合理地开发与利用，为人类健康贡献一份力量。

2. 科学技术内容

(提要：从总体思路、研究成果或技术方案、实施效果三方面总结)

(1) 总体思路



(2) 技术方案

①陕产矿物药的矿物学肉眼鉴定特征研究

主要通过矿物学的肉眼鉴定，观察形态、光学性质、力学性质等，再与陕西省药材公司的样品进行对比分析。

②陕产矿物药的矿物学地球化学分析测试

通过光谱半定量测试、X射线衍射技术(XRD)、红外光谱分析测试、差热分析等技术手段，将陕西省一些具有矿物药资源产地的样品与陕西省药材公司的矿物药进行对比测试，看化学成分差异、其中重金属及其它有害物质成分是否符合国家入药标准，从而判断作为矿物药资源开发利用的可行性。

③陕产矿物药的初步药理研究

在对一些矿物学归类为一种矿物，但矿物药名称、药理不同，通过分析测试发现矿物药的成分、结构或其它矿物学特征差异，进行初步的药理差异与之相关度分析。

④陕产矿物药的资源开发研究

(3) 研究方法

①调研法：市场调研法、文献研究法及野外勘查、调研法

对国内外、尤其是省内的雄黄及其它种类的矿物药比较全面地收集市场销售中的鉴定情况，地质产地的资源分布情况，从而推测未来矿物药的侧重研究方向，并做出分析、综合。其中对国内外雄黄及其它种类的矿物药鉴定及使用研究情况主要通过网上文献检索、网上药店咨询等方式，陕西省内通过市场考察方式。

地质产地的矿物药资源主要通过文献中总结前人开采情况，选择几个省内典型的目前仍处于开采阶段的产地进行野外勘查方法，简单对矿产资源进行评估。

②实验法

矿物学肉眼鉴定特征：肉眼鉴定矿物主要是根据矿物的颜色、光泽、条痕、解理、硬度的特点来进行鉴定工作。那么肉眼鉴定矿物所需的简易工具有：瓷板（用来刻划条痕）、小刀（用来刻硬度）、放大镜（用来看解理特点等）。有时还可以随身带一小瓶盐酸、小磁铁。

光谱半定量化学分析测试：光谱半定量分析是根据元素的特征谱线确定被测元素的存在，然后根据谱线的黑度估计其含量的光谱分析。

X射线衍射测试：当一束单色X射线入射到晶体时，由于晶体是由原子规则排列成的晶胞组成，这些规则排列的原子间距离与入射X射线波长有相同数量级，故由不同原子散射的X射线相互干涉，在某些特殊方向上产生强X射线衍射，衍射线在空间分布的方位和强度，与晶体结构密切相关。

红外光谱分析：当一束具有连续波长的红外光通过物质，物质分子中某个基团的振动频率或转动频率和红外光的频率一样时，分子就吸收能量由原来的基态振(转)动能级跃迁到能量较高的振(转)动能级，分子吸收红外辐射后发生振动和转动能级的跃迁，该处波长的光就被物质吸收。所以，红外光谱法实质上是一种根据分子内部原子间的相对振动和分子转动等信息来确定物质分子结构和鉴别化合物的分析方法。将分子吸收红外光的情况用仪器记录下来，就得到红外光谱图。红外光谱图通常用波长(λ)或波数(σ)为横坐标，表示吸收峰的位置，用透光率(T%)或者吸光度(A)为纵坐标，表示吸收强度。

(4) 实施效果

①交叉学科错位发展

我国矿物药资源丰富且入药已有几千年历史，但受其研究涉及中医药学、地质学、药理学、化学等多个学科，而少有跨学科的学者相互渗透、配合研究，而使行业一度出现萎靡现状。笔者从我校现有医药、矿物学、宝石学等优势专业联合角度下，从规范药用矿物市场、学科竞争等方面分析矿物学与药学交叉学科平台建设的必要性。

我校为地方高校，而地方高校的学科建设立足在内容特点上形成与众不同的特色或优势，从而使得本校的学科具有相比其他高校同类学科更多的内涵或价值。“矿物药”研究机构就是在这种思路的引导下考虑成立的。经过调查研究，珠宝学院虽然在西北地区首屈一指，但是在全国范围内来说优势并不明显，尤其是国内开办矿物学相关专业的重点院校有数十家，而我院办学思路基本沿用了传统思路与方法，科研方面力量相对薄弱；我校医药学院依托步长集团，校内相对发展较快，但是由于陕西省乃至全国医药类高校较多，而无法形成突出的竞争优势。因此需要侵入现代观念与同类学科竞争会形成差异，在同类高校中建立“异质”，从而寻求发展空间。

目前国内高等院校中同时设有矿物学和医药相关专业的院校少之又少，而陕西国际商贸学院不仅同时开设医药学院，同时开设与矿物学紧密相关的珠宝学院。“矿物药”研究在国内相对起步较晚，且受学科结合、人才方面的困难，从事该方面的研究机构极少，如果在两者错位中汇聚人才、构建平台、进行学术研究，避开与强校、强势学科相同的发展方向或发展路径，走自己的路，利用自身优势去发展学科特色，必定会取得良好效果。

在学科建设中实施差异化发展和错位竞争策略的同时，还需要树立正确的学科生态观、学科竞争观、学科内涵观：首先，学科之间要构建生态平衡，相互适应，形成学科交叉；其次，基础学科和应用学科、自然科学学科协调发展；再次，学科多样化和综合相联伴生，比如联合申请综合型大型科研项目，产生整体效应和边缘效应。

②特色学科优势发展

随着国内人民生活水平的提高，珠宝首饰不再是高奢产品，而随着人们消费观念的更新，消费者对首饰的要求不断提高，这就要求首饰制作者们挖空心思，不断开发具有多种用途的新产品。除自身的装饰功能外，还具有保健功能，这就是所谓的保健首饰。

最常见的保健首饰分为两大类，一种是以玉、玛瑙首饰为主的天然饰品。玉和玛瑙的质地本身就具有清凉、消暑、镇静的作用。还有一类产品是经过加工而成的，即在饰品中加入特定的物质，起到特定的保健作用。如目前市场上热销的磁性保健首饰，可预

防和治疗风湿病、关节炎、高血压、神经衰弱和肌肉劳损等多种疾病，对一般人的保健都有所裨益。这类饰品不含铅等有害物质，对皮肤无刺激，长期佩戴无不良反应。保健饰品的形式多种多样，如项链、戒指、耳环、胸针、手镯等。目前，科学家们已经发明了科技含量更高的保健首饰，但因其费用巨大，现在只作为科技成果，例如体温戒指、防瞌睡戒指、防晕手镯、芳香耳环等。

我校珠宝学院作为西北地区最大的珠宝学院，具有引领珠宝行业革新的重大使命，办出特色是当务之急，除规避常规的鉴定、营销专业方向外，可设置特色的矿物药首饰设计方向，为行业创新人才的培养做出贡献。

③陕产矿物药资源开发

主要通过陕西省内雄黄、石膏、碧石、大青盐、光明盐几种矿物药的产地资源情况探究，通过矿物学、地球化学测试分析手段，将几个产地的矿物药进行鉴定分析，与陕西省药材公司的样品进行对比测试，研究是否可作为矿物药资源加以开发利用，并通过初步的化学成分对比分析进行初步的药理探究。

3. 本研究的发现点、发明点和创新点

(1) 研究发现

①陕西省矿物药资源丰富，从矿物学角度分析可分为单矿物类、多矿物（岩石）类及含矿物类，其中单矿物类种类最多且应用最广泛，地质学角度描述了4种陕西省矿物药（自然铜、石膏、白石英、滑石）资源类型及药用功效。

②主要通过陕西省内雄黄、石膏、礬石、大青盐、光明盐几种矿物药的产地资源情况探究，通过矿物学、地球化学测试分析手段，将几个产地的矿物药进行鉴定分析，与陕西省药材公司的样品进行对比测试，研究是否可作为矿物药资源加以开发利用，并通过初步的化学成分对比分析进行初步的药理探究。

②陕西省西乡县产出的石膏符合矿物药条件，可作为矿物药资源进行开采。矿物学肉眼鉴定特征对比显示两种不同来源的矿物药石膏略有差异，可从形态、光泽加以区分。两者的曲线及光谱特征高度相似，细微差异，均反映了化学成分非常纯净，矿物石膏含量接近百分之百。差热分析测试中，陕西省药材公司石膏样品只在130℃出现了一个中等强度的吸热谷，陕西省西乡县产出的石膏样品在140℃、180℃时出现明显的双吸热谷特征，与矿物药中是否含有含水矿物——硬石膏有关。主要化学成分测试及微量元素光谱半定量测试显示两者主要化学成分一致，其中微量元素均含有较多Cu、Sr，相对陕西省药材公司的石膏中杂质元素种类较多，数量较高，与两种不同产地的地质地球化学背景存在差异有关。

③陕西省凤县铅硐山矿物药礬石具有资源开发条件。利用主要化学成分分析、微量元素光谱半定量、红外光谱、X射线衍射、X射线粉晶数据等不同测试技术对矿物药礬石进行鉴定，主要化学分析（重量百分比）为Fe 36.63, As 32.014, S 31.75，微量元素主要为Zn、Pb、Ag、Co、Nb、Cu、Ni等，杂质含量微弱，符合药材要求；红外光谱分析表明，礬石成分纯净，几乎百分百为毒砂；X射线衍射曲线表明，主要衍射线均为2.674、2.433，主要矿物为毒砂；X射线粉晶分析结果基本一致，成分纯净。

④陕西省蒲城县伏头地区盛产矿物药自然铜，可作为矿物药资源进行开采。通过与陕西省药材公司及省内白河县里端沟、华阴县全堆城、略阳县煎茶岭及西乡县余家山几种不同来源、不同产地的自然铜矿物药进行矿物学对比分析，结合肉眼及反光镜鉴定，利用主要化学成分分析、微量元素光谱半定量、红外光谱、X射线衍射等不同技术对其进行矿物学测试分析。

4. 与当前国内外同类学科技研究现状与水平比较

目前国内外中医药中对矿物药的通过比较丰富，但缺乏矿物药为矿物的研究基础，未能将其药理、资源评价以矿物学的角度进行分析，例如收集国内外关于矿物药雄黄的研究表明，雄黄具有以下药用价值：抗肿瘤作用，能抑制移植性小鼠肉瘤 S-180 的生长，并对细胞有腐蚀作用；杀虫作用；水浸剂对金黄色葡萄球菌、结核杆菌、变形杆菌不同程度的抑制作用等。相反，肠道吸收后能引起吐、泻、眩晕、惊厥甚至慢性中毒，损害肝、肾，氧化成为我们俗称的砒霜。传统风俗中，部分地区端午节会喝“雄黄酒”饮品，作为解毒剂或杀虫药，但缺乏用量的科学根据。

国内外药材市场发现，由于中药采集或销售人员矿物学知识的欠缺，导致出现较多“此雄黄非彼雄黄”类似情况，即名称与矿物晶体不符、矿物与共生矿物集合体共同销售等情况，从而导致隐患；同时，作为临床外用矿物药剂量合理性研究也存在着定量问题，炮制方法及毒性分析与矿物学特征联系存在不紧密的特点。

5. 应用情况（经济效益、社会效益情况）

陕西国际商贸学院张丽倩、刘养杰等同志撰写的《陕西省旬阳县公馆地区朱砂矿物药的矿物学鉴定及成分对比研究》《陕西省蒲城县伏头地区自然铜矿物药的矿物学鉴定及成分对比研究》《陕西省凤县铅硐山矿物药碧石矿物学鉴定及分析》《两种不同来源的矿物药石膏矿物学分析及鉴定》《陕西省雄黄矿物药资源开发可行性分析》《4种陕西省单矿物类中药资源及功效》等矿物药论文，提交到淄博橘源血管病研究所、桓台城区橘源堂中医诊所（市级非物质文化遗产重点保护示范基地）等单位后，受到了单位的采用，并进行矿物药的药理探究与治疗实施，同时指导了郑雯乐等同学实施了陕西省大学生创新创业项目“矿物药智能珠宝”，尝试将各种具有不同功效的矿物药应用于珠宝首饰等保健产品中。

实践证明，关于陕西省产矿物药的学术论文对于省内外中药行业的发展起到了一定的理论参考价值和实践作用。

6. 申请、获得知识产权情况

四、项目主要完成人员情况表

第 1 完成人：

姓 名	张丽倩	性别	女	年龄	33
所在单位	陕西国际商贸学院			文化程度	硕士
从事专业	矿物学			技术职称	讲师
参加本项目的起止时间	2016-06-30 至 2020-05-31				
对项目的主要创造性贡献	作为主持人完成了矿物药相关项目 2 项，在研 1 项，第一参与人 4 项，同时作为成果第一完成人公开发表了核心论文 5 篇。				
声 明	本人严格按照《陕西高等学校科学技术奖励办法》的具体要求，对推荐书及其附件进行了审阅，确认全部内容和材料属实，并符合相关保密规定。如有不符，本人愿意承担相应后果并接受相应处理。				
本人签名：_____					
年 月 日					

第 2 完成人：

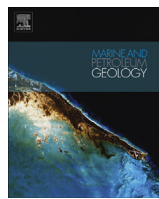
姓 名	刘养杰	性别	女	年龄	65
所在单位	陕西国际商贸学院			文化程度	硕士
从事专业	矿物药			技术职称	教授
参加本项目的起止时间	2016-06-30 至 2020-05-31				
对项目的主要创造性贡献	作为项目主持人在研项目 4 项，作为主要参与人完成了项目 2 项，同时作为成果第二完成人公开发表了核心论文 5 篇，出版了专著 1 部。				
声 明	本人严格按照《陕西高等学校科学技术奖励办法》的具体要求，对推荐书及其附件进行了审阅，确认全部内容和材料属实，并符合相关保密规定。如有不符，本人愿意承担相应后果并接受相应处理。				
本人签名：_____					
年 月 日					

第3完成人：

姓 名	王成	性别	男	年龄	30
所在单位	长安大学		文化程度	无	
从事专业	矿物学、地球化学		技术职称	讲师	
参加本项目的起止时间	2016-06-30 至 2020-05-31				
对项目的主要创造性贡献	作为项目主要参与人完成了项目1项，在研项目2项，作为第一作者发表了相关SCI论文1篇，核心论文第五作者1篇。				
声 明	本人严格按照《陕西高等学校科学技术奖励办法》的具体要求，对推荐书及其附件进行了审阅，确认全部内容和材料属实，并符合相关保密规定。如有不符，本人愿意承担相应后果并接受相应处理。				
本人签名：_____					
年 月 日					

五、附件目录

附件大类	子类	序号	附件名称
一、论文著作证明	主要论文著作	1	SCI 论文
一、论文著作证明	检索证明	2	SCI 检索证明
一、论文著作证明	主要论文著作	3	4 种陕西省单矿物类中药资源及功效
一、论文著作证明	主要论文著作	4	两种不同来源的矿物药石膏矿物学分析及鉴定
一、论文著作证明	主要论文著作	5	陕西省蒲城县伏头地区自然铜矿物药的矿物学鉴定及成分对比研究
一、论文著作证明	主要论文著作	6	陕西省雄黄矿物药资源开发可行性分析
一、论文著作证明	主要论文著作	7	陕西省凤县铅硐山矿物药碧石矿物学鉴定及分析
三、应用证明	应用证明	8	淄博橘源血管病研究所应用证明
五、其他证明	其他证明	9	项目结题证明
三、应用证明	应用证明	10	桓台城区橘源堂中医诊所应用证明
五、其他证明	其他证明	11	大学生创新创业项目立项



Research paper

Petrographic and geochemical characteristics of the lacustrine black shales from the Upper Triassic Yanchang Formation of the Ordos Basin, China: Implications for the organic matter accumulation

Cheng Wang ^{a, d}, Qinxian Wang ^{a, *}, Guojun Chen ^b, Long He ^{a, d}, Yong Xu ^{b, d},
Linying Chen ^c, Duofu Chen ^{a, c, **}

^a CAS Key Laboratory of Ocean and Marginal Sea Geology, Guangzhou Institute of Geochemistry, Chinese Academy of Sciences, Guangzhou 510640, China

^b Key Laboratory of Petroleum Resources Research, Chinese Academy of Sciences, Lanzhou 730000, China

^c Shanghai Engineering Research Center of Hadal Science and Technology, College of Marine Sciences, Shanghai Ocean University, Shanghai 201306, China

^d University of Chinese Academy of Sciences, Beijing 100049, China

ARTICLE INFO

Article history:

Received 8 October 2016

Received in revised form

25 March 2017

Accepted 9 May 2017

Available online 11 May 2017

Keywords:

Black shale

Organic matter accumulation

Primary productivity

Redox conditions

Sedimentation rate

Volcanic ash

Upper Triassic

Ordos basin

ABSTRACT

The lacustrine black shales in the Chang7 Member from the Upper Triassic Yanchang Formation of the Ordos Basin in Central China are considered one of the most important hydrocarbon source rocks. However, the mechanism of organic accumulation in the black shales remains controversial. To resolve the controversy, with the former paleontological data of Yanchang Formation and sedimentation rate data of the Chang7 black shales, we investigated the typical intervals of the Chang7 black shales (TICBS) which were obtained by drilling in Yaowan at the southern margin of the Ordos Basin and performed various sedimentary, isotopic and geochemical analysis, including the sedimentary petrography, pyrite morphology, total organic carbon (TOC) and total sulfur (TS), the ratio of pyritic Fe to total Fe (DOP_r), major and trace elements, together with pyritic sulfur isotopes ($\delta^{34}\text{S}_{\text{py}}$). The high sulfur content, enrichment of redox-sensitive trace metals, and the lower sedimentation rate of the TICBS in addition to the presence of marine spined acritarchs and coelacanth fossils indicate that the TICBS were deposited in a lacustrine environment possibly influenced by seawater. The petrographic observations show a thick layer of black shale with interlayers of thin layered siltstone (silty mudstone) and laminated tuff, which were related to the turbidity currents and volcanism, respectively. The U/Th, C-S, and Mo-U covariations, pyrite morphology, DOP_r, combined with the $\delta^{34}\text{S}_{\text{py}}$, suggest that the deposition occurred beneath the anoxic-sulfidic bottom waters, which was intermittently influenced by the oxygen-containing turbidity. The Ni/Al and Cu/Al possibly show extremely high to high primary productivity in the water column, which might be connected with the substantial nutrients input from seawater or frequently erupted volcanic ash entering the lake. In addition, the coincidence of an increased abundance of TOC with increased P/Al, Ni/Al, Cu/Al and U/Th, as well as relatively consistent Ti/Al suggest that the accumulation of the organic matter might be irrelevant to the clastic influx, and was mainly controlled by the high primary productivity and anoxic-sulfidic conditions. Further, the covariations of TOC vs. P/Al and TOC vs. Ba/Al indicate that the high primary productivity led to the elevated accumulation and burial of organic matter, while the anoxic to sulfidic conditions were likely resulted from an intense degradation of the organic matter during the early diagenesis. In summary, the organic matter accumulation is ultimately attributed to the high primary productivity possibly resulted from seawater or volcanic ash entering the lake.

© 2017 Elsevier Ltd. All rights reserved.

* Corresponding author. CAS Key Laboratory of Ocean and Marginal Sea Geology, Guangzhou Institute of Geochemistry, Chinese Academy of Sciences, Guangzhou 510640, China.

** Corresponding author. Shanghai Engineering Research Center of Hadal Science and Technology, College of Marine Sciences, Shanghai Ocean University, Shanghai 201306, China.

E-mail addresses: qinxianwang@gig.ac.cn (Q. Wang), cdf@gig.ac.cn (D. Chen).

1. Introduction

The deposition of black shales and the accumulation of organic matter in black shales not only involves the basic biogeochemical processes on Earth, including photosynthesis, oxidation, bacterial sulfate reduction and humification, etc., but also makes an important contribution to the primary source of hydrocarbons and other economic mineral deposits (Arthur and Sageman, 1994; Hedges and Keil, 1995; Burdige, 2007). The preservation and enrichment of the organic matter in the sediments is controlled by many factors, such as primary productivity, bottom-water oxygen supply, nutrient availability, clastic influx and the activity of such degradation processes as bacterial sulfate reduction (e.g. Demaison and Moore, 1980; Pedersen and Calvert, 1990; Murphy et al., 2000; Wei et al., 2012; Lash and Blood, 2014; Fu et al., 2015; Yan et al., 2015). However, the most important factors are attributed to primary productivity, redox conditions, and sedimentation rate. Correspondingly, three “simple” models on the accumulation of organic matter have been proposed, including the models on productivity, preservation and sedimentation rate (Katz, 2005). The productivity model suggests that a high level of primary productivity, which is induced by a high nutrient supply from the sedimentary environments, results in a large accumulation of organic matter (Pedersen and Calvert, 1990; Hay, 1995; Parrish, 1995). The preservation model argues that bottom dysoxia/anoxia ought to be regarded as the main control on organic matter preservation, which enhances organic matter accumulation by limiting the benthic activity and reducing the consumption of organic matter (Demaison and Moore, 1980). The sedimentation rate model suggests that there is a critical threshold in the sedimentation rate (Ibach, 1982). When the sedimentation rate is below this threshold, the oxidation and bioturbation of the organic matter potentially decrease with increasing sedimentation rate. However, above this threshold, as the sedimentation rate continues to increase, the dilution of organic matter increases whilst the amount of accumulated organic matter decreases. Therefore, it is difficult to explain organic accumulation with a single factor in all sediments and different sedimentary settings may have specific factors that control the accumulation of organic matter (Arthur and Sageman, 1994; Canfield, 1994; Rimmer et al., 2004; Yan et al., 2015; Zeng et al., 2015).

The lacustrine black shales in the Chang7 Member from the Upper Triassic Yanchang Formation of the Ordos Basin, Central China, have a high abundance of organic matter with a strong potential for hydrocarbon generation and expulsion (Yang and Zhang, 2005). The preservation of a large amount of cyanobacteria, green algae and acritarchs shows that the productivity was high during the deposition of the shales (Ji et al., 2012). Laminated black shales, biomarkers and trace elements indicate that the Chang7 black shales were deposited in an anoxic setting (Yang and Zhang, 2005; Zhang et al., 2008; Yang et al., 2010; Qiu et al., 2014). Further, volcanic eruptions and lake-bottom hydrothermal activities during the same periods may have been the sources for significant nutrients, resulting in an enhanced biological productivity (Qiu et al., 2009b; Zhang et al., 2009, 2010). Lastly, the identification of marine spined acritarchs and coelacanth fossils from the Chang7 black shales suggest conditions with a marine influence (Su, 1984; Xu et al., 2003). Despite previous studies dealing with the Chang7 black shales, the factors controlling the enrichment of organic matter are not well understood. Further, the hypothesis of marine incursion events is not generally accepted and it is even unclear whether those events have influenced the accumulation of organic matter in shales.

Using traditional sedimentology and sediment geochemistry in conjunction with the published data of paleontology and

sedimentation rate, we re-evaluate the depositional environment of the Yanchang Formation and re-assess various sediment parameters pertaining to the typical intervals of the Chang7 black shales (TICBS). By so doing, we explored the mechanism of organic matter accumulation and factors controlling the deposition of the TICBS.

2. Geological background, samples and analytical methods

The Ordos Basin spans five provinces namely, Shaanxi, Gansu, Ningxia, Inner Mongolia and Shanxi, and is a multicycle cratonic basin (Yang and Zhang, 2005). It has a significant resource potential, amounting to about one-third of China's total oil and gas production (Yang et al., 2013). The Ordos Basin has experienced different stages of evolution, including the Early Paleozoic marginal ocean basin, Early to the Late Paleozoic littoral basin, Late Permian to Middle Triassic large interior basin and Late Triassic to the Early Cretaceous para-foreland basin, before finally developing into the tectonic framework of the current basin. In the foreland basin stage during the Late Triassic, the North China plate and Yangtze plate collided and integrated, resulting in the closure of the relict of Youjiang and Qinling troughs and the formation of the Qinling Mountains (Yang, 2002). The tectonic process provided a large depositional space for the Ordos Basin (Liu, 1998; Liu and Yang, 2000) and subsequently deposited a set of fluvial-lacustrine sediments with a thickness of about 1300 m - the Upper Triassic Yanchang Formation (Deng et al., 2008). It is subdivided into 10 members from bottom to top (Qiu et al., 2010) and the depositional period of Chang7 was the pinnacle of the basin development. Meanwhile, intense subsidence allowed large-scale deposition of organic-rich source rocks in the deep to semi-deep water of the lake (Yang and Zhang, 2005). The Chang7 member can be subdivided into 3 sub-members based on the sedimentary cycles, named Chang7₁ to Chang7₃ from top to bottom. Chang7₃ is mainly a developed, thick layer of oil shale with tuff layers at the bottom, Chang7₂ has developed mudstone with thin tuff intercalations in the lower part and development of silty mudstone in the upper part, and lastly Chang7₁ is mainly composed of mudstone and silty mudstone (Qiu, 2011).

The well Yaowan 1 (N35° 13'; E109° 01') lies in the Tongchuan area at the southern margin of the Ordos Basin, which is 35 km north of Tongchuan City (Fig. 1A). The total thickness of the drilled core is 168 m including the Chang6, Chang7 and Chang8 strata of the Yanchang Formation. The Chang6 and Chang8 strata are mainly thick-bedded fine-grained gray-green sandstone, whereas the Chang7 strata are predominantly black shale and siltstone with intercalations of gray mudstone, silty mudstone, and tuff. In this paper, we collected samples from the typical intervals of black shales (108.5–117.5 m with the total length of 9 m) mostly developed in Chang7₂. The sampling interval is from 0.3 to 0.5 m with a total of 25 samples (Fig. 1B; Table 1).

Thin sections of sedimentary rock samples were prepared at the Guangzhou Institute of Geochemistry, Chinese Academy of Sciences, and were studied in detail using an optical microscope (Leica DMRX 888056) and a scanning electron microscope (SEM; Carl Zeiss SUPRA55 SAPPHIRE). Powdered samples were taken from the drilled core using a hand-held dental drill (ROTEX™ 782E), and care was taken to avoid mixing those powders with tuff and phosphate nodules, and subsequently, samples were pulverized to <200 mesh sizes with an agate mortar.

Major and trace elements were measured at the Institute of Geochemistry, Chinese Academy of Sciences. Powdered samples were placed in Teflon beakers and dissolved in 1 mL of hydrofluoric acid (HF) and 1 mL of nitric acid (HNO₃). Subsequently, the sealed beakers were placed into an electric oven and heated to 185 °C for

about 36 h. Thereafter, the solutions were evaporated on a hot plate overnight and then treated with 2 mL of HNO_3 and 3 mL of ultra-pure distilled water. The beakers were sealed again and heated to 135 °C for about 5 h to dissolve the residue. Major and trace elements were determined using a Varian Vista Pro ICP-AES and a Perkin-Elmer Sciex ELAN 6000 ICP-MS following the method described by Qi et al. (2005). Certified reference materials (GSR-1, OU-6, 1633-a, GXR-2, GXR-5) were used for quality control. The precision and accuracy were both above 5% for Al, Ti, P, Fe, Ba, Cu, Ni, Th, U, and 10% for Mo.

The total organic carbon (TOC) and total sulfur (TS) contents were measured using a vario EL cube elemental analyzer at the Guangzhou Institute of Geochemistry, Chinese Academy of Sciences. At first, the total carbon and total sulfur contents were measured. Secondly, samples were decalcified with 6 mol/L HCl to remove inorganic carbon, and were washed twice with de-ionized water before dried at 60 °C for TOC determination. Certified reference material (sulfanilamide) was used for quality control. The precision and accuracy of the TOC and TS measurements were both above 0.5%.

Sulfur isotopic measurement was conducted by the Oxy-Anion Stable Isotope Consortium (OASIC) at Louisiana State University. Firstly, the sample split was treated with 1 M chromium dichloride (CrCl_2) solution and 6 N hydrochloric acid (HCl) + 10 mL alcohol. The hydrogen sulfide was immediately purged by nitrogen stream and was trapped and collected in a zinc acetate (ZnAc) solution to which 2% silver nitrate (AgNO_3) + 6 N ammonium hydroxide (NH_4OH) solutions were added to precipitate silver sulfide (Ag_2S), which was then filtered, rinsed and dried. All these procedures were based on the method of Canfield et al. (1986). Afterward, the dried Ag_2S was mixed with vanadium pentoxide (V_2O_5) and then converted to sulfur dioxide (SO_2) by combustion with an elemental analyzer at 980 °C. Finally, the sulfur isotopic ratio of the purified SO_2 , namely, the pyrite sulfur isotope value ($\delta^{34}\text{S}_{\text{py}}$), was analyzed by using a Finnigan Delta-S mass spectrometer. The standard deviation associated with the $\delta^{34}\text{S}$ analysis was $\pm 0.3\text{\textperthousand}$ and was reported according to the VCDT (Vienna Canyon Diablo Troilite) standard.

3. Results

3.1. Petrographic characteristics

The TICBS from well Yaowan 1 is thick, with interlayers of thin siltstone (silty mudstone) and laminated tuff. The interlayers of siltstone and silty mudstone are rare compared to the tuff interlayers and they often abruptly shift to black shale at the bottom with a flame-like sedimentary structure (Fig. 2A), which is considered to be the characteristic of deepwater deposits formed by turbidity currents (Feng et al., 2012; Qiu, 2011). The interlayers of tuff developed in the whole shales are mainly ash lamina, which is usually a centimeter to less than a millimeter. Phosphate nodules are often found above ash lamina (Fig. 2B and D).

Under the single-polar microscope, the ash lamina are composed of coarse crystal fragments of plagioclase which are scattered in the matrix of tiny volcanic dust. The contents of the crystal fragments of plagioclase are 50–70% with a particle size of about 0.05–0.3 mm (Fig. 2C). In addition, there are usually small amounts of volcanic crystal fragments found in the organic lamina (Fig. 2C).

3.2. The characteristics of TOC, TS, and $\delta^{34}\text{S}_{\text{py}}$

The TOC and TS contents of the black shales are both high and highly variable, ranging from 7.21% to 32.28% (avg. 18.35%), and

3.84%–16.83% (avg. 7.57%), respectively. The TOC and TS contents of siltstones and silty mudstones are relatively low with small variations, ranging from 2.84% to 4.27% (avg. 3.55%) and 0.58%–1.94% (avg. 1.16%), respectively (Fig. 3; Table 1).

The $\delta^{34}\text{S}_{\text{py}}$ of the TICBS range between $-2.4\text{\textperthousand}$ and $+8.7\text{\textperthousand}$, with the majority being positive. The $\delta^{34}\text{S}_{\text{py}}$ fluctuate significantly in the profile and are generally lower in the black shales with high TOC contents (Fig. 3).

3.3. The characteristics of major and trace elements

The aluminum (Al) and titanium (Ti) contents of the TICBS are relatively variable with the similar trends (Fig. 3). The Ti/Al is relatively steady, while the Ti/Al of siltstones and silty mudstones (0.036–0.061, avg. 0.049) are slightly higher than those of the associated black shales (0.025–0.058, avg. 0.043) (Fig. 3; Table 1).

To eliminate the influence of terrigenous clastics, the productivity indicators, including phosphorus (P), barium (Ba), nickel (Ni) and copper (Cu) are normalized to aluminum (Al) (Algeo and Tribouillard, 2009). The profiles of the P/Al, Ni/Al and Cu/Al of the TICBS correlate well, with the Ba/Al showing a different trend (Fig. 4). Generally, the mean P/Al, Ni/Al and Cu/Al of the black shales (131.5×10^{-4} , 7.89×10^{-4} and 22.89×10^{-4}) are significantly higher than those of the siltstones and silty mudstones (85.79×10^{-4} , 2.74×10^{-4} and 5.92×10^{-4} ; one anomaly is the sample A-24 with extremely high P/Al, mostly likely caused by phosphate nodules in the shales). Meanwhile, the mean Ba/Al is lower than those of the black shales (73.86×10^{-4}) compared to the siltstones and silty mudstones (97.70×10^{-4}) (Table 1).

The enrichment factor (M_{EF}) is used to describe the degree of element enrichment in shale, which is calculated according to the following equation: $M_{\text{EF}} = (X/\text{Al})_{\text{sample}} / (X/\text{Al})_{\text{PAAS}}$, where X and Al represent the concentration of elements X and Al, respectively. Samples are normalized using the post-Archean average shale (PAAS) of McLennan (1989). $M_{\text{EF}} > 1$ represents an element enrichment to the PAAS concentrations, $M_{\text{EF}} > 3$ represents a detectable enrichment and $M_{\text{EF}} > 10$ indicates a moderate to a strong degree of enrichment (Algeo and Tribouillard, 2009). The enrichment factors of phosphorus (P), iron (Fe), molybdenum (Mo), uranium (U), barium (Ba), thorium (Th), nickel (Ni) and copper (Cu) (P_{EF} , F_{EF} , M_{EF} , U_{EF} , Ba_{EF} , Th_{EF} , Ni_{EF} and Cu_{EF}) of the TICBS are shown in Table 1 and Fig. 5. In the black shales, the Mo and U are strongly enriched, Fe and Cu are detectably enriched, while the other elements show minor to no enrichment. In siltstones and silty mudstones, the Mo has a detectable to moderate enrichment, P, U, Ba, and Cu show slight enrichment, Fe, and Th show no enrichment, and Ni is depleted.

4. Discussion

4.1. The depositional setting: lacustrine or marine?

It is generally believed that the major basins in central and western China, including the Ordos Basin, have been transformed from sea-land interaction (marine or offshore lake) into a freshwater lake in Late Permian (Ji et al., 2006). However, marine fossils were found in the Late Triassic sediments from the southwestern Ordos Basin. For example, a typical marine coelacanth fossil with a rounded tail was found in the Chang3³ (Chang4-6) of the Upper Triassic Yanchang Formation in Huachi area (Liu et al., 1999); a broken marine coelacanth fossil was discovered in the Tongchuan Formation (Chang7) in Tongchuan area (Su, 1984); spined acritarchs fossils belonging to marine planktonic algae were identified in the Chang2, 3, 6 and 7 members of the Upper Triassic Yanchang Formation in the southwestern of the Ordos basin (Xu et al., 2003;

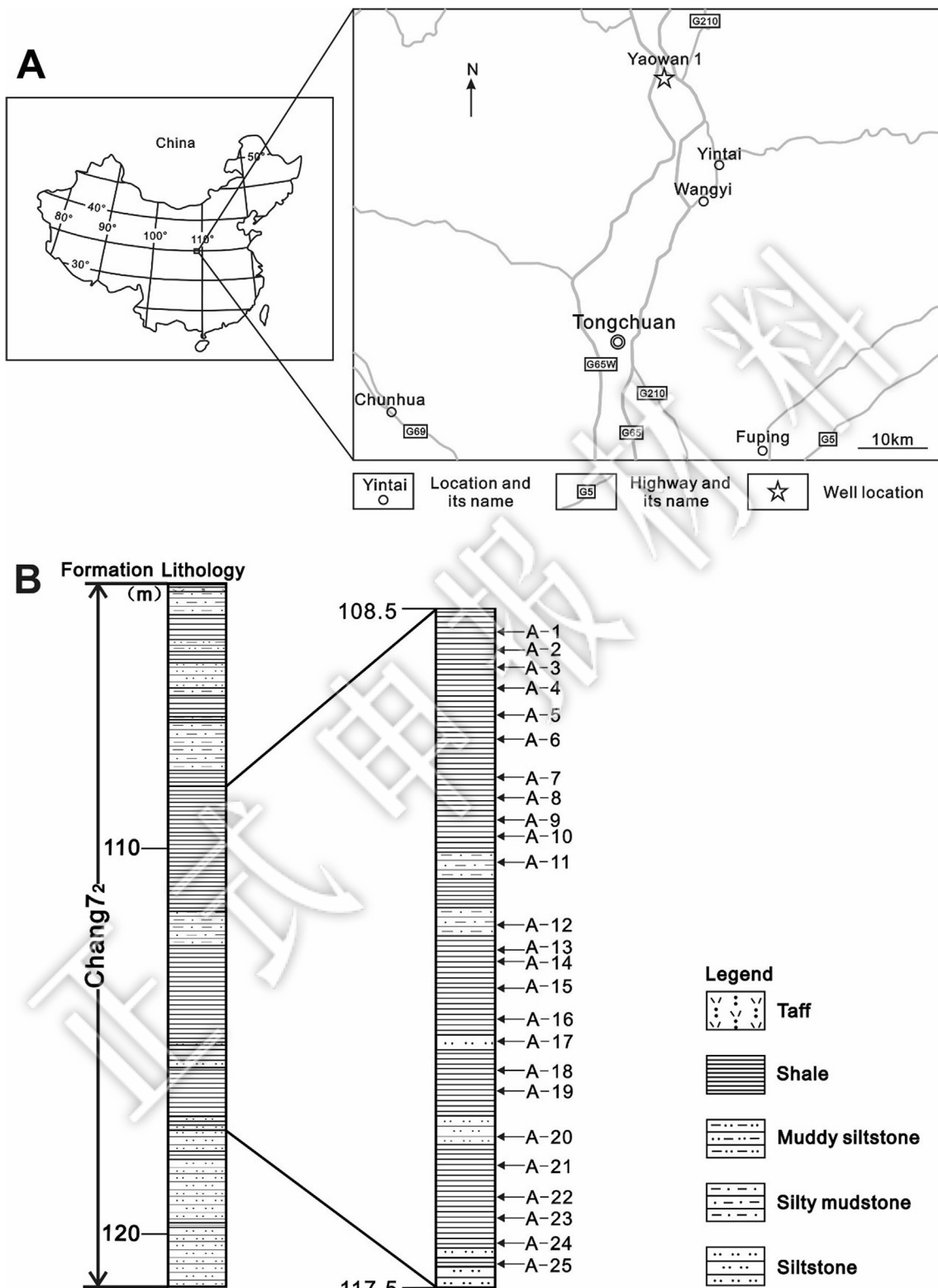


Fig. 1. (A) Study site (left) and an expanded view (right) of the Tongchuan area with the location of well Yaowan 1; and (B) Vertical profile in which lithologies of the Chang7₂ strata and the position of samples in this study are shown.

Ji et al., 2006). In addition, the high sulfur content (avg.6.54%, Max >15, Fig. 3), the enrichment of Mo, U and other redox-sensitive trace metals (Fig. 5) of the TICBS suggest the characteristics of the marine environment (Berner and Raiswell, 1984; Rimmer,

2004). Lastly, the sedimentation rate of Chang7 shales is in the range of limited marine basins (see below section 4.4 for discussion). Therefore, it is possible that seawater intruded into the Ordos Basin, and some sediments of the Yanchang Formation

Table 1

Variation of the multiple geochemical parameters of the samples from the typical intervals of the Chang7 black shales.

Samples	Depth(m)	Lithology	TOC (%)	TS (%)	Al (%)	Ti (%)	Fe (%)	P (ug/g)	Mo (ug/g)	U (ug/g)	Ba (ug/g)	Th (ug/g)	Ni (ug/g)	Cu (ug/g)	
A-1	108.80	Black shale	31.66	7.71	4.81	0.19	7.40	982.8	80.7	50.5	344.0	10.4	40.7	131.0	
A-2	109.00	Black shale	10.59	3.84	8.09	0.20	4.37	513.4	34.7	32.1	408.0	15.7	26.8	67.6	
A-3	109.25	Black shale	17.59	6.26	6.37	0.27	6.65	730.5	55.6	53.0	391.0	11.6	44.9	113.0	
A-4	109.50	Black shale	24.80	7.51	5.75	0.26	7.31	1260.0	90.5	73.6	431.0	10.4	53.6	127.0	
A-5	109.85	Black shale	7.21	4.44	8.69	0.50	4.18	615.5	23.9	27.9	931.0	14.8	25.2	73.8	
A-6	110.20	Black shale	15.21	5.36	5.65	0.30	5.94	567.0	26.9	20.2	377.0	13.2	51.2	79.4	
A-7	110.70	Black shale	14.02	9.36	4.74	0.23	8.55	328.1	64.0	59.4	383.0	9.1	33.6	145.0	
A-8	110.95	Black shale	26.79	11.27	4.05	0.17	9.92	708.5	94.1	52.0	248.0	7.4	47.2	183.0	
A-9	111.25	Black shale	32.28	8.27	3.75	0.17	6.98	1093.0	57.7	44.9	280.0	7.2	30.4	101.0	
A-10	111.45	Black shale	14.55	8.58	6.01	0.24	8.32	561.7	40.5	49.8	325.0	12.5	41.3	109.0	
A-11	111.80	Silty mudstone	3.83	0.95	8.11	0.29	5.11	701.4	7.1	10.0	583.0	13.2	23.1	47.5	
A-12	112.65	Silty mudstone	4.27	1.15	7.24	0.44	2.98	906.5	12.8	9.8	697.0	14.2	30.1	70.0	
A-13	113.00	Black shale	10.96	5.97	6.99	0.27	6.82	490.4	37.2	30.0	350.0	12.5	81.0	108.0	
A-14	113.10	Black shale	9.08	3.97	7.35	0.29	6.65	440.5	27.4	22.2	366.0	13.9	39.4	74.8	
A-15	113.45	Black shale	9.81	7.21	7.41	0.31	7.28	425.4	48.6	53.7	449.0	12.4	42.6	97.8	
A-16	113.90	Black shale	19.86	8.11	3.27	0.16	7.22	516.2	55.9	34.5	228.0	7.6	31.2	104.0	
A-17	114.20	Siltstone	2.84	1.94	9.18	0.53	2.68	519.1	6.0	4.2	1210.0	12.4	7.2	19.6	
A-18	114.60	Black shale	17.71	10.52	4.63	0.21	9.48	375.0	96.7	33.6	300.0	7.0	32.5	132.0	
A-19	114.85	Black shale	17.08	4.78	5.36	0.27	5.12	527.9	36.0	32.4	396.0	10.1	53.3	85.1	
A-20	115.40	Siltstone	3.27	0.58	7.50	0.30	2.50	560.6	4.4	4.4	680.0	10.1	23.8	45.2	
A-21	115.80	Black shale	29.90	16.83	2.66	0.12	14.36	509.2	99.4	66.4	223.0	5.6	39.6	165.0	
A-22	116.20	Black shale	17.51	8.98	4.68	0.21	7.79	856.4	61.5	54.5	396.0	6.7	28.0	107.0	
A-23	116.50	Black shale	19.00	7.94	5.60	0.22	7.39	960.3	55.7	57.0	389.0	10.6	41.8	112.0	
A-24	116.80	Black shale	19.08	7.29	5.53	0.21	6.91	5484.0	59.5	80.8	609.0	8.8	33.3	124.0	
A-25	117.15	Black shale	20.67	4.77	5.71	0.20	4.97	898.6	60.5	37.6	750.0	7.7	47.5	112.0	
Ti/Al	P/Al ($\times 10^{-4}$)	Ba/Al ($\times 10^{-4}$)	Ni/Al ($\times 10^{-4}$)	Cu/Al ($\times 10^{-4}$)	P _{EF}	Fe _{EF}	Mo _{EF}	U _{EF}	Ba _{EF}	Th _{EF}	Ni _{EF}	Cu _{EF}	U/Th	$\delta^{34}\text{S}_{\text{py}} (\text{\textperthousand})$	DOP _T
0.040	204.49	71.58	8.47	27.26	2.92	3.06	168.09	33.90	1.10	1.48	1.54	5.46	4.85	3.2	0.91
0.025	63.46	50.43	3.31	8.36	0.91	1.07	42.93	12.82	0.78	1.33	0.60	1.67	2.05	0.4	0.77
0.042	114.75	61.42	7.05	17.75	1.64	2.08	87.43	26.88	0.95	1.25	1.28	3.55	4.57		0.82
0.045	219.10	74.95	9.32	22.08	3.13	2.53	157.53	41.31	1.15	1.24	1.70	4.42	7.07	-2.4	0.90
0.057	70.82	107.12	2.90	8.49	1.01	0.96	27.53	10.36	1.65	1.17	0.53	1.70	1.88	7.9	0.93
0.053	100.30	66.69	9.06	14.05	1.43	2.09	47.63	11.56	1.03	1.60	1.65	2.81	1.53	4.1	0.79
0.048	69.21	80.78	7.09	30.58	0.99	3.59	135.11	40.43	1.24	1.31	1.29	6.12	6.54		0.96
0.042	174.99	61.25	11.66	45.20	2.50	4.88	232.65	41.51	0.94	1.24	2.12	9.05	7.08	0.3	0.99
0.046	291.30	74.62	8.10	26.92	4.17	3.70	153.93	38.68	1.15	1.32	1.47	5.39	6.24		1.04
0.041	93.43	54.06	6.87	18.13	1.34	2.75	67.44	26.76	0.83	1.43	1.25	3.63	3.99		0.90
0.035	86.52	71.92	2.85	5.86	1.24	1.26	8.82	3.99	1.11	1.12	0.52	1.17	0.76		0.16
0.061	125.28	96.33	4.16	9.67	1.79	0.82	17.71	4.38	1.48	1.35	0.76	1.94	0.69	3.4	0.34
0.038	70.20	50.10	11.60	15.46	1.00	1.94	53.31	13.87	0.77	1.23	2.11	3.10	2.40		0.77
0.040	59.93	49.79	5.36	10.18	0.86	1.80	37.31	9.73	0.77	1.30	0.98	2.04	1.59	-1.3	0.52
0.042	57.44	60.63	5.75	13.21	0.82	1.96	65.69	23.43	0.93	1.15	1.05	2.64	4.33		0.87
0.050	157.96	69.76	9.55	31.82	2.26	4.40	171.21	34.04	1.07	1.59	1.74	6.37	4.54	1.3	0.98
0.057	56.57	131.85	0.78	2.14	0.81	0.58	6.58	1.47	2.03	0.93	0.14	0.43	0.34	8.7	0.63
0.044	81.08	64.86	7.03	28.54	1.16	4.08	209.28	23.46	1.00	1.04	1.28	5.71	4.79	3	0.97
0.050	98.46	73.87	9.94	15.87	1.41	1.90	67.22	19.54	1.14	1.29	1.81	3.18	3.21		0.82
0.040	74.78	90.71	3.17	6.03	1.07	0.66	5.89	1.91	1.40	0.92	0.58	1.21	0.44	1.7	0.20
0.044	191.35	83.80	14.88	62.01	2.74	10.74	373.92	80.52	1.29	1.44	2.71	12.41	11.87	0.7	1.03
0.044	182.93	84.58	5.98	22.85	2.62	3.31	131.49	37.58	1.30	0.98	1.09	4.58	8.16	3.4	1.01
0.039	171.46	69.45	7.46	20.00	2.45	2.63	99.55	32.88	1.07	1.30	1.36	4.00	5.38		0.94
0.038	991.43	110.10	6.02	22.42	14.18	2.49	107.67	47.15	1.70	1.09	1.10	4.49	9.17	3.7	0.92
0.036	157.32	131.30	8.32	19.61	2.25	1.73	106.02	21.27	2.02	0.93	1.51	3.93	4.88		0.84

(including Chang7) might have marine deposits with the characteristics of offshore lakes in the Late Triassic.

However, it has been debated regarding the origin of seawater. Liu et al. (1999) proposed that (1) the trough of northern margin of the Ordos Basin has been closed in the late Permian; (2) there was no seawater connected from the eastern and southern margin of the Ordos Basin after the Permian as indicated by the regular sedimentary sequence of regression from eastern and southern margin into interior of the Ordos Basin; (3) the northern part of the western basin margin is a set of coarse debris continental sediments in the Permian and Triassic while the southern part of the western basin margin has Early to Middle Triassic marine strata (Fig. 6). Taking into consideration of all the evidence it is suggested that the Ordos Basin was possibly connected to the sea in the southwest margin.

4.2. Redox conditions

4.2.1. Pyrite morphology and DOP_T

Pyrite framboid diameter is a potential tool to distinguish anoxic-euxinic conditions from oxic-dysoxic conditions (Wilkin and Barnes, 1997; Wignall and Newton, 1998; Riquier et al., 2006). Wilkin and Barnes (1996) suggested the mean framboid diameter ($\pm 1\sigma$, σ stands for standard deviation) from sediments of anoxic-euxinic and oxic-dysoxic environments are $5.0 \pm 1.7 \mu\text{m}$ and $7.7 \pm 4.1 \mu\text{m}$, respectively. They also think fewer than 4% of framboids are $>10 \mu\text{m}$ in euxinic sediments; generally 10–50% of framboids are $>10 \mu\text{m}$ in non-euxinic sediments. The size distributions of framboidal pyrite from the black shales of the TICBS is 4–8 μm with rather constant and small sizes, and only a few of those framboidal pyrite (<10%) are $>10 \mu\text{m}$ (Fig. 7 A, B and D).

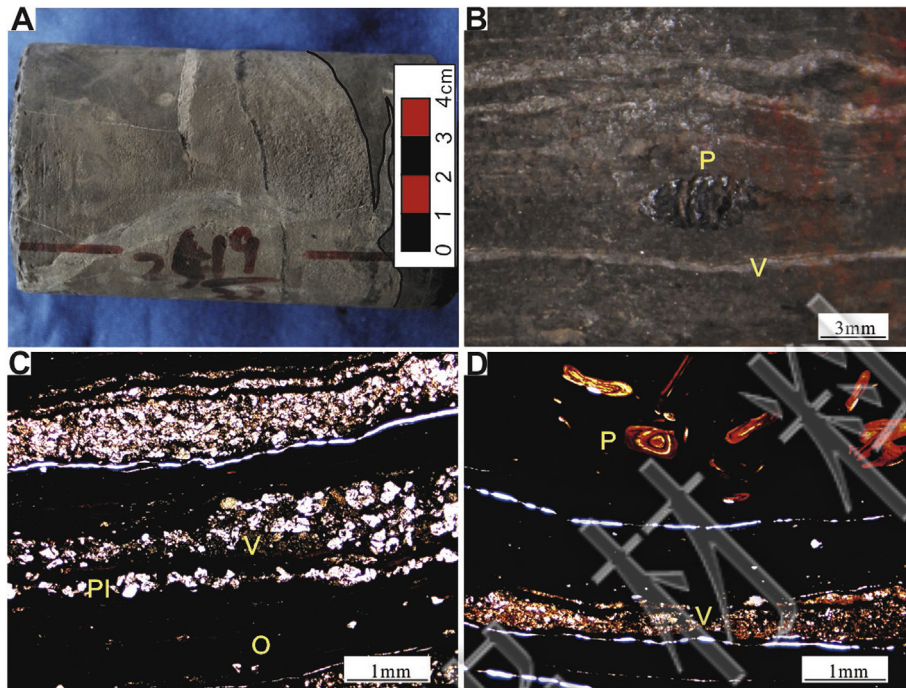


Fig. 2. Characteristics of the TICBS. (A) Black shale and turbidite siltstone with a flame-like sedimentary structure (black line); (B) Volcanic ash layers (light-colored layer marked "V") and phosphate nodule (dark nodule marked "P") developed in the black shale samples; (C) Organic matter lamina (dark layer marked "O") and millimeter thin volcanic ash layer (bright layer marked "V") in which the crystals are plagioclase (sample A-24) and volcanic ash layer (the bright layer marked "V") of sample A-24. The fine bright bands in C and D are fractures, artefacts produced by the process of making thin sections. Note that A and B are sample photographs, and C and D are photographs taken under the single-polar microscope. (For interpretation of the references to colour in this figure legend, the reader is referred to the web version of this article.)

Therefore, the black shales were possibly deposited in anoxic-euxinic bottom water. In contrast to the shales, the siltstones and silty mudstones have a few pyrite framboids and often 30% of framboids are $>10 \mu\text{m}$ (Fig. 7C), which likely indicate the oxic-dysoxic environment.

The degree of pyritization (DOP), a ratio of pyritic Fe to total reactive Fe within a sample, is used as a paleoredox proxy (Raiswell et al., 1988). Generally, $\text{DOP} < 0.42$ indicates an oxic, $0.46 < \text{DOP} < 0.75$ the suboxic, and $\text{DOP} > 0.75$ anoxic-euxinic environment (Raiswell et al., 1988; Sageman et al., 2003). The DOP_T , the

ratio of pyritic Fe (based on total S) to total Fe, can be used in place of the true DOP values, if pyrite S composes the bulk of total S and reactive Fe compose the bulk of total Fe (Algeo and Maynard, 2008; Algeo et al., 2008b). This is true for many black shale formations including the Pennsylvanian shales, Appalachian Basin Devonian black shales, and Late Triassic Chang7 shales (Rimmer et al., 2004; Algeo and Maynard, 2008; Yuan et al., 2016b). In current study, the DOP_T of the shales is between 0.52 and 1.04 (Fig. 4), almost all of them higher than 0.75, which suggests an anoxic-euxinic environment. In contrast to the shales, the DOP_T of the siltstones and

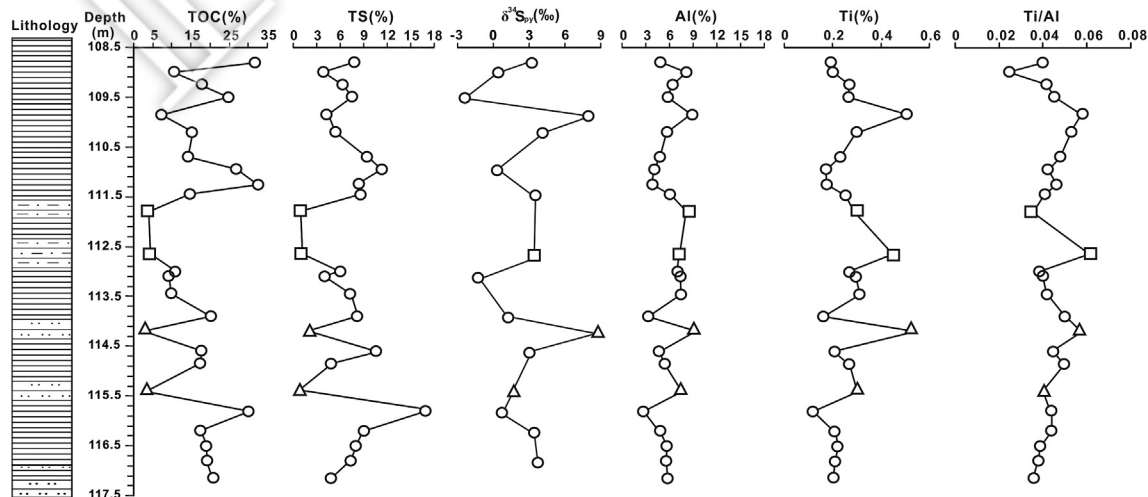


Fig. 3. Down-core variations of TOC contents, TS contents, $\delta^{34}\text{S}_{\text{py}}$ ratios, Al contents, Ti contents and Ti/Al ratios of the TICBS. Unfilled circles, squares, and triangles represent black shales, silty mudstones, and siltstones, respectively.

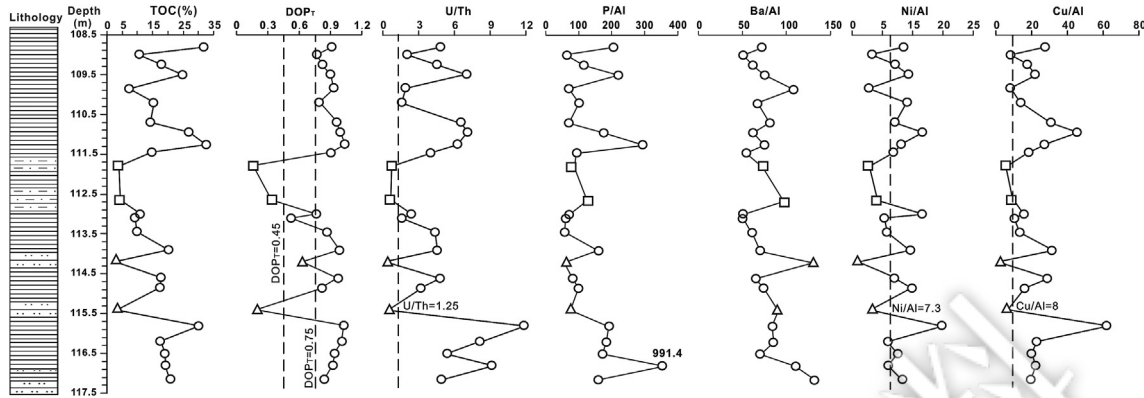


Fig. 4. Down-core variations of the TOC contents, DOP_T, U/Th, P/AI ($\times 10^{-4}$), Ba/Al ($\times 10^{-4}$), Ni/Al ($\times 10^{-4}$) and Cu/Al ($\times 10^{-4}$) of the TICBS. The five vertical dashed lines mark in DOP_T, U/Th, Ni/Al ($\times 10^{-4}$) and Cu/Al ($\times 10^{-4}$) panels at 0.45, 0.75, 1.25, 7.3, and 8.0, respectively (Raiswell et al., 1988; Wignall and Twitchett, 1996; Böning et al., 2012). Unfilled circles, squares, and triangles represent black shales, silty mudstones and siltstones, respectively.

silty mudstones range from 0.16 to 0.62 (Fig. 4), which indicates an oxic-suboxic environment.

4.2.2. U/Th

Under oxidizing conditions, Th exists as insoluble Th⁴⁺, and U exists as the dissolved form of U⁶⁺. Under strong reducing conditions, Th is still in the insoluble form Th⁴⁺, but U transforms from the dissolved state of U⁶⁺ to insoluble U⁴⁺, and is enriched in sediments (Wignall and Twitchett, 1996; Kimura and Watanabe, 2001). Therefore, the U/Th are typically greater than 1.25 in an anoxic environment and less than 0.75 in an oxygen-enriched environment (Wignall and Twitchett, 1996). The U/Th of the black shales are greater than 1.25 with the highest value of 11.87 and its average of 5.05. In addition, the U/Th of the siltstones and silty mudstones are close to or less than 0.75 (Fig. 4; Table 1). These data indicate that the black shales were deposited in an intensely anoxic environment, while the siltstones and silty mudstones were deposited in an oxic to the suboxic environment.

4.2.3. C-S-Fe relationship

The theoretical composition of pyrite (FeS₂) is Fe 46.55 wt%, S 53.45 wt% and S/Fe = 1.15. In the Fe-S scatter plot, there is a good correlation between Fe and S (Fig. 8A solid line, R² = 0.92) and the TICBS are near the theoretical line of pyrite (Fig. 8A dotted line), indicating that the sulfur contained in the samples may almost entirely exist as pyrite (Dean and Arthur, 1989). Thus, the pyrite sulfur can be estimated by the total sulfur (Algeo and Maynard, 2004; Rimmer, 2004; Rimmer et al., 2004).

The C-S relationship in the sediments can be used to assess the oxygen level of bottom waters (Hofmann et al., 2000). It is based on the principle that organic matter is catabolized by bacteria, while sulfates are concurrently reduced by means of the bacteria sulfate reduction (BSR) to form hydrogen sulfides that react with iron so as to form pyrites in the sediment, resulting in the C-S covariation (Leventhal, 1987). In the C-S plot, sediments (rocks) deposited under the oxic conditions generally distribute along a line through the origin with S/C = 0.36 (Berner and Raiswell, 1984). In contrast to the oxic conditions, the euxinic environments with abundant reactive iron are characterized by S/C higher than 0.36 with positive intercepts on the S axis (Leventhal, 1983; Berner, 1984). The positive intercept indicates that the pyrite is formed in sulfidic water columns (Raiswell and Berner, 1985; Lyons and Berner, 1992). Additionally, the euxinic environments with limited reactive iron are characterized by a fairly constant or relatively high sulfur content independent of the organic carbon content (Hofmann et al., 2000).

The TICBS show a good correlation between C and S (R² = 0.57), and their trend line with a positive intercept (Fig. 8B solid line a) is close to the line of S/C = 0.36 (Fig. 8B dotted line). This shows that the TICBS may be deposited in an environment crossing from oxic to anoxic, even to sulfidic. If the samples from the siltstone and silty mudstone were excluded, the correlation between C and S becomes worse (R² = 0.34), still with a positive intercept (Fig. 8B solid line b), and a relatively high S content, indicating the sedimentary characteristics of anoxic to sulfidic environment with limited reactive iron. In summary, the black shales may have been deposited in an anoxic to the sulfidic environment, while the siltstones and silty mudstones may have been deposited in an oxic to the suboxic environment.

4.2.4. Mo-U covariation

U and Mo are redox indicators with minimal detrital influences and can truly reflect the redox conditions during sediment deposition (Tribouillard et al., 2006). As the U enrichment begins under suboxic conditions (Fe³⁺ is transforming to Fe²⁺), whereas Mo enrichment requires the presence of H₂S (i.e., euxinic conditions) and the redox cycle of Mo potentially being influenced by particulate shuttles, the patterns of U-Mo covariations have been shown to be particularly useful proxies for paleoenvironmental reconstruction (Algeo and Tribouillard, 2009; Tribouillard et al., 2012; Luo et al., 2017).

Mo and U show strong enrichment in the black shales, whereas Mo and U shows detectable to moderate and detectable enrichment, respectively, in the siltstones and silty mudstones (Fig. 9; Table 1). Additionally, the Mo_{EF} are much higher than the U_{EF} in the black shales and slightly higher than the U_{EF} in the siltstones and silty mudstones. These data indicate that the black shales were possibly deposited in a water column with abundant H₂S, whereas siltstones and silty mudstones were deposited in water with scarce H₂S. In the diagram of the Mo-U covariation, the black shales correspond to an anoxic to the sulfidic environment, whereas the siltstones and silty mudstones correspond to an oxic to the suboxic environment (Fig. 9). Given that the siltstones and silty mudstones belongs to the turbidites (Qiu, 2011; Feng et al., 2012.), the TICBS were generally deposited in an anoxic to the sulfidic environment, but occasionally affected by the oxygen-containing turbidity.

4.2.5. Characteristics of sulfur isotopes

Studies have shown that sulfur isotopes can record changes in the redox conditions in ocean and lake systems (e.g., Strauss, 1997; Watanabe et al., 2004; Thompson and Kah, 2012). The principle is

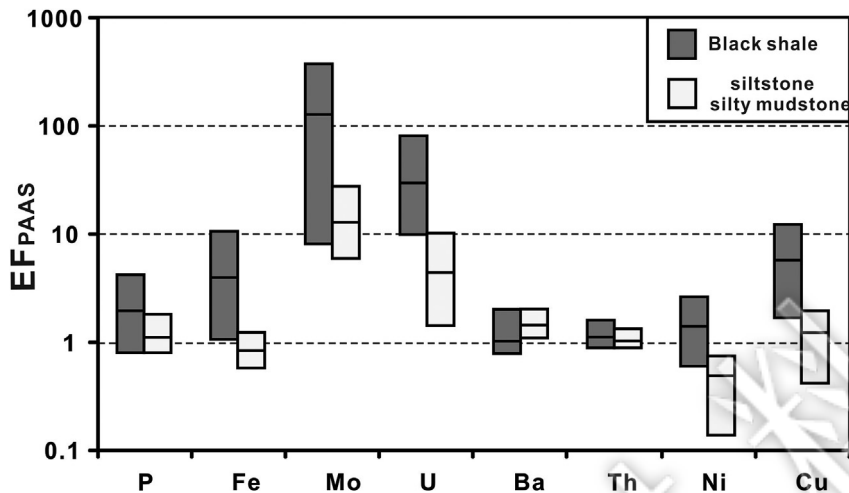


Fig. 5. Enrichment factors of some major and trace elements of the TICBS. The extent of the boxes corresponds to the range of values (min-max) and the inner line to the average values.

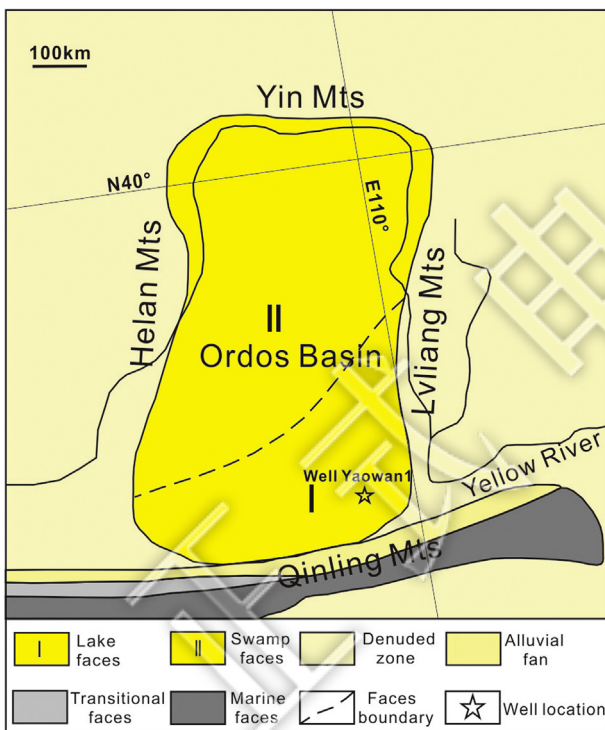


Fig. 6. Late Triassic palaeogeographic map of the Ordos Basin with well location (Modified from Qiu et al., 2009a).

that the bacterial sulfate reduction (BSR) activity induces a fractionation of the stable isotopes ^{34}S and ^{32}S , resulting in a depletion of ^{34}S in the produced sulfide relative to coeval sulfate (Kaplan and Rittenberg, 1964; Canfield, 2001). Although the sulfur isotope fractionation caused by the BSR is widespread, the degree of fractionation is ultimately controlled by the sulfate availability. In an open environment, the supply of sulfate is sufficient and the sulfur isotope fractionation is generally greater than 20–22‰ (Zaback et al., 1993; Habicht and Canfield, 1997), whereas in a closed environment, the sulfate concentration is very low and the sulfur isotope fractionation is often less than 25‰ (Schwarcz and Burnie, 1973; Chambers, 1982; Habicht and Canfield, 1996, 1997;

Watanabe et al., 2004).

The $\delta^{34}\text{S}_{\text{py}}$ of the TICBS range from -2.4 to +8.7‰ (Table 1). As the marine incursion events possibly occurred when the shales were deposited (see section 4.1), so we assume that the sulfate $\delta^{34}\text{S}$ of the Late Triassic lake water in the Ordos Basin was the same as coeval open-marine waters ($15.5 \pm 0.4\text{‰}$; Boschetti et al., 2011), then the maximum fractionation of the sulfur isotope would be 6.4–18.3‰. It is lower than 20‰ representing the fractionation value of the sulfur isotope caused by the BSR in an open environment with sufficient sulfate, but much higher than the maximum fractionation of the sulfur isotope (4.6‰) in Late Cretaceous Songliao Basin experienced from marine incursion (Huang et al., 2013). This possibly shows that the Late Triassic Ordos Basin was a semi-closed environment, although other reasons could have caused a small S-isotope fractionations, e.g., near-quantitative consumption of water-column or porewater sulfate, more reactive (i.e., more easily metabolized) organic matter associated with greater rates of sulfate reduction (Algeo et al., 2015; Canfield, 2001).

Further, the $\delta^{34}\text{S}_{\text{py}}$ fluctuates significantly, being lighter in black shales with high TOC and heavier in black shales with low TOC or siltstones (silty mudstones) (Fig. 3). These fluctuations may possibly be related to the migration of the redox interface. It appears that when black shales with low TOC or siltstones (silty mudstones) were deposited, the redox interface was possibly located under or at the sediment-water interface, which limited the supply of sulfate in the pore water system, resulting in the formation of pyrite with heavier $\delta^{34}\text{S}_{\text{py}}$. On the other hand, when black shales with high TOC were deposited, the redox interface possibly moved up to the bottom water, which enhanced the supply of sulfate and BSR, leading to the formation of pyrite with lighter $\delta^{34}\text{S}_{\text{py}}$.

To summarize, the present data (U/Th, C-S, and Mo-U covariations, DOP_T and $\delta^{34}\text{S}_{\text{py}}$) and pyrite morphology as stated above indicate that the sediments from the TICBS, even though existing short-term oxidation to sub-oxidation, were mainly deposited in the anoxic-sulfidic depositional environment.

4.3. Primary productivity

P, Ba, Ni and Cu are potential proxies for primary productivity (Tribouillard et al., 2006). They usually represent the relative level of primary productivity and be used to compare with TOC in order to ensure the relationship between primary productivity and

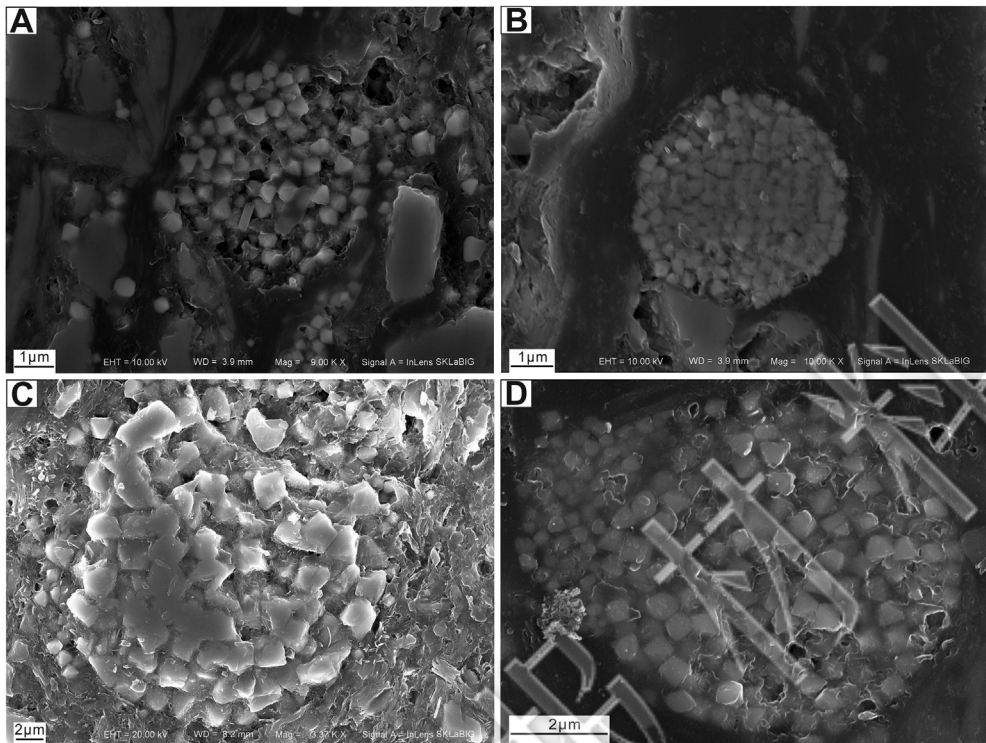


Fig. 7. Photomicrographs obtained by using a scanning electron microscope (SEM) of pyrite from studied samples: (A) Pyrite framboids in sample A-7; (B) Framboidal pyrite made up of uniform microcrystals in sample A-8; (C) Pyrite framboids in sample A-11; and (D) Pyrite framboids with a tail in sample A-22.

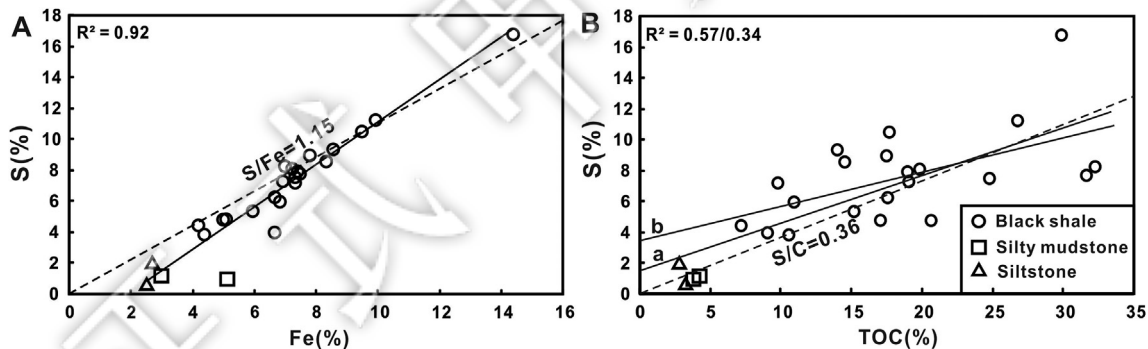


Fig. 8. The relationship of iron and organic carbon to the sulfur content of the TICBS.

organic matter enrichment (e.g. Böning et al., 2012; Wei et al., 2012; Yan et al., 2015). However, we need to certify that the TOC above refers to the organic matter produced by algae organisms (primary productivity) before compare (Pedersen and Calvert, 1990). In fact, previous research had certified that the organic matter of the Chang7 black shales was mainly algae coming from primary productivity. For instance, the kerogen of the Chang7 black shales was consisted of average value being 91.08% amorphous liptinite and less than 10% the vitrinite (terrestrial debris) (Yang and Zhang, 2005; Kong, 2007); the kerogen's $\delta^{13}\text{C}$ of the Chang7 black shales ranges from $-30\text{\textperthousand}$ to $-28\text{\textperthousand}$ (Guo et al., 2014; Ji et al., 2007), which is in the range of algae (Meyers, 1994); the abundance of cyanobacteria fossils in the Chang7 black shales is closely related to the organic carbon contents of black shales (Ji et al., 2012). Therefore, TOC in our paper can be compared with the productivity proxies and the details are as follows.

Phosphorus is considered as an important nutrient which limits biological growth (Ingall et al., 1993; Vink et al., 1997; Slomp et al.,

2004). The distributions of phosphorous (P) in sediments are often linked to supply of organic matter, possibly resulting from a high productivity, which makes P an important indicator for biological productivity (Schmitz et al., 1997). The P/Al in the black shales are higher with a larger range, while in siltstones (silty mudstones), it is lower with a smaller range. As a whole, the P/Al shows a rapid and frequent change (Fig. 4). These data suggest that a significant change possibly occurred in primary productivity when the TICBS were deposited. In addition, the P/Al and TOC have nearly the same profile trends, indicating that the primary productivity is likely to exert an important influence on the enrichment of organic matter.

Nickel (Ni) and copper (Cu) are predominantly delivered to the sediments in association with the OM (organometallic complexes), so the contents of sedimentary organic matter are often proportional to Ni and Cu (Tribouillard et al., 2006). Consequently, organic matter may be partially or completely degraded after deposition, whereas the Ni and Cu released by the organic matter are trapped by pyrite and are retained within the sediments (Huerta-Diaz and

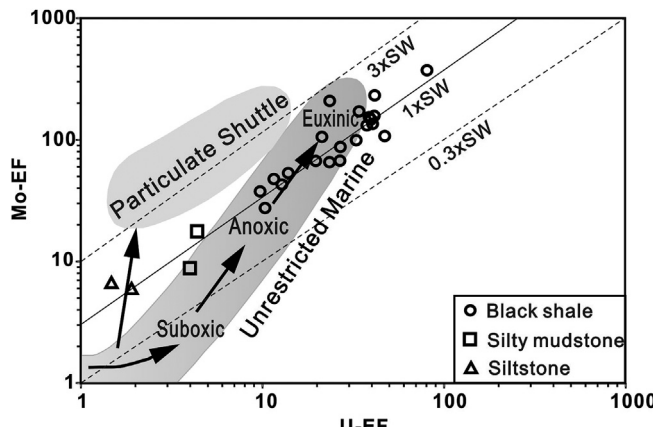


Fig. 9. U_{EF} versus Mo_{EF} for the TICBS. The lines show Mo/U molar ratios equal to the seawater value (SW) and to the fractions thereof ($3 \times SW$, $0.3 \times SW$). The pattern of U_{EF} and Mo_{EF} are compared to the model proposed by Algeo and Tribouillard (2009).

Morse, 1992; Algeo and Maynard, 2004; Nameroff et al., 2004; Piper and Perkins, 2004); hence, the Ni and Cu can be used as indicators for paleoproductivity (Tribouillard et al., 2006). The average Cu/Al and Ni/Al of the Peru upwelling area (Productive area) are 8.00×10^{-4} and 7.30×10^{-4} , and their background values with TOC being zero are 1.8×10^{-4} or 2.7×10^{-4} and 0.7×10^{-4} or 1.4×10^{-4} , respectively (Böning et al., 2012). The Cu/Al of the black shales are much higher than those of Peru, and Ni/Al are slightly higher than those of Peru (Fig. 4), whilst the background values with TOC being zero (1.14×10^{-4} and 2.63×10^{-4} , respectively) (Fig. 10D and C) are similar to the Peru area. Therefore, the paleoproductivity of the black shales was possibly very high. In addition, the coincidence of an increased abundance of total organic carbon (TOC) with increased Cu/Al , Ni/Al , and P/Al (Fig. 4) indicates that the organic matter accumulation in the TICBS was mainly controlled by increased primary productivity.

The barite accumulation rate shows a positive correlation with primary productivity in the marine sediments (Dymond et al., 1992; Dymond and Collier, 1996; Paytan, 1996; Paytan and Griffith, 2007). Therefore, the Ba/Al ratio can be used in order to quantitatively evaluate the paleoproductivity (Dean et al., 1997). However, when the primary productivity is very high, a strong BSR may cause barite dissolution and Ba loss in the sediments, thus reducing the reliability of the Ba/Al proxy (Van Os et al., 1991; Torres et al., 1996; Van Santvoort et al., 1996; Tribouillard et al., 2006). The profile variations of Ba/Al are very different from the Cu/Al , Ni/Al , P/Al and TOC contents, with Ba/Al values of most black shale samples lower than the values of the siltstone (silty mudstone) samples (Fig. 4). Combined with the characteristics of the abundant reduced sulfur and pyritic sulfur isotopes in the black shales, these data indicate that the intense BSR possibly led to barite dissolution in the sediments and transformed the original Ba content in shales. Thus, the Ba/Al in this profile cannot reflect the true paleoproductivity.

4.4. Clastic influx

Clastic influx is indicative of the fact that the diluents and absorbents of organic matter may directly affect the content of organic matter in the sediments (Ibach, 1982; Rimmer, 2004), and thus indirectly affect the burial rate and bacteria degradation efficiency of the organic matter (Canfield, 1994). Al in sediments is all from clay, feldspar and other aluminum silicate minerals, while Ti is partly from clay minerals, and partly from silt-sized grains of heavy minerals (such as ilmenite, sphene, and augite) (Rimmer, 2004).

Thus, the Ti/Al can be used as a reliable indicator of the siliciclastic grain size (Bertrand et al., 1996). As the grains of sediment increase with the sedimentation rates, higher Ti/Al represent the larger grains and faster sedimentation rates (Murphy et al., 2000).

The Ti/Al of the TICBS in the profile show a relatively steady trend (Fig. 3). The Ti/Al of the siltstones and silty mudstones are slightly higher than those of the black shales, but all of them are lower than the anoxic marine sediments (e.g., Longmaxi Formation in South China in which the Ti/Al is 0.058; Yan et al., 2015). Meanwhile, based on the age model which was constructed using the zircon U-Pb age of tuff and strata thickness (Yang and Deng, 2013), and Milankovitch cycle (Earth orbital cycle) (Yuan et al., 2016a), the average sedimentation rate of the Chang7 shales is 1.5 cm/kyr (5 cm/kyr by taking into account the compaction rate of the mudstone (70%, Chen and Wan, 1984)) and 1.35 cm/kyr, respectively, which are between the open marine settings (<1 cm/kyr, Loutit et al., 1988; Katz, 2005) and the strongly limited marine basins (e.g. Black sea Unit II, 7.8–21.4 cm/kyr, Arthur and Dean, 1998), so the information deduced by Ti/Al is nearly consistent with the sedimentation rate here, namely, the sedimentation rate may have been lower when the TICBS were deposited. In addition, the Ti/Al and TOC data show a very weak negative correlation ($R^2 = 0.02$) (Fig. 10E) suggesting that the enrichment of the organic matter possibly has no relationship with the detrital input/sedimentation rate. Therefore, the burial of organic matter in the TICBS was not simply a function of clastic starvation or the increased surface area for organic matter adsorption associated with finer grains.

4.5. The mechanism of organic matter accumulation

The factors controlling organic matter enrichment include surficial primary productivity (Pedersen and Calvert, 1990; Caplan and Bustin, 1999), sedimentation rate (clastic influx) (Murphy et al., 2000; Sageman et al., 2003) and redox conditions (Demaison and Moore, 1980; Mort et al., 2007). The clastic influx indicator (Ti/Al) of the TICBS has a relatively steady trend (Fig. 3) and has no correlation with the TOC contents ($R^2 = 0.02$) (Fig. 10 E) suggesting that the change of clastic influx was not the main factor controlling the enrichment of the organic matter in the TICBS. The redox (U/Th) and productivity (Cu/Al , Ni/Al , and P/Al) indicators and TOC contents show a similar trend (Fig. 4), as well as the U/Th , Cu/Al , and Ni/Al with TOC have good positive correlations ($R^2 = 0.59$, 0.62 and 0.56 , respectively) (Fig. 10). This indicates that the anoxic conditions and high productivity joined together to enhance preservation and accumulation of sedimentary organic matter, resulting in the deposition of the TICBS.

However, which factor on Earth is more important? Schoepfer et al. (2015) proposed that the covariant relations of TOC vs. P and TOC vs. Ba can be used to distinguish the relative importance between the redox conditions and productivity levels in the process of organic matter enrichment. When the redox conditions are more critical, in reducing conditions, TOC tends to save, while P and Ba prefer to activate and are lost as their adsorption carriers (ferromanganese hydroxide) are reduced and dissolved. In oxidizing conditions, the TOC is easily consumed by oxygen, while P and Ba tend to be buried and deposited. Therefore, either in oxidizing or reducing conditions, the TOC vs. P and TOC vs. Ba always show an anti-covariant relationship (Tyson, 2005). When primary productivity is more important, the output of organic matter in surface water is the main factor controlling for the TOC, P, and Ba in sediments. The redox conditions will generally not affect the strong positive correlation of TOC vs. P and TOC vs. Ba (Tyson, 2005); however, the correlation of TOC vs. Ba may possibly be lost as a result of the intense sulfate reduction (Reichart et al.,

1997; Muñoz et al., 2012).

The P/Al and TOC of the TICBS show a good positive correlation (Fig. 10A solid line a, $R^2 = 0.71$, excluding the sample A-24), and the black shales (excluding siltstones and silty mudstones) exhibits a better positive correlation ($R^2 = 0.81$, Fig. 10A solid line b), suggesting that the organic matter enrichment in the TICBS may have been predominantly derived by primary productivity. However, the Ba/Al and TOC do not show any correlation ($R^2 = 0.02$, Fig. 10B), which may have been related to the intense sulfate reduction, possibly resulting in by high productivity (see section 4.3). Therefore, we suggest that the primary productivity was more important in organic matter enrichment in the TICBS, and the anoxic to sulfidic conditions in the lake may have been the result of the intense degradation of organic matter.

The level of primary productivity is largely controlled by nutrient availability in any sedimentary basins (Katz, 1995). For one thing, as the marine incursion events possibly occurred when the TICBS were deposited, so the nutrients were possible seawater-sourced and entered the basin through lateral advection when the shales deposited. That is to say, surface waters flow oceanward and deep waters cratonward while nutrients are brought in with the laterally advected deep waters. Then, they recycled between the surface and deep layers of the basin, such as the Permian Phosphoria Formation on the western margin of North America (Stephens and Carroll, 1999), as well as the Late Pennsylvanian Midcontinent Sea of North America (Algeo et al., 2008a; Algeo and Heckel, 2008). For another thing, experimental research shows that

the volcanic ashes can release large amounts of major and trace nutrients such as P, Si, Fe, Zn, Mn, Ni, Co, and Cu, etc. in 1–2 h, thus creating favorable conditions for a large-scale phytoplankton blooms (Frogner et al., 2001). Field observations have also confirmed the rapid blooms of phytoplankton in lakes and oceans after deposition of ash and aerosols. For example, the eruption of Mount St. Helens in Washington on May 18, 1980, was followed by a proliferation of phytoplankton in its nearby lakes (Smith and White, 1985); In August 2008, when the Kasatochi volcano of the Aleutian Islands erupted, volcanic ashes were deposited over a large area, with satellite observations showing a massive increase in the biological chlorophyll within the Northeast Pacific region (Hamme et al., 2010). It is noteworthy that there are abundant volcanic ash layers in the TICBS and overlying those volcanic layers, phosphate nodules were also found (Fig. 2B and D), which could be possibly related to high productivity. Furthermore, the P/Al and TOC also show a strong positive correlation. All these data suggest that the increase of paleoproductivity in the Chang7 period was likely driven by lateral advection of seawater-freshwater or the deposition of volcanic ash supplying abundant nutrients.

5. Conclusions

Sedimentary petrographic and geochemical data in conjunction with the published paleontological and sedimentation rate data were used to reveal the depositional environments and processes of organic matter accumulation in the black shales from the

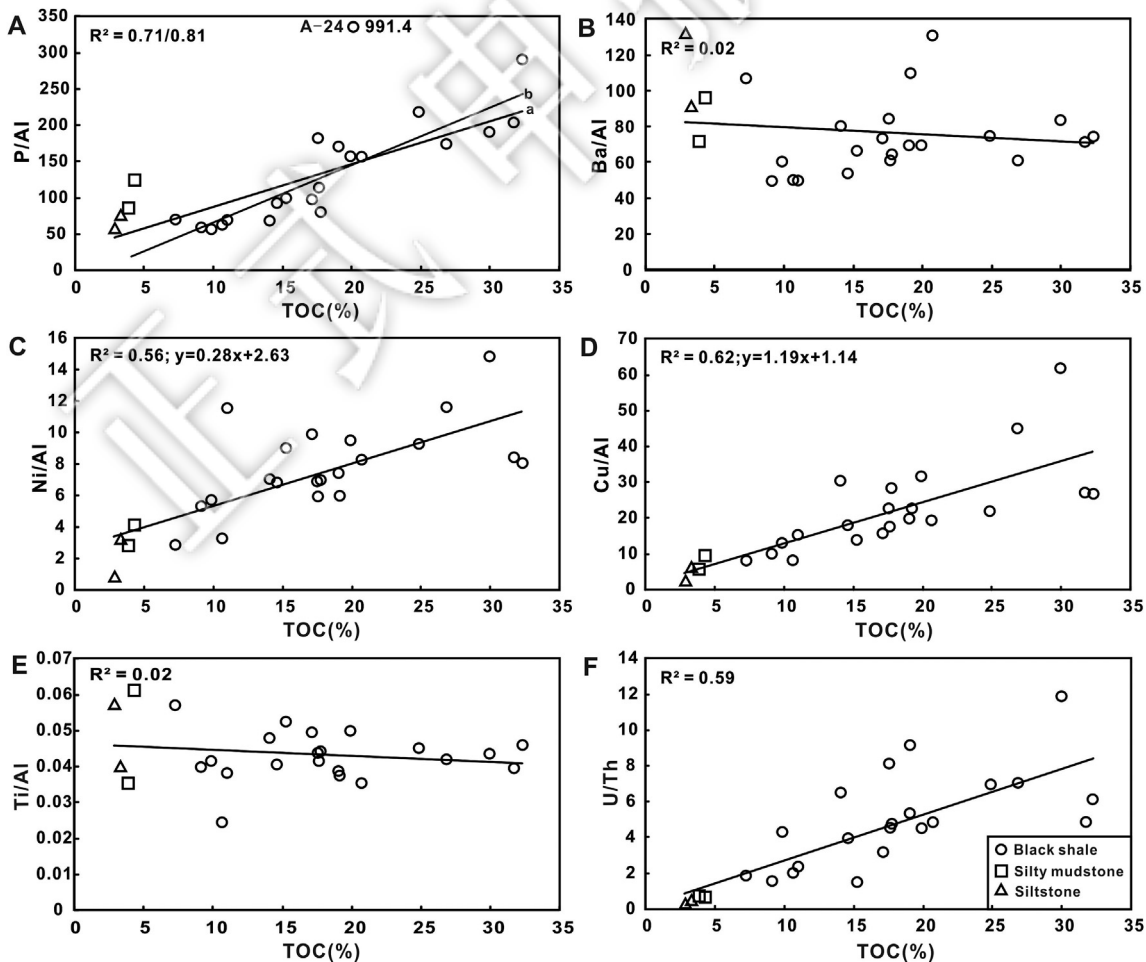


Fig. 10. The relationship of TOC to P/Al ($\times 10^{-4}$), Ba/Al ($\times 10^{-4}$), Ni/Al ($\times 10^{-4}$), Cu/Al ($\times 10^{-4}$), Ti/Al, and U/Th of the TICBS.

Yanchang Formation of the Ordos Basin. Our findings are summarized as follows:

- (1) The typical intervals of the Chang7 black shales were deposited in a lacustrine environment possibly intruded by seawater.
- (2) The typical intervals of the Chang7 black shales are mainly composed of black shale intercalated with thin siltstone (silty mudstone) caused by the turbidity currents and laminated tuff from volcanism.
- (3) The typical intervals of the Chang7 black shales were mainly deposited under anoxic to sulfidic bottom water conditions, which were interrupted by the oxygen-containing turbidity currents.
- (4) Organic matter enrichment was controlled by primary productivity, which was possibly increased in unison with an influx of nutrients from seawater or volcanic eruptions. This along with the anoxic to sulfidic water mass, which was possibly caused by the intense degradation of the organic matter during early diagenesis of the accumulated organic matter, results in enhanced organic matter accumulation and preservation in the typical intervals of the Chang7 black shales.

Acknowledgements

We would like to thank Liang Qi from the Institute of Geochemistry, Chinese Academy of Sciences, for the major and trace metals analysis. This research was supported by the National Natural Science Foundation of China (41321002 and 41272144) and the scientific and technological project B of the strategic precursor, the Chinese Academy of Sciences (XDB10000000). We would like to extend thank you for improving the grammar of the manuscript by Prof. Harunur Rashid, the insightful comments and suggestions by Thomas Algeo and an anonymous reviewer, and Editor-in-chief Andrew Bell is highly acknowledged. This paper is Contribution No. IS-2394 from GIGCAS.

References

- Algeo, T.J., Heckel, P.H., 2008. The Late Pennsylvanian midcontinent sea of North America: a review. *Palaeogeogr. Palaeoclimatol. Palaeoecol.* 268, 205–221.
- Algeo, T.J., Heckel, P.H., Maynard, J.B., Blakey, R.C., Rowe, H., 2008a. Modern and Ancient Epeiric Seas and the Super-estuarine Circulation Model of Marine Anoxia. *Dynamics of Epeiric Seas: Sedimentological, Paleontological and Geochemical Perspectives*. Geological Association Canada Special Publication, pp. 7–38.
- Algeo, T.J., Luo, G.M., Song, H.Y., Lyons, T.W., Canfield, D.C., 2015. Reconstruction of secular variation in seawater sulfate concentrations. *Biogeosciences* 12, 2131–2151.
- Algeo, T.J., Maynard, J.B., 2004. Trace-element behavior and redox facies in core shales of Upper Pennsylvanian Kansas-type cycloths. *Chem. Geol.* 206, 289–318.
- Algeo, T.J., Maynard, J.B., 2008. Trace-metal covariation as a guide to water-mass conditions in ancient anoxic marine environments. *Geosphere* 4, 872–887.
- Algeo, T.J., Rowe, H., Hower, J.C., Schwark, L., Herrmann, A., Heckel, P., 2008b. Changes in ocean denitrification during Late Carboniferous glacial-interglacial cycles. *Nat. Geosci.* 1, 709–714 (supplementary information).
- Algeo, T.J., Tribouillard, N., 2009. Environmental analysis of paleoceanographic systems based on molybdenum–uranium covariation. *Chem. Geol.* 268, 211–225.
- Arthur, M.A., Dean, W.E., 1998. Organic-matter production and preservation and evolution of anoxia in the Holocene Black Sea. *Paleoceanography* 13, 395–411.
- Arthur, M.A., Sageman, B.B., 1994. Marine shales: depositional mechanisms and environments of ancient deposits. *Annu. Rev. Earth Planet. Sci.* 22, 499–551.
- Böning, P., Fröllje, H., Beck, M., Schnetger, B., Brumsack, H.-J., 2012. Underestimation of the authigenic fraction of Cu and Ni in organic-rich sediments. *Mar. Geol.* 323, 24–28.
- Berner, R.A., 1984. Sedimentary pyrite formation: an update. *Geochimica Cosmochimica Acta* 48, 605–615.
- Berner, R.A., Raiswell, R., 1984. C/S method for distinguishing freshwater from marine sedimentary rocks. *Geology* 12, 365–368.
- Bertrand, P., Shimmield, G., Martinez, P., Grousset, F., Jorissen, F., Paterne, M., Pujol, C., Bouloubassi, I., Menard, P.B., Peypouquet, J.-P., 1996. The glacial ocean productivity hypothesis: the importance of regional temporal and spatial studies. *Mar. Geol.* 130, 1–9.
- Boschetti, T., Cortecchi, G., Toscani, L., Iacumin, P., 2011. Sulfur and oxygen isotope compositions of Upper Triassic sulfates from Northern Apennines (Italy): palaeogeographic and hidrogeochemical implications. *Geol. Acta* 9, 129–147.
- Burdige, D.J., 2007. Preservation of organic matter in marine sediments: controls, mechanisms, and an imbalance in sediment organic carbon budgets? *Chem. Rev.* 107, 467–485.
- Canfield, D.E., 1994. Factors influencing organic carbon preservation in marine sediments. *Chem. Geol.* 114, 315–329.
- Canfield, D.E., 2001. Biogeochemistry of sulfur isotopes. In: Valley, J.W., Cole, D.R. (Eds.), *Reviews in Mineralogy and Geochemistry: Stable Isotope Geochemistry*, 43. Mineralogical Society of America, pp. 607–636.
- Canfield, D.E., Raiswell, R., Westrich, J.T., Reaves, C.M., Berner, R.A., 1986. The use of chromium reduction in the analysis of reduced inorganic sulfur in sediments and shales. *Chem. Geol.* 54, 149–155.
- Caplan, M.L., Bustin, R.M., 1999. Palaeoceanographic controls on geochemical characteristics of organic-rich Exshaw mudrocks: role of enhanced primary production. *Org. Geochem.* 30, 161–188.
- Chambers, L.A., 1982. Sulfur isotope study of a modern intertidal environment, and the interpretation of ancient sulfides. *Geochimica Cosmochimica Acta* 46, 721–728.
- Chen, Z.M., Wan, L.G., 1984. A calculating method on the fossil thickness of stratigraphy. *Oil Gas Geol.* 5, 47–54 (in Chinese with English abstract).
- Dean, W.E., Arthur, M.A., 1989. Iron-sulfur-carbon relationships in organic-carbon-rich sequences I: cretaceous western interior seaway. *Am. J. Sci.* 289, 708–743.
- Dean, W.E., Gardner, J.V., Piper, D.Z., 1997. Inorganic geochemical indicators of glacial-interglacial changes in productivity and anoxia on the California continental margin. *Geochimica Cosmochimica Acta* 61, 4507–4518.
- Demaison, G.T., Moore, G.T., 1980. Anoxic environments and oil source bed genesis. *Org. Geochem.* 2, 9–31.
- Deng, X.Q., Lin, F.X., Liu, X.Y., Pang, J.L., Lv, J.W., Li, S.X., Liu, X., 2008. Discussion on relationship between sedimentary evolution of the triassic Yanchang Formation and the early indosian movement in Ordos basin. *J. Palaeogeogr.* 10, 159–166 (in Chinese with English abstract).
- Dymond, J., Collier, R., 1996. Particulate barium fluxes and their relationships to biological productivity. *Deep Sea Res. Part II Top. Stud. Oceanogr.* 43, 1283–1308.
- Dymond, J., Suess, E., Lyle, M., 1992. Barium in deep-sea sediment: a geochemical proxy for paleoproduction. *Paleoceanography* 7, 163–181.
- Feng, P.J., Li, W.H., Ou, Y.Z.J., 2012. Sedimentary characters and geological implication of turbidite of the Chang 6 and Chang 7 intervals of upper triassic Yanchang Formation in Huangling area, Ordos basin. *J. Palaeogeogr.* 14, 295–302 (in Chinese with English abstract).
- Frogner, P., Gislason, S.R., Öskarsson, N., 2001. Fertilizing potential of volcanic ash in ocean surface water. *Geology* 29, 487–490.
- Fu, X.Z., Wang, J., Chen, W.B., Feng, X.L., Wang, D., Song, C.Y., Zeng, S.Q., 2015. Organic accumulation in lacustrine rift basin: constraints from mineralogical and multiple geochemical proxies. *Int. J. Earth Sci.* 104, 495–511.
- Guo, H.J., Jia, W.L., Peng, P.A., Lei, Y.H., Luo, X.R., Cheng, M., Wang, X.Z., Zhang, L.X., Jiang, C.F., 2014. The organic geochemistry, mineralogy and methane sorption of lacustrine shales from the Upper Triassic Yanchang Formation, Ordos Basin, China. *Mar. Petroleum Geol.* 57, 509–520.
- Habicht, K.S., Canfield, D.E., 1996. Sulphur isotope fractionation in modern microbial mats and the evolution of the sulphur cycle. *Nature* 382, 342–343.
- Habicht, K.S., Canfield, D.E., 1997. Sulfur isotope fractionation during bacterial sulfate reduction in organic-rich sediments. *Geochimica Cosmochimica Acta* 61, 5351–5361.
- Hamme, R.C., Webley, P.W., Crawford, W.R., Whitney, F.A., DeGrandpre, M.D., Emerson, S.R., Eriksen, C.C., Giesbrecht, K.E., Gower, J.F.R., Kavanaugh, M.T., Pena, M.A., Sabine, C.L., Batten, S.D., Coogan, L.A., Grundle, D.S., Lockwood, D., 2010. Volcanic ash fuels anomalous plankton bloom in subarctic northeast Pacific. *Geophys. Res. Lett.* 37, 470–479.
- Hay, W.W., 1995. Paleoceanography of marine organic-carbon-rich sediments. In: Huc, A.-Y. (Ed.), *Paleogeography, Paleoclimate, and Source Rocks*, 40. American Association of Petroleum Geologists, Studies in Geology, pp. 21–59.
- Hedges, J.I., Keil, R.G., 1995. Sedimentary organic matter preservation: an assessment and speculative synthesis. *Mar. Chem.* 49, 81–115.
- Hofmann, P., Ricken, W., Schwark, L., Leythaeuser, D., 2000. Carbon-sulfur-iron relationships and $\delta^{34}\text{S}$ of organic matter for late Albian sedimentary rocks from the North Atlantic Ocean: paleoceanographic implications. *Paleoceanography* 163, 97–113.
- Huang, Y.J., Yang, G.S., Gu, J., Wang, P.K., Huang, Q.H., Feng, Z.H., Feng, L.J., 2013. Marine incursion events in the Late Cretaceous Songliao Basin: constraints from sulfur geochemistry records. *Palaeogeogr. Palaeoclimatol. Palaeoecol.* 385, 152–161.
- Huerta-Diaz, M.A., Morse, J.W., 1992. Pyritization of trace metals in anoxic marine sediments. *Geochimica Cosmochimica Acta* 56, 2681–2702.
- Ibach, L.E.J., 1982. Relationship between sedimentation rate and total organic carbon content in ancient marine sediments. *AAPG Bull.* 66, 170–188.
- Ingall, E.D., Bustin, R.M., Cappellen, P.V., 1993. Influence of water column anoxia on the burial and preservation of carbon and phosphorus in marine shales. *Geochimica Cosmochimica Acta* 57, 303–316.

- Ji, L.M., Wang, S.F., Xu, J.L., 2006. Acritarch Assemblage in Yanchang Formation in Eastern Gansu Province and its Environmental Implications. *Earth Science-Journal of China University of Geosciences* 31, pp. 798–806 (in Chinese with English abstract).
- Ji, L.M., Wu, T., Li, L.T., 2007. Geochemical characteristics of kerogen in Yanchang Formation source rocks, Xifeng area, Ordos basin. *Petroleum Explor. Dev.* 34, 424–428 (in Chinese with English abstract).
- Ji, L.M., Xu, J.L., Song, Z.G., 2012. Lacustrine cyanobacteria from the Yanchang Formation in Ordos basin and its implication of oil source. *Acta Micropalaeontologica Sin.* 3, 270–281 (in Chinese with English abstract).
- Kaplan, I.R., Rittenberg, S.C., 1964. Microbiological fractionation of sulphur isotopes. *J. General Microbiol.* 34, 195–212.
- Katz, B.J., 1995. Factors controlling the development of lacustrine petroleum source rocks—an update. In: Huc, A.-Y. (Ed.), *Paleogeography, Paleoclimate, and Source Rocks*, vol. 40. American Association of Petroleum Geologists, *Studies in Geology*, pp. 61–79.
- Katz, B.J., 2005. Controlling factors on source rock development—a review of productivity, preservation, and sedimentation rate. *Soc. Sediment. Geol.* 82, 7–16.
- Kimura, H., Watanabe, Y., 2001. Oceanic anoxia at the Precambrian-Cambrian boundary. *Geology* 29, 995.
- Kong, Q.F., 2007. The organic maceral characteristic of Yanchang source rock in Ordos Basin. *Xinjiang Pet. Geol.* 28, 163–166 (in Chinese with English abstract).
- Lash, G.G., Blood, D.R., 2014. Organic matter accumulation, redox, and diagenetic history of the Marcellus Formation, southwestern Pennsylvania, Appalachian basin. *Mar. Petroleum Geol.* 57, 244–263.
- Leventhal, J.S., 1983. An interpretation of carbon and sulfur relationships in Black Sea sediments as indicators of environments of deposition. *Geochimica Cosmochimica Acta* 47, 133–137.
- Leventhal, J.S., 1987. C and S relationships in Devonian shales from the Appalachian basin as an indicator of environment of deposition. *Am. J. Sci.* 287, 33–49.
- Liu, G.B., Zhu, Z.X., Zhang, X.L., Ai, F., 1999. A coelacanthid fossil from Huachi area, Gansu province. *Geol. J. China Univ.* 4, 474–480 (in Chinese with English abstract).
- Liu, S., 1998. The coupling mechanism of basin and orogen in the western Ordos Basin and adjacent regions of China. *J. Asian Earth Sci.* 16, 369–383.
- Liu, S., Yang, S., 2000. Upper Triassic–Jurassic sequence stratigraphy and its structural controls in the western Ordos Basin, China. *Basin Res.* 12, 1–18.
- Loutit, T.S., Hardenbol, J., Vail, P.R., Baum, G.R., 1988. Condensed sections: the key to age determination and correlation of continental margin sequences. *SEPM* 42, 183–213.
- Luo, M., Algeo, T.J., Tong, H.P., Gieskes, J., Chen, L.Y., Shi, X.F., Chen, D.F., 2017. More reducing bottom-water redox conditions during the Last Glacial Maximum in the southern Challenger Deep (Mariana Trench, western Pacific) driven by enhanced productivity. *Deep Sea Res. Part II Top. Stud. Oceanogr.* <http://dx.doi.org/10.1016/j.dsro.2017.01.006>.
- Lyons, T.W., Berner, R.A., 1992. Carbon-sulfur-iron systematics of the uppermost deep-water sediments of the Black Sea. *Chem. Geol.* 99, 1–27.
- Meyers, P.A., 1994. Preservation of elemental and isotopic source identification of sedimentary organic matter. *Chem. Geol.* 114, 289–302.
- McLennan, S., 1989. Rare earth elements in sedimentary rocks; influence of provenance and sedimentary processes. *Rev. Mineralogy Geochem.* 21, 169–200.
- Mort, H., Jacquat, O., Adatte, T., Steinmann, P., Föllmi, K., Matera, V., Berner, Z., Stüben, D., 2007. The Cenomanian/Turonian anoxic event at the Bonarelli Level in Italy and Spain: enhanced productivity and/or better preservation? *Cretac. Res.* 28, 597–612.
- Muñoz, P., Dezileau, L., Cárdenas, L., Sellanes, J., Lange, C.B., Inostroza, J., Muratli, J., Salamanca, M.A., 2012. Geochemistry of trace metals in shelf sediments affected by seasonal and permanent low oxygen conditions off central Chile, SE Pacific (-36° S). *Cont. Shelf Res.* 33, 51–68.
- Murphy, A.E., Sageman, B.B., Hollander, D.J., Lyons, T.W., Brett, C.E., 2000. Black shale deposition and faunal overturn in the Devonian Appalachian Basin: clastic starvation, seasonal water-column mixing, and efficient biolimiting nutrient recycling. *Paleoceanography* 15, 280–291.
- Nameroff, T.J., Calvert, S.E., Murray, J.W., 2004. Glacial-interglacial variability in the eastern tropical North Pacific oxygen minimum zone recorded by redox-sensitive trace metals. *Paleoceanography* 19, 373–394.
- Parrish, J.T., 1995. Paleogeography of C org-rich rocks and the preservation versus production controversy. In: Huc, A.Y. (Ed.), *Paleogeography, Paleoclimate, and Source Rocks*, vol. 40. American Association of Petroleum Geologists, *Studies in Geology*, pp. 1–20.
- Paytan, A., 1996. Glacial to interglacial fluctuations in productivity in the Equatorial Pacific as indicated by marine barite. *Science* 274, 1355–1357.
- Paytan, A., Griffith, E.M., 2007. Marine barite: recorder of variations in ocean export productivity. *Deep Sea Res. Part II Top. Stud. Oceanogr.* 54, 687–705.
- Pedersen, T.F., Calvert, S.E., 1990. Anoxia vs. productivity: what controls the formation of organic-carbon-rich sediments and sedimentary Rocks? *AAPG Bull.* 74, 454–466.
- Piper, D.Z., Perkins, R.B., 2004. A modern vs. Permian black shale—the hydrography, primary productivity, and water-column chemistry of deposition. *Chem. Geol.* 206, 177–197.
- Qi, L., Zhou, M.F., Malpas, J., Sun, M., 2005. Determination of rare earth elements and Y in ultramafic rocks by ICP-MS after preconcentration using Fe(OH)_3 and Mg(OH)_2 coprecipitation. *Geostand. Geanalytical Res.* 29, 131–141.
- Qiu, D.Z., Xie, Y., Li, X.Q., Huang, F.X., 2009a. Geological characteristics of lithofacies paleogeography and hydrocarbon accumulation in Asian tethyan tectonic domain. *Mar. Orig. Pet. Geol.* 14, 41–51.
- Qiu, X.W., 2011. Characteristics and Dynamic Settings of Yanchang Period Hydrocarbon-rich Depression in Ordos Basin (PhD Dissertation). Northwest University, Xi'an (in Chinese with English abstract).
- Qiu, X.W., Liu, C.Y., Li, Y.H., Mao, G.Z., Wang, J.Q., 2009b. Distribution characteristics and geological significances of tuff interlayers in Yanchang formation of Ordos basin, China. *Acta Sedimentol. Sin.* 27, 1138–1146 (in Chinese with English abstract).
- Qiu, X.W., Liu, C.Y., Mao, G.Z., Deng, Y., Wang, F.F., 2010. Enrichment feature of thorium element in tuff interlayers of Upper Triassic Yanchang formation in Ordos basin, China. *Geol. Bull. China* 29, 1185–1191 (in Chinese with English abstract).
- Qiu, X.W., Liu, C.Y., Mao, G.Z., Deng, Y., Wang, F.F., Wang, J.Q., 2014. Major, trace and platinum-group element geochemistry of the Upper Triassic nonmarine hot shales in the Ordos basin, Central China. *Appl. Geochem.* 53, 42–52.
- Raiswell, R., Berner, R.A., 1985. Pyrite formation in euxinic and semi-euxinic sediments. *Am. J. Sci.* 285, 710–724.
- Raiswell, R., Buckley, F., Berner, R.A., Anderson, T.F., 1988. Degree of pyritization of iron as a paleoenvironmental indicator of bottom-water oxygenation. *J. Sediment. Res.* 58, 812–819.
- Reichart, G.J., Dulik, M.D., Visser, H.J., Weijden, C.H.V.D., Zachariasse, W.J., 1997. A 225 kyr record of dust supply, paleoproduction and the oxygen minimum zone from the Murray Ridge (northern Arabian Sea). *Palaeogeogr. Palaeoclimatol. Palaeoecol.* 134, 149–169.
- Rimmer, S.M., 2004. Geochemical paleoredox indicators in devonian-mississippian black shales, central Appalachian Basin (USA). *Chem. Geol.* 206, 373–391.
- Rimmer, S.M., Thompson, J.A., Goodnight, S.A., Robl, T.L., 2004. Multiple controls on the preservation of organic matter in Devonian–Mississippian marine black shales: geochemical and petrographic evidence. *Palaeogeogr. Palaeoclimatol. Palaeoecol.* 215, 125–154.
- Riquier, L., Tribouillard, N., Averbuch, O., Devleeschouwer, X., Riboulleau, A., 2006. The Late Frasnian Kellwasser horizons of the Harz Mountains (Germany): two oxygen-deficient periods resulting from different mechanisms. *Chem. Geol.* 233, 137–155.
- Sageman, B.B., Murphy, A.E., Werne, J.P., Ver Straeten, C.A., Hollander, D.J., Lyons, T.W., 2003. A tale of shales: the relative roles of production, decomposition, and dilution in the accumulation of organic-rich strata, Middle–Upper Devonian, Appalachian basin. *Chem. Geol.* 195, 229–273.
- Schmitz, B., Charisi, S.D., Thompson, E.I., Speijer, R.P., 1997. Barium, SiO_2 (excess), and P_2O_5 as proxies of biological productivity in the Middle East during the Palaeocene and the latest Palaeocene benthic extinction event. *Terra nova* 9, 95–99.
- Schoepfer, S.D., Shen, J., Wei, H., Tyson, R.V., Ingall, E., Algeo, T.J., 2015. Total organic carbon, organic phosphorus, and biogenic barium fluxes as proxies for paleo-marine productivity. *Earth-Science Rev.* 149, 23–52.
- Schwarz, H.P., Burnie, S.W., 1973. Influence of sedimentary environments on sulfur isotope ratios in clastic rocks: a review. *Miner. Deposita* 8, 264–277.
- Slomp, C.P., Thomson, J., Lange, G.J.D., 2004. Controls on phosphorus regeneration and burial during formation of eastern Mediterranean sapropels. *Mar. Geol.* 203, 141–159.
- Smith, M.A., White, M.J., 1985. Observations on lakes near Mount St. Helens: phytoplankton. *Arch. Fuer Hydrobiol.* 104, 345–362.
- Stephens, N.P., Carroll, A.R., 1999. Salinity stratification in the Permian Phosphoria sea: a proposed paleoceanographic model. *Geology* 27, 899–902.
- Strauss, H., 1997. The isotopic composition of sedimentary sulfur through time. *Palaeogeogr. Palaeoclimatol. Palaeoecol.* 132, 97–118.
- Su, D.Z., 1984. A new palaeoniscoid fish from the Yanchang Group of North Shaanxi and its biostratigraphic significance. *Vertebr. Palasiat.* 22, 14–21 (in Chinese with English abstract).
- Thompson, C.K., Kah, L.C., 2012. Sulfur isotope evidence for widespread euxinia and a fluctuating oxycline in Early to Middle Ordovician greenhouse oceans. *Palaeogeogr. Palaeoclimatol. Palaeoecol.* 313, 189–214.
- Torres, M.E., Brumsack, H.J., Bohrman, G., Emeis, K.C., 1996. Barite front in continental margin sediments: a new look at barium remobilization in the zone of sulfate reduction and formation of heavy barites in diagenetic fronts. *Chem. Geol.* 127, 125–139.
- Tribouillard, N., Algeo, T.J., Baudin, F., Riboulleau, A., 2012. Analysis of marine environmental conditions based on molybdenum-uranium covariation—Applications to Mesozoic paleoceanography. *Chem. Geol.* 324, 46–58.
- Tribouillard, N., Algeo, T.J., Lyons, T., Riboulleau, A., 2006. Trace metals as paleoredox and paleoproductivity proxies: an update. *Chem. Geol.* 232, 12–32.
- Tyson, R.V., 2005. The “productivity versus preservation” controversy: cause, flaws, and resolution. *Spec. Publ.* 82, 17–33.
- Van Os, B.J.H., Middelburg, J.J., de Lange, G.J., 1991. Possible diagenetic mobilization of barium in sapropelic sediments from the eastern Mediterranean. *Mar. Geol.* 100, 125–136.
- Van Santvoort, P.J.M., de Lange, G.J., Thomson, J., Cussen, H., Wilson, T.R.S., Krom, M.D., Ströhle, K., 1996. Active postdepositional oxidation of the most recent sapropel (S1) in sediments of the eastern Mediterranean Sea. *Geochimica Cosmochimica Acta* 60, 4007–4024.
- Vink, S., Chambers, R.M., Smith, S.V., 1997. Distribution of phosphorus in sediments from Tomales Bay, California. *Mar. Geol.* 139, 157–179.
- Watanabe, T., Naraoka, H., Nishimura, M., Kawai, T., 2004. Biological and environmental changes in lake Baikal during the late quaternary inferred from carbon, nitrogen and sulfur isotopes. *Earth Planet. Sci. Lett.* 222, 285–299.

- Wei, H., Chen, D., Wang, J., Yu, H., Tucker, M.E., 2012. Organic accumulation in the lower Chihsia Formation (Middle Permian) of South China: constraints from pyrite morphology and multiple geochemical proxies. *Palaeogeogr. Palaeoclimatol. Palaeoecol.* 353, 73–86.
- Wignall, P.B., Twitchett, R.J., 1996. Oceanic anoxia and the End Permian mass extinction. *Science* 272, 1155–1158.
- Wignall, P.B., Newton, R., 1998. Pyrite framboid diameter as a measure of oxygen deficiency in ancient mudrocks. *Am. J. Sci.* 298, 537–552.
- Wilkin, R.T., Barnes, H.L., 1996. Pyrite formation by reactions of iron monosulfides with dissolved inorganic and organic sulfur species. *Geochimica Cosmochimica Acta* 60, 4167–4179.
- Wilkin, R.T., Barnes, H.L., 1997. Formation processes of framboidal pyrite. *Geochimica Cosmochimica Acta* 61, 323–339.
- Xu, W., Wang, W.Y., Zhang, Q., 2003. Primary discussion on the recent development of the geological theory in China. *China Pet. Explor.* 8, 18–24 (in Chinese with English abstract).
- Yan, D., Wang, H., Fu, Q., Chen, Z., He, J., Gao, Z., 2015. Geochemical characteristics in the Longmaxi Formation (early silturian) of South China: implications for organic matter accumulation. *Mar. Petroleum Geol.* 65, 290–301.
- Yang, H., Deng, X.Q., 2013. Deposition of Yanchang Formation deep-water sandstone under the control of tectonic events, Ordos Basin. *Petroleum Explor. Dev.* 40, 513–520 (in Chinese with English abstract).
- Yang, H., Li, S.X., Liu, X.Y., 2013. Characteristics and resource prospects of tight oil and shale oil in Ordos basin. *Acta Pet. Sin.* 34, 1–11 (in Chinese with English abstract).
- Yang, H., Zhang, W.Z., 2005. Leading effect of the seventh member high-quality source rock of Yanchang Formation in Ordos Basin during the enrichment of low-penetrating oil-gas accumulation: geology and geochemistry. *Geochimica* 34, 147–154 (in Chinese with English abstract).
- Yang, H., Zhang, W., Wu, K., Li, S., Peng, P.A., Qin, Y., 2010. Uranium enrichment in lacustrine oil source rocks of the Chang 7 member of the Yanchang Formation, Erdos Basin, China. *J. Asian Earth Sci.* 39, 285–293.
- Yang, J.J., 2002. Tectonic Evolution and Oil-gas Reservoirs Distribution in Ordos Basin. Petroleum Industry Press, Beijing, pp. 36–37 (in Chinese).
- Yuan, W., Liu, G.D., Luo, W.B., 2016a. Deposition rate of the seventh member of Yanchang Formation, Ordos Basin and its impact on organic matter abundance of hydrocarbon source rock (Natural Science Edition). *J. Xi'an Shiyou Uni.* 31, 20–26 (in Chinese with English abstract).
- Yuan, W., Liu, G.D., Stebbins, A., Xu, L.M., Niu, X.B., Luo, W.B., Li, C.Z., 2016b. Reconstruction of redox conditions during deposition of organic-rich shales of the upper triassic Yangchang formation, Ordos basin, China. *Palaeogeogr. Palaeoclimatol. Palaeoecol.* <http://dx.doi.org/10.1016/j.palaeo.2016.12.020>.
- Zaback, D.A., Pratt, L.M., Hayes, J.M., 1993. Transport and reduction of sulfate and immobilization of sulfide in marine black shales. *Geology* 21, 141–144.
- Zeng, S., Wang, J., Fu, X., Chen, W., Feng, X., Wang, D., Song, C., Wang, Z., 2015. Geochemical characteristics, redox conditions, and organic matter accumulation of marine oil shale from the Changliang Mountain area, northern Tibet, China. *Mar. Petroleum Geol.* 64, 203–221.
- Zhang, W.Z., Yang, H., Peng, P.A., Yang, Y.H., Zhang, H., Shi, X.H., 2009. The influence of Late Triassic volcanism on the development of Chang7 high grade hydrocarbon source rock in Ordos Basin. *Geochimica* 38, 573–582 (in Chinese with English abstract).
- Zhang, W.Z., Yang, H., Xie, L.Q., Yang, Y.H., 2010. Lake-bottom hydrothermal activities and their influences on the high-quality source rock development: a case from Chang 7 source rocks in Ordos Basin. *Petroleum Explor. Dev.* 424–429 (in Chinese with English abstract).
- Zhang, W.Z., Yang, H., Yang, Y.H., Kong, Q.F., Wu, K., 2008. Petrology and element geochemistry and development environment of Yanchang Formation Chang 7 high quality source rocks in Ordos basin. *Geochimica* 37, 59–64 (in Chinese with English abstract).

检索工具	SCI-EXPANDED数据库	查证日期	2019年10月30日
署名作者	王成 陈多福	署名单位	中国科学院广州地球化学研究所
查证单位	长安大学图书馆	地址	西安市长安大学图书馆信息部 029-82334377
检索人	徐继维	审核人	徐 芳

标题: Petrographic and geochemical characteristics of the lacustrine black shales from the Upper Triassic Yanchang Formation of the Ordos Basin, China: Implications for the organic matter accumulation

作者: Wang, C (Wang, Cheng); Wang, QX (Wang, Qinxiang); Chen, GJ (Chen, Guojun); He, L (He, Long); Xu, Y (Xu, Yong); Chen, LY (Chen, Linying); Chen, DF (Chen, Duofu)

来源出版物: MARINE AND PETROLEUM GEOLOGY 卷: 86 页: 52-65 DOI: 10.1016/j.marpetgeo.2017.05.016 出版年: SEP 2017

Web of Science 核心合集中的 "被引频次": 6

被引频次合计: 7

使用次数 (最近 180 天): 3

使用次数 (2013 年至今): 43

引用的参考文献数: 118

摘要: The lacustrine black shales in the Chang7 Member from the Upper Triassic Yanchang Formation of the Ordos Basin in Central China are considered one of the most important hydrocarbon source rocks. However, the mechanism of organic accumulation in the black shales remains controversial. To resolve the controversy, with the former paleontological data of Yanchang Formation and sedimentation rate data of the Chang7 black shales, we investigated the typical intervals of the Chang7 black shales (TICBS) which were obtained by drilling in Yaowan at the southern margin of the Ordos Basin and performed various sedimentary, isotopic and geochemical analysis, including the sedimentary petrography, pyrite morphology, total organic carbon (TOC) and total sulfur (TS), the ratio of pyritic Fe to total Fe (DOPT), major and trace elements, together with pyritic sulfur isotopes (δ S-34(py)). The high sulfur content, enrichment of redox-sensitive trace metals, and the lower sedimentation rate of the TICBS in addition to the presence of marine spined acritarchs and coelacanth fossils indicate that the TICBS were deposited in a lacustrine environment possibly influenced by seawater. The petrographic observations show a thick layer of black shale with interlayers of thin layered siltstone (silty mudstone) and laminated tuff, which were related to the turbidity currents and volcanism, respectively. The U/Th, C-S, and Mo-U covariations, pyrite morphology, DOPT, combined with the δ S-34(py), suggest that the deposition occurred beneath the anoxic-sulfidic bottom waters, which was intermittently influenced by the oxygen-containing turbidity. The Ni/Al and Cu/Al possibly show extremely high to high primary productivity in the water column, which might be connected with the substantial nutrients input from seawater or frequently erupted volcanic ash entering the lake. In addition, the coincidence of an increased abundance of TOC with increased P/Al, Ni/Al, Cu/Al and U/Th, as well as relatively consistent Ti/Al suggest that the accumulation of the organic matter might be irrelevant to the clastic influx, and was mainly controlled by the high primary productivity and anoxic-sulfidic conditions. Further, the covariations of TOC vs. P/Al and TOC vs. Ba/Al indicate that the high primary productivity led to the elevated accumulation and burial of organic matter, while the anoxic to sulfidic conditions were likely resulted from an intense degradation of the organic matter during the early diagenesis. In summary, the organic matter accumulation is ultimately attributed to the high primary productivity possibly resulted from seawater or volcanic ash entering the lake. (C) 2017 Elsevier Ltd. All rights reserved.

入藏号: WOS:000411296600004

语言: English

文献类型: Article

作者关键词: Black shale; Organic matter accumulation; Primary productivity; Redox conditions; Sedimentation rate; Volcanic ash; Upper Triassic; Ordos basin

KeyWords Plus: SULFUR ISOTOPE FRACTIONATION; RARE-EARTH-ELEMENTS; APPALACHIAN BASIN; PYRITE FORMATION; SULFATE REDUCTION; SEDIMENTARY-ROCKS; OCEANIC ANOXIA; BARIUM FLUXES; TRACE-METALS; CARBON

地址: [Wang, Cheng; Wang, Qinxiang; He, Long; Chen, Duofu] Chinese Acad Sci, Guangzhou Inst Geochem, CAS Key Lab Ocean & Marginal Sea Geol, Guangzhou 510640, Guangdong, Peoples R China.

[Chen, Guojun; Xu, Yong] Chinese Acad Sci, Key Lab Petr Resources Res, Lanzhou 730000, Gansu, Peoples R China.

[Chen, Linying; Chen, Duofu] Shanghai Ocean Univ, Coll Marine Sci, Shanghai Engn Res Ctr Hadal Sci & Technol, Shanghai 207306, Peoples R China.

[Wang, Cheng; He, Long; Xu, Yong] Univ Chinese Acad Sci, Beijing 100049, Peoples R China.

通讯作者地址: Wang, QX (通讯作者), Chinese Acad Sci, Guangzhou Inst Geochem, CAS Key Lab Ocean & Marginal Sea Geol, Guangzhou 510640, Guangdong, Peoples R China.

Chen, DF (通讯作者), Shanghai Ocean Univ, Coll Marine Sci, Shanghai Engn Res Ctr Hadal Sci & Technol, Shanghai 207306, Peoples R China.

电子邮件地址: qinxiwang@gig.ac.cn; cdf@gig.ac.cn

出版商: ELSEVIER SCI LTD

出版商地址: THE BOULEVARD, LANGFORD LANE, KIDLINGTON, OXFORD OX5 1GB, OXON, ENGLAND

Web of Science 类别: Geosciences, Multidisciplinary

研究方向: Geology

IDS 号: FH6OM

ISSN: 0264-8172

eISSN: 1873-4073

29 字符的来源出版物名称缩写: MAR PETROL GEOL

ISO 来源出版物缩写: Mar. Pet. Geol.

来源出版物页码计数: 14

基金资助致谢:

We would like to thank Liang Qi from the Institute of Geochemistry, Chinese Academy of Sciences, for the major and trace metals analysis. This research was supported by the National Natural Science Foundation of China (41321002 and 41272144) and the scientific and technological project B of the strategic precursor, the Chinese Academy of Sciences (XDB10000000). We would like to extend thank you for improving the grammar of the manuscript by Prof. Harunur Rashid, the insightful comments and suggestions by Thomas Algeo and an anonymous reviewer, and Editor-in-chief Andrew Bell is highly acknowledged. This paper is Contribution No. IS-2394 from GIGCAS.

4种陕西省单矿物类中药资源及功效

张丽倩 胡海燕

(陕西国际商贸学院 陕西 西安 712046)

摘要:陕西省矿物药资源丰富,从矿物学角度分析可分为单矿物类、多矿物(岩石)类及含矿物类,其中单矿物类种类最多且应用最广泛,本文从地质学角度描述了4种陕西省矿物药资源类型及药用功效,以为矿物药入药提供依据。

关键词:矿物药资源;功效;陕西省

【中图分类号】O741+.2

【文献标识码】B

【文章编号】2236-1879(2017)08-0254-01

1 陕西省药用矿物资源形成的地质条件

在我国,矿物入药治病有两千多年的悠久历史,长期以来为人类的健康事业做出了重要贡献^[1-2]。药用矿物的形成或富集都是在特定地质作用的产物,它们的分布规律与地质构造、地层、岩浆活动、火山喷发及沉积作用密切相关,往往通过矿化区及矿化带明显的表现出来。陕西省属鄂尔多斯地台的一部分,南侧毗邻渭河断陷,秦岭东西褶皱带横亘中央,陕南跨扬子地台西北一隅。这种独具一格的地质构造基础,支配着本省药用矿物的地质分布规律。

2 陕西省药用矿物的类型及功效

关于药用矿物分类方法繁多,国内目前尚未统一,根据凡由地质作用和生物化学等作用形成的一些单矿物和多矿物组成的岩石及含有矿物成分的动物化石,能够单独入药或与其他植物药材、动物药材组方配伍在一起治疗疾病者,我们将其统称为矿物药材。根据矿物药材的矿物组成情况来看,大体分为三大类:单矿物药材、多矿物药材、含矿物药材。其中单矿物药材种类最多,应用最广。

2.1 自然铜。原矿物是黄铁矿,其化学成分为 FeS_2 。别名称为石髓铅、接骨丹、铜矿石。自然铜是地壳中分布最广泛的硫化物矿物,它可在各种地质条件下形成,所以它在自然界的成因类型和产状多种多样,本省自然铜的主要成因类型包括有沉积型、沉积变质型、岩浆型、热液型、火山型及斑岩型。自然铜属等轴晶系,晶体通常呈立方体、五角十二面体及八面体,集合体常呈粒状、致密块状及结核状。颜色呈浅铜黄色,条痕绿黑色,不透明,强金属光泽,无解理,性较脆,参差状断口,硬度6-6.5,比重4.9-5.2。

自然铜味苦,性平,微毒,其功效主要是散瘀、行血、止痛、续筋接骨折。历代中医外科多以自然铜为首药组方配伍,主治跌打损伤和骨折,疗效显著。还可治腋臭,聰耳明目,疗女人血气及心痛。

2.2 石膏。原矿物是石膏,其化学组成为 $\text{Ca}[\text{SO}_4] \cdot 2\text{H}_2\text{O}$ 。别名可称为大石膏、细理纹、寒水等。石膏主要是外生条件下化学沉积作用的产物,由溶解在内海及咸潮中的硫酸钙,在蒸发量很大的环境中结晶沉淀而形成,往往成巨大的矿层或透镜体存在于石灰岩、红色页岩及砂岩、泥灰岩、粘土岩之间,常与硬石膏、石盐等共生;在硫化矿床氧化带,原生硫化物矿物被氧化后生成硫酸水溶液,再与石灰岩质之围岩作用,可生成石膏,由这种方式形成的石膏,多赋存于氧化带的下部,以及原生矿石带的上部裂隙中;硬石膏经水化作用,亦可形成石膏。本省的石膏分布广泛,所赋存的地层,在陕北地区的第三系,关中地区的二叠系,陕南地区的三叠系,其中以赋存于三叠系地层中的石膏质量最好。石膏属单斜晶系,晶体呈板状、柱状,集合体呈纤维状及细晶粒状块体;颜色一般为白色、灰白色,也有无色透明的。但往往由于含其他杂质而被染成灰、浅黄、浅褐等色调。条痕为白色,透明,玻璃光泽,解理面现珍珠光泽,解理完全,性脆。硬度1.5-2,比重2.3。

石膏味辛、甘,性热寒,无毒。具有清热泻火、止渴除烦之功能。主治各种热性症,如皮肤热、中风寒热、口干舌焦、腹胀暴气、咽热、头痛发热、肺热咳嗽、口齿肿痛,除肠胃中结气,解肌发汗等。

2.3 白石英。原矿物为石英,别名又可称为水晶。石英是地壳中分布最广泛的矿物之一,在岩浆岩、变质岩和沉积岩中均有产出。但能作为药材用的是由伟晶作用和热液作用形成的比较完整的巨晶及晶簇状石英。本省各地均有出产,以商南、丹凤等地的花岗伟晶岩和潼关小秦岭地区含金石英脉中为最多。

石英,属三方晶系,单晶为六方柱发育,上、下两端出现多个三角形晶面,柱体晶面上常有水平线条。一般为致密块状或不规则粒状,无解理。断面为贝壳状或不平坦参差状,硬度7,比重2.65。颜色为白色或灰白色,透明至半透明,无色透明者称为水晶。

白石英味甘,性微温,主消渴不足、咳逆、胸膈间久寒。益气,除风湿痹。疗肺痨,下气。利小便,补五脏,久服轻身长年。镇心,治惊悸。益毛发,悦颜色。

2.4 滑石。药用滑石的原矿物并非都是矿物学上的单矿物滑石,其中有一部分是由高岭石或水云母等粘土矿物所组成的“类滑石”。矿物学上的滑石为含羟基的偏硅酸镁,属典型的热液蚀变型矿物。即是一种镁质岩石如超基性岩、白云岩、白云质灰岩在含 SiO_2 或 CO_2 的热水溶液作用下形成的。此外,在区域变质作用和接触变质作用中,也可以形成滑石。

高岭石和水云母(又称伊利石)均系粘土矿物,为含羟基的偏硅酸铝,属典型的风化产物。前者一般由长石、似长石及其他铝硅酸盐矿物风化而成的,且最适合于在缺乏碱金属和碱土金属的介质中形成;后者是由白云母风化而成的,而且是白云母遭受风化作用而转变成粘土矿物的中间过渡产物,可以在各种气候条件下和不同浓度的碱性介质中形成。

滑石在本省分布比较普遍,如略阳县的煎茶岭、马家山、金家沟等地,宁强县的婆婆沟、香树坪等地。

滑石($\text{Mg}_3[\text{Si}_4\text{O}_{10}](\text{OH})_2$),属单斜晶系,晶体呈假六方或菱形的片状,偶见。通常呈致密块状、叶片状、纤维状、放射状集合体。无色透明或白色,但因含少量杂质而呈现浅绿、浅黄、浅棕甚至浅红色,解理面上呈珍珠光泽。硬度1, $\langle 001 \rangle$ 解理完全,手触有滑腻感,薄片具挠性,相对密度2.82。

滑石味甘,性寒,具有清暑解热、渗湿利尿之功能。主治暑热烦渴,暑便不利,小便短赤等病。内服还能止泻并保护肠壁。外用治溃疡、湿疹、痱子等。

参考文献

[1] 赵学敏.本草纲目拾遗[M].人民卫生出版社,1998.

[2] 陈贵廷.本草纲目通释[M].学苑出版社,1992.

基金项目:陕西省教育厅项目;陕西省雄黄矿物药资源开发与研究;陕西国际商贸学院校级科研项目;雄黄矿物药资源开发与研究(SMXY201606)。

作者简介:张丽倩(1985—),女,河北乐亭人,讲师,硕士,主要从事矿物药相关教学、科研工作。

两种不同来源的矿物药石膏矿物学分析及鉴定

张丽倩¹, 刘养杰^{1,2}

(1. 陕西国际商贸学院, 陕西 咸阳 712046; 2. 西北大学, 西安 710069)

摘要: 目的 从矿物学角度, 对陕西省矿物药石膏产地西乡县及陕西省药材公司两种不同来源的石膏矿物药进行系列测试分析及鉴定, 以确定是否符合入药条件。方法 肉眼鉴定矿物学特征、X射线衍射、红外光谱、差热分析等进行了对比测试, 并综合前人X射线粉晶数据, 对其进行化学分析及光谱半定量分析。结果 2种不同来源的矿物药石膏矿物学特征相似, 陕西省西乡县所产矿物药石膏符合入药条件。结论 经对比, 笔者认为陕西省西乡县产出的石膏符合矿物药开发标准, 可作为矿物药资源进行开采。

关键词: 矿物药; 石膏; 矿物学; 分析; 鉴定

中图分类号: R284

文献标志码: A

文章编号: 1003-5699(2018)10-1206-03

Mineralogical analysis and identification of two different sources of mineral medicine gypsum

ZHANG Liqian¹, LIU Yangjie^{1,2}

(1. Shaanxi Institute of International Trade and Commerce, Xianyang 712046, Shaanxi Province, China;
2. Shaanxi Northwestern University, Xi'an 710069, China)

Abstract: Objective From the viewpoint of mineralogy, a series of test analysis and identification of Shaanxi province mineral medicine gypsum production in Xixiang county and Shaanxi Province medicine company from two kinds of gypsum mineral drug, to determine compliance with the conditions. Methods The mineralogical characteristics of naked eye were characterized by X-ray diffraction, infrared spectrum and differential thermal analysis. The X-ray powder crystal data were analyzed by chemical analysis and semi-quantitative analysis. Results The mineralogical characteristics of two kinds of mineral medicine gypsum were similar, and the mineral medicine gypsum produced in Shaanxi County of Xixiang province was in accordance with the medical conditions. Conclusion Through comparison, the author believes that the gypsum produced in Shaanxi County of Xixiang province conforms to the mineral drug development standard and can be used as mineral medicine resources for exploitation.

Keywords: mineral medicine; gypsum; mineralogy; analysis; identification

矿物药石膏, 药材名称为大石膏、细理石、软石膏、寒水、玉大石、白虎、冰石^[1,2], 始载于《神农本草经》, 列为中品, 主要成分为含水硫酸钙, 还含有锌、铜、铁、锰等丰富的微量元素^[3]。首载于《神农本草经》, 临床应用广泛而历史悠久^[3]。性大寒, 味甘辛, 有透表解肌之力, 具有清热泻水、除烦止渴等功效,

是最常见的矿物性中药之一^[6]。汉代张仲景在《伤寒论》中指出, 以石膏为主药, 将石膏30 g, 知母10 g, 甘草3 g, 粳米15 g熬制成白虎汤主治阳明热盛, 或温病热在气分证, 以达清热目的^[1]。现代临床中石膏也是退热必用中药之一^[2], 并且在治疗乙型脑膜炎等热性病也有较好的效果^[3,7]。药理研究成果颇丰^[8-9]。

基金项目: 陕西省教育厅2017年度专项科学计划(17JK0945); 校级重点科研项目(SMXY201606)。

作者简介: 张丽倩(1985-), 女, 讲师, 理学硕士, 主要从事矿物药等教学与科学工作。

笔者调研陕西省内主要药材市场发现,不同产地的矿物药石膏存在“此药非彼药”或成分不符等现象,主要原因因为不同产地的石膏含有的成分不一,需要对其进行矿物学分析、鉴定以判断是否符合入药条件。多采用X射线衍射、红外光谱及指纹图谱等方法^[10-13],也有部分学者根据不同地区在售的石膏矿物药化学成分进行质量评价探索^[14]。

笔者从陕西省主要产地西乡县及陕西省药材公司进行样品采集、测试,从矿物学角度,肉眼鉴定特征、光谱半定量测试、X射线衍射、红外光谱、差热分析等进行了对比测试分析及鉴定,并结合近年来的X射线粉晶数据,以判断陕西省西乡县矿物药石膏是否符合本省的药材市场入药条件,以期为资源开发提供些许参考。

1 矿物学肉眼鉴定特征分析

陕西省药材公司矿物药石膏的主要矿物学肉眼鉴定特征形态为长块状或不规则形态的扁平块状,少量为纤维状的集合体,粒径相差较悬殊。颜色为白色,由于内部含有少量的杂质而略带灰黄色调,略有透明度有影响,但仍以透明度高为特征,玻璃光泽,解理及纤维状集合体位置可见丝绢光泽,质地疏松易碎^[15]。陕西省西乡县矿物药石膏产地的主要矿物学肉眼鉴定特征形态为纤维状集合体^[16],即由针状单晶体呈放射状或纤维状组成。颜色为白色或无色,内部几乎未见杂质,透明度高,丝绢光泽,硬度可用指甲刻划,小于2,沿纤维状的延长方向及垂直方向略有差异。

2 对比测试分析

2.1 X射线衍射对比测试分析 为了明确陕西省西乡县矿物药石膏与陕西省药材公司矿物药石膏的差异,笔者首先对两种样品分别进行了X射线衍射技术测试,曲线图如图1、图2。由X射线衍射曲线可看出,陕西省药材公司的石膏占100%,曲线特征为7.595(10)、3.797(7)、3.062(7);西乡县矿物药石膏的特征为石膏占99%,曲线特征为7.880(10)、3.791(7)、3.062(9)。

2.2 红外光谱测试 笔者又分别对2个样品进行了红外光谱测试,测试结果基本与X射线衍射技术一致,2种矿物药质地均很纯净,几乎百分之百为石膏矿物成分,未见杂质元素对应的红外光谱特征。

陕西省药材公司石膏矿物药红外光谱图显示比例100%,3546、3403、1688、1621、1143、1116、668、598、465、312、230 cm⁻¹。

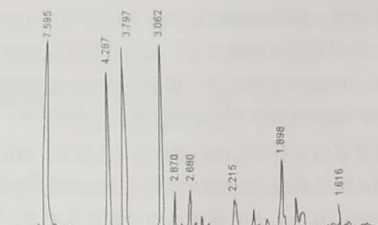


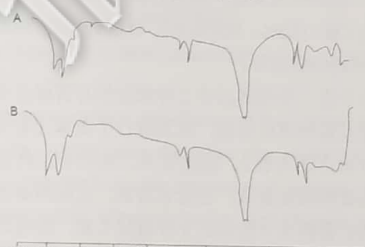
图1 陕西省药材公司矿物药石膏的X射线衍射曲线



图2 陕西省西乡县矿物药石膏的X射线衍射曲线

陕西省西乡县产出的石膏矿物药红外光谱图显示比例99%,3548、3401、3240、1689、1621、1143、1116、668、600、465、312、235 cm⁻¹。

同时结合近年来^[17]关于西乡县石膏的X射线衍射粉晶分析数据,也证明该地的石膏矿物药纯净程度较高,只含有极少量的杂质(详见表1)。



A: 陕西省药材公司采购样品; B: 陕西省西乡县产出样品

图3 2种石膏样品红外光谱图对比

表1 陕西省西乡县矿物药石膏的X射线粉晶数据

I	d	I	d	I	d
6	7.80	5	2.70	4	1.81
2	4.70	1	2.60	2	1.63
10	4.30	2	2.48	2	1.36
2	3.81	3	2.22	3	1.24
2	3.40	5	2.09	3	1.20
9	3.07	1	2.00	3	1.13
4	2.89	6	1.88		

注:数据来源于叶芳等《陕西矿物》,1985

2.3 差热分析测试 图4两种石膏样品的差热分析对

比曲线表明,陕西省药材公司石膏样品只在130℃出现了一个中等强度的吸热谷,其他位置未见明显的吸热效应,与炮制过程对于石膏的处理有一定关系;也可能与矿物药的保存不当导致轻微水化有关。

陕西省西乡县产出的石膏样品在140℃、180℃时出现明显吸热效应,且出现双谷特征,推测与天然产出,未经炮制,其中石膏生药中含有少量水分有关,也即石膏与硬石膏存在转化关系,导致在100℃之后其中的水分逸出不彻底,而在180℃时再次出现吸热谷。



A: 陕西省药材公司采购样品; B: 陕西省西乡县产出样品
图4 2种样品矿物药石膏的差热分析对比曲线

2.4 主量化学分析及微量元素光谱半定量对比分析 分别对2种不同来源的石膏样品进行化学成分分析,其中陕西省药材公司石膏样品主要化学成分基本与理论值一致,表现为CaO 32.3%、SO₄ 46.6%、H₂O 20.3%,陕西省西乡县产出的石膏样品所测的化学成分数据为CaO 32.2%、SO₄ 46.4%、H₂O 19.3%,相对含有约3.1%的杂质组分。

为了进一步明确其中2种来源的石膏样品中含有微量元素种类及含量,对其进行了微量元素光谱半定量分析,详见表2。由此可见,陕西省药材公司的微量元素种类较复杂,含量也较高,而陕西省西乡县产出的石膏样品只检测出2种微量元素,推测原因主要是陕西省药材公司的样品产地的地质环境与陕西省西乡县不同,导致元素的地球化学元素富集、分散程度有异,但2者均含有较多的Cu、Sr,可能与样品内含物相同有关,机械混入物中含有2种元素。

表2 2种不同来源矿物药石膏微量元素光谱半定量分析结果

样品来源	Cu	Sr	Ti	Pb	Ga	Mo	V	ppm
陕西省药材公司	15	800	<200	350	1	10	50	
陕西省西乡县产样	<5	200	-	-	-	-	-	

3 结论

近年来,中药的安全性问题备受关注^[18],尤其含重金属的矿物药安全引起科学界的广泛关注^[19]。笔者调研发现,近年来对含钙类矿物药进行了鉴定与分析^[20],

具体产地的石膏矿物药鉴定具有更深远的意义。综上所述,陕西省西乡县产出的石膏符合矿物药开发标准,可作为矿物药资源进行开采。

参考文献:

- [1] 喻嘉言.尚论张仲景伤寒论三百九十七法[M].北京:人民军医出版社,2011.
- [2] 杨柳,张义生,徐惠芳,等.矿物类中药石膏清热作用研究进展[J].中国药师,2016,19(10):1943-1945.
- [3] 王风霞.石膏的药性功效及临床应用文献整理研究[D].北京:北京中医药大学,2015.
- [4] 王建华.矿物药石膏中有害元素的研究[D].长沙:湖南中医药大学,2013.
- [5] 杨柳,张义生,徐惠芳,等.矿物类中药石膏清热作用研究进展[J].中国药师,2016,19(10):1943-1945.
- [6] 孙姝.石膏的药理作用与微量元素的探究[J].中国中医药现代远程教育,2009,7(5):170.
- [7] 祝之友.石膏古今临床应用解读[J].中国中医药现代远程教育,2017(9).
- [8] 龚传美,管喜义,周永良.生石膏煎剂的药理作用观察[C]/全国矿物药学术会议,1989.
- [9] 吕晓霞,郭春萍.中药矿物药研究及发展概况[J].吉林中医药,1997(3):42-43.
- [10] 张涵,李祥,陈建伟.药用石膏生、煅品与类似含钙矿物药X-衍射谱的比较[J].南京中医药大学学报,2009,25(1):42-45.
- [11] 闫晶.硫酸盐类矿物药红外指纹图谱研究[D].广州:广东药科大学,2016.
- [12] 李祥,李凡,刘元芬.中药石膏X射线衍射分析及指纹图谱的确定[C]/2006中国科协年会,2006:91-93.
- [13] 闫晶,曾柏琳,孟江等.石膏红外图谱鉴定研究[J].光谱学与光谱分析,2016,36(7):2098-2103.
- [14] 罗燕梅.市售中药石膏的鉴定及质量考察[J].中草药,2000(2):61.
- [15] 赵珊英,边秋娟,王勤燕.结晶学及矿物学[M].北京:高等教育出版社,2011.
- [16] 白学让.陕西省药用矿物[M].西安:陕西人民教育出版社,1992.
- [17] 叶芳,雷宗荣,周胜利,等.陕西矿物[M].陕西省地质矿产局西安测试中心,1985.
- [18] 朱葛馨,王丽霞,全小林.中药安全性研究[J].长春中医药大学学报,2015,31(1):32-34.
- [19] 韩炜.含矿物类中药制剂中砷的质量控制[J].云南中医学报,2017(4):98-102.
- [20] 梁素娇.六种常用含钙类矿物药鉴别分析[J].光明中医,2015,30(6):1349-1350.

(责任编辑:赵玉芝 收稿日期:2017-08-14)

- [18] 常青, 陈振江, 段丹. 四种胶类药材及蜂王浆的高效电泳鉴别[J]. 湖北中医药学院学报, 2006, 8(4): 15-17.
[19] 徐莹. 蜜蚕炮制前后蛋白质的差异研究[D]. 镇江: 江苏大学, 2016.
[20] Li C H, Zuo H L, Zhang Q, et al. Analysis of soluble proteins

in natural *Cordyceps sinensis* from different producing areas by sodium dodecyl sulfate-polyacrylamide gel electrophoresis and two-dimensional electrophoresis[J]. *Pharmacogn Res*, 2017, 9(1): 34-38.

自然铜矿物药的矿物学鉴定及成分对比

张丽倩¹、刘养杰^{1,2}

(1. 陕西国际商贸学院, 陕西 咸阳 712046; 2. 西北大学 陕西 西安 710069)

摘要: 目的 对自然铜矿物药进行矿物学鉴定并对比其成分。方法 结合外观及反光镜鉴定, 利用主要化学成分分析、微量元素光谱半定量、红外光谱、X射线衍射等不同技术进行矿物学测试分析。结果 外观鉴定显示矿物药自然铜实际矿物为黄铁矿, 反光镜显示反射率53%, 无内反射, 为均质体; 主要化学成分结果为Fe 46.6%、S 53.4%, 光谱半定量分析显示其中主要微量元素为Cu、Mo、Co、Yb、Mn、K, 与其它不同来源的样品微量元素的种类及含有量均有差异; X射线衍射显示蒲城县样品中黄铁矿含有量为100%; 与陕西省药材公司样品对比显示黄铁矿含有量为95%; 此外, 红外光谱曲线显示蒲城县样品中黄铁矿含有量95%以上; 陕西省药材公司样品中黄铁矿含有量95%。

结论 蒲城县伏头地区矿物药自然铜符合药材资源标准。

关键词: 自然铜; 矿物药; 矿物学; 鉴定; 成分对比

中图分类号: R284.1 文献标志码: B

文章编号: 1001-1528(2018)08-1863-04

doi:10.3969/j.issn.1001-1528.2018.08.045

矿物药自然铜, 别名石髓铅、接骨丹、铜矿石^[1-2], 矿物学归属问题仍存在较大争议, 可认为矿物药自然铜实际矿物成分为单矿物, 如自然铜^[3]、黄铜矿^[4-5]、黄铁矿^[6-7]; 也可认为矿物集合体, 如自然铜与黄铁矿混合物^[8], 自然铜、黄铜矿、赤铜矿、斑铜矿、黑铜矿等含铜矿物的混合物^[9]。随着矿物学测试技术的不断更新, 近年来关于矿物药自然铜的研究成果颇丰^[10]; 部分学者进行了自然铜辨析、成分测试及矿物学归属研究^[11-13]、中药炮制研究^[14-17]、药理分析^[18-20]、毒性分析^[21]。课题组发现对不同产地、来源的矿物药自然铜的鉴定及成分对比研究仍接近空白。

前期调研发现, 陕西省内自然铜矿物药产地包括白河县、华阴县等, 明确其矿物学归属、比较其中化学成分异同对于自然铜矿物药的质量评价具有一定的意义, 课题组分别采集了省内5个不同产地的自然铜样品, 同时购买了陕西省药材公司在售品。首先进行了简项化学成分分析、微量元素光谱半定量分析; 再根据矿产开采条件、初步药材质量评价选择蒲城县伏头地区样品进行详细的分析测试, 以期对陕西省内自然铜矿物药资源的合理开发与利用提供

参考。

1 仪器与材料

DX-2500X射线衍射仪(上海精密仪器仪表有限公司); BRUKER Tenser27型傅里叶变换红外光谱仪(德国BRUKER公司)。溴化钾为分析纯试剂; 自然铜矿物药购自陕西省药材公司, 由西北大学刘养杰教授鉴定为正品。

2 不同来源自然铜矿物药化学成分对比

2.1 化学成分测试 为了分析不同产地、来源的矿物药自然铜的矿物学归属, 课题组分别对陕西省药材公司在售品、蒲城县伏头地区、白河县里端沟、华阴县全堆城、略阳县煎茶岭及西乡县余家山6种不同来源的自然铜样品进行了主要简项化学成分测试(见表1)。结果显示主要化学成分为Fe、S, 除华阴县全堆城地区样品外, 其它杂质组分含有量均小于5%, 即矿物学中应归属为黄铁矿, 而非其它矿物。

2.2 光谱半定量分析 光谱半定量分析方法是利用原子发射光谱进行近似定量, 具有简单、快捷的特点, 上世纪90年代末到20世纪初在矿物药的成分测试中得到了较为普遍

收稿日期: 2017-09-18

基金项目: 陕西省教育厅2017年度专项科学计划(17JK0945); 陕西省雄黄矿物药资源的开发与研究、校级重点科研项目雄黄矿物药资源的开发与研究(SMXY201606); 宝石工艺技术创新团队(2018)

作者简介: 张丽倩(1985—), 女, 硕士, 讲师, 院长助理, 从事矿物药等教学与科学研究。Tel: (029) 33694428, E-mail: zlq1218@163.com

1868

表1 矿物药自然铜化学成分(%)

产地	Fe	S
陕西省药材公司	45.40	52.30
蒲城县伏头地区	46.60	53.40
白河县里端沟	45.50	51.30
华阴县全堆城	44.30	50.10
略阳县煎茶岭	45.20	53.50
西乡县余家山	44.80	52.70

的应用^[22-24]。课题组分别对6种矿物药自然铜进行了微量元素光谱半定量分析(见表2),结果显示不同产地、来源的矿物药种类及含有量均存在较大差异,其中蒲城县高阳乡某矿区的自然铜相对于陕西省药材公司的自然铜微量元素元

素种类接近,均含有Cu、Mo、Co、Mn、K,含有量略有差异。白河县里端沟、华阴县全堆城、略阳县煎茶岭及西乡县余家山的样品测试数据显示其与陕西省药材公司的微量元素存在较大差异,其中白河县里端沟样品中微量元素种类少,华阴县全堆城中微量元素种类多,而略阳县煎茶岭及西乡县余家山样品中只有2~3种微量元素。

3 矿物学外观鉴定及特征分析

调研发现,蒲城县伏头地区存在煤矿,具有良好的交通及矿产开采等条件、较大的自然铜资源开采前景。为了进一步明确其中的矿物组成,与陕西省药材公司在售品矿物组成的异同,课题组依次进行了矿物学外观鉴定及特征分析、X射线衍射及红外光谱测试。

表2 自然铜微量元素光谱半定量分析结果($\text{mg} \cdot \text{kg}^{-1}$)

来源	Cu	Zn	Pb	Sn	Cr	Ni	Mo	V	Co	Ag	Yb	Y
陕西省药材公司	35	500	60				15		150	7		5
蒲城县伏头地区	<5						15		10		15	
白河县里端沟	120	800	15	<10		120	5	<10	50	5	2	15
华阴县全堆城	10	100	20				1	10			3	15
略阳县煎茶岭							1 600	6 400				
西乡县余家山	1 810						1 284		1 080			
来源	Zr	As	Mn	Ti	Na	K	Bi	B	Nb	Ca	Mg	Al
陕西省药材公司	20	1 500	200	500	500	>10	20					
蒲城县伏头地区			<200			>10						
白河县里端沟	20			100								
华阴县全堆城		300	200	200	8 000		5	120	10	500	<100	1%
略阳县煎茶岭											10%	4.8
西乡县余家山												3.5

矿物学中自然铜成分应为Cu,含有少量或微量的Fe、Ag、Au、Hg等,完好晶体少见,主要为不规则树枝状、片状或纤维状集合体,物理性质为铜红色,表面常见黑色被膜,条痕铜红色,锯齿状断口^[25-28]。

而陕西省药材公司在售样品特征表现为规则立方体,表面平坦,青黄或表面棕褐色,断面亮白色;经西北大学刘养杰教授鉴定为黄铁矿(见图1),晶体以立方体为主,少量五角十二面体、八面体,集合体常呈粒状、致密块状、结核状,晶面可见平行条纹,且条纹方向与邻面垂直,浅铜黄色;反光镜下为亮白色,反射率53%,无内反射,见图2。

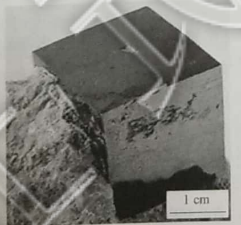


图1 自然铜外观特征

4 测试分析

4.1 X射线衍射 X衍射技术是研究物质物相和晶体结构



图2 自然铜反目镜下特征

的新方法之一,根据中药化学成分与其X射线衍射Fourier图谱的——对应关系,可实现对中药的鉴定^[29]。课题组阅读相关文献发现X射线衍射技术用于中药和中成药的鉴定具有较好的效果^[30]。仪器采用DX-2500X射线衍射仪;先将样品粉碎,过100目筛,压制为可供X射线衍射实验用的薄片样品。

实验条件采用定性扫描方式;工作电压为40 kV;工作电流为40 mA;扫描范围(2θ) 5° ~ 60° ;扫描速度为 $8^\circ/\text{min}$;步长为 0.02° ;预置时间为0.2 s。

X射线衍射曲线横坐标表示扫描范围 2θ ,纵坐标表示衍射强度I,结果见图3。陕西省药材公司在售的自然铜中黄铁矿含有量为95%,主要衍射线为2.704(10)、1.631(9)、1.912(8),褐铁矿5%,2.704(10)、4.156(8)、2.513(8);陕西省蒲城县某矿区所产自然铜中黄铁矿含有量为100%,主要衍射线为2.702(10)、1.630(9)、2.417(7)。

- [12] 李钢, 秦涛, 黄长高, 等. 矿物中药自然铜的组成与热稳定性研究[J]. 化学学报, 2009, 67(6): 466-470.
- [13] 李建芬, 徐方铭. 自然铜及其混淆品的鉴别[J]. 时珍国医国药, 2005, 16(4): 286.
- [14] 张亚敏, 何淑华, 牟树田, 等. 自然铜炮制品溶出成分与矿物组分探讨[J]. 中药材, 1993(10): 26-28.
- [15] 王静, 孟祥才, 陈玉义. 矿物中药自然铜煅制工艺研究[J]. 佳木斯大学学报(自然科学版), 2013, 31(3): 399-401.
- [16] 叶定江, 丁安伟, 蔡宝昌. 中药自然铜的炮制[J]. 中成药, 1980(1): 13-15.
- [17] 张志杰, 蔡宝昌, 李伟东, 等. 自然铜不同炮制品矿相及化学成分的研究[J]. 中草药, 2005, 36(6): 834-836.
- [18] 毛碧峰. 中药自然铜低频超声透入给药促进骨折愈合的实验研究[D]. 沈阳: 辽宁中医药大学, 2009.
- [19] 范思敏, 刘凤权. 中药自然铜功效本草考证[J]. 黑龙江中医药, 2000(4): 54-55.
- [20] 沈海葆. 铜类矿物药的应用概况[J]. 江西中医药, 1987(4): 58-59.
- [21] 孙波. 不同产地自然铜的元素分析及其毒性研究[D]. 南京: 南京师范大学, 2013.
- [22] 周晶, 陈刚, 张恢联, 等. 光谱半定量分析在微量物证检验中的应用[J]. 刑事技术, 2001(4): 45.
- [23] 白学让. 陕西省药用矿物[M]. 西安: 陕西人民教育出版社, 1992.
- [24] 刘墨庄, 赵霖, 许贵新, 等. 中药姜石矿物成分的研究[J]. 中国药学杂志, 1984(2): 54.
- [25] 潘兆橹. 结晶学及矿物学[M]. 北京: 地质出版社, 1993.
- [26] 赵珊琪, 边秋娟, 王勤燕. 结晶学及矿物学[M]. 北京: 高等教育出版社, 2011.
- [27] 李胜荣. 结晶学与矿物学[M]. 北京: 地质出版社, 2008.
- [28] 赵建刚. 结晶学与矿物学基础[M]. 北京: 中国地质大学出版社, 2009.
- [29] 裴汉幸. X衍射技术在中药鉴定中的应用新进展[J]. 中国药业, 2005, 14(7): 89-91.
- [30] 黄燕, 姚国菁. X射线衍射法在中药鉴定中的应用[J]. 山东中医杂志, 2004, 23(4): 232-234.

紫地榆不同提取物对脱矿牛切牙再矿化的影响

卢燕¹, 王丽梅^{1,2}, 杨淋¹, 蓝海¹, 杨晓莉¹

(1. 大理大学药学与化学学院, 云南大理 671000; 2. 大理大学第三附属医院, 大理州医院口腔科, 云南大理 671000)

摘要: 目的 探讨紫地榆不同提取物对脱矿牛切牙再矿化的影响。方法 先将牛切牙浸泡于脱矿液建立牙齿脱矿釉质模型, 测试硬度, 然后分别用紫地榆不同溶剂提取物、去离子水和氟化钠处理脱矿釉质, 最后用显微硬度仪测试各组牙齿的釉质表面硬度, 用扫描电子显微镜观察脱矿区表面。结果 紫地榆不同溶剂提取物对脱矿牛切牙有不同程度的影响。结论 紫地榆不同溶剂提取物能增强脱矿牛切牙硬度, 有再矿化作用。

关键词: 紫地榆; 牛切牙; 再矿化; 显微硬度; 扫描电镜

中图分类号: R284.1

文献标志码: B

文章编号: 1001-1528(2018)08-1871-04

doi:10.3969/j.issn.1001-1528.2018.08.046

随着生活水平的提高, 龋病越来越成为日常生活中困扰大家的疾病。2010年, 全球有超过50亿的人患过龋病^[1]。目前, 中国的龋病发病率高达70%~80%, 在婴幼儿中高达90%以上, 龋病防治工作迫在眉睫。牙体病损先发生脱矿, 再形成龋洞, 进而形成较严重的并发症^[1]。国内外对天然药物防龋研究较多, 但关于紫地榆防龋的研究鲜有报道。研究证实紫地榆的乙醇粗提物具有较好的抗龋活性^[2,3], 本实验将研究不同溶剂的紫地榆提取物对牛切牙硬度的影响, 为紫地榆防龋作用机制提供理论依据。

1 仪器与材料

303-A-I型电热恒温培养箱(萧山永发电器有限公司沪南实验室厂); 402MVD自动转塔数显显微维氏硬度计(依工测试测量仪器上海有限公司); ZQX-1全自动金相试样镶嵌机(苏州欧卡精密光学仪器有限公司); YMP-2B金相试样磨抛机(苏州欧卡精密光学仪器有限公司); BCD-193容声牌电冰箱(中国广东科龙电器股份有限公司)。氯化钾、乙醇、石油醚、乙酸乙酯、三氯甲烷、氟化钠、正丁醇(均为分析纯)。人工唾液KCl 0.4125 g、NaCl 0.4020 g,

收稿日期: 2017-12-25

基金项目: 国家自然科学基金(81260512)

作者简介: 卢燕(1993—), 女, 硕士生, 从事药理学研究。Tel: 17608725572, E-mail: 853048157@qq.com

*通信作者: 杨晓莉(1977—), 女, 副教授, 研究方向为药事管理。E-mail: yteacher@126.com

陕西省雄黄矿物药资源的开发可行性分析

张丽倩 王修杭

(1.陕西国际商贸学院 陕西 西安 712046;
2.陕西省宝石学实验教学示范中心 陕西 西安 712046)

摘要:本文旨在通过陕西省雄黄矿物药资源的浅谈,分析本省资源开发的可行性。

关键词:雄黄;矿物药资源;开发;可行性

【中图分类号】R282.7

【文献标识码】B

【文章编号】2236-1879(2017)08-0187-02

1 国内外研究现状和发展趋势

1.1 国外研究现状。随着里约奥运会的进行,中医中的“火罐”、“针灸”在国际运动场上展示出来,中医药文化引起国内外的广泛关注,一定程度上将推动我国中医、中药的发展。

矿物药指在中医药临床应用中可作为制作中成药或中药方剂的天然矿物或岩石^[1],包括天然矿物、岩石、生物化石等,以矿物为主。矿物药在中药资源中占据重要地位,在传统中医药治疗中已有几千年的历史。

调查发现,矿物药资源的开发与应用在韩国、日本等国家发展较快,其中雄黄矿物药资源的研究主要集中在药用价值,抗肿瘤作用,能抑制移植性小鼠肉瘤S-180的生长,并对细胞有腐蚀作用;杀虫作用;水浸剂对金黄色葡萄球菌、结核杆菌、变形杆菌不同程度的抑制作用等。相反,肠道吸收后能引起吐、泻、眩晕、惊厥甚至慢性中毒,损害肝、肾,氧化成为我们俗称的砒霜。传统风俗中,部分地区端午节会喝“雄黄酒”饮品,作为解毒剂或杀虫药。

1.2 国内研究现状。雄黄是中医内治外用常用药之一,最早收载于《神农本草经》距今已有几千年历史。雄黄又名石黄,其性辛温、味苦,有毒。2005年版《中国药典》收载含雄黄的中成药共26种,约占药典成方总数的4.6%。传统医学认为雄黄具有解毒、杀虫、燥湿、祛瘀、截疟等功能。自20世纪60年代以来,国内医者将含雄黄的复方制剂或单方用于治疗血液系统疾病、恶性淋巴系统疾病甚至实体瘤,取得了明显的治疗效果,引起人们广泛的关注。

1.3 研究述评。由于其研究涉及中医药学、地质学、药理学、化学等多个学科,而少有跨学科的学者相互渗透、配合研究,致使矿物药资源相关研究在国内近于止步不前。笔者走访西安周边药材市场发现,由于中药采集或销售人员矿物学知识的欠缺,导致出现较多“此雄黄非彼雄黄”的情况,即名称与矿物晶体不符、雄黄与共生矿物集合体共同销售等情况,从而导致隐患;同时,作为临床外用雄黄剂量合理性研究也存在着定量问题,炮制方法及毒性分析与矿物学特征联系存在不紧密的特点。本项目组成员想尝试通过对雄黄矿物药资源的矿物学、药理等基础特征进行研究,对其矿物学特征与药用紧密结合起来,进行充分、合理地开发与利用,为人类健康贡献一份力量。

2 研究内容及关键技术

2.1 研究内容。雄黄矿物药研究涉及中医药学、地质学、药理学、化学等多个学科,前人研究多仅从中药学角度出发进行研究,而少有跨学科的学者相互渗透、配合研究。调研发现,陕西省部分中药市场中,雄黄矿物药的销售出现混有类似矿物、共生矿物混合销售、产地不明确等情况,本项目成员既有矿物药研究人员、执业药师,又有地质学、矿物学研究人员,

通过交叉学科综合研究,从不同角度进行陕西省雄黄矿物药资源的开发与研究。

将主要从以下几个方面进行研究:

(1)调研陕西省内不同中药市场雄黄矿物药的销售现状:陕西省内中药市场大多集中在西安,通过走访不同的中药市场,调查雄黄矿物药资源的主要产地,购买不同中药市场的药品以备实验室进行矿物学测定、药理测试等,同时可确定雄黄矿物药的销售中是否存在名称与成分不符、与共生矿物混合销售等情况。

(2)野外调查陕西省不同雄黄矿物药产地的地质情况;对陕西省不同雄黄矿物药产地进行野外地质勘查,野外记录地层特征,采集样品以备后期测试不同产地雄黄矿物药的矿物学特征及药理对比。

(3)室内进行雄黄矿物学特征研究:通过电子探针、X射线衍射(XRD)、扫描电镜(SEM)、热重—差热分析(TG-DTA)、等离子发射光谱(ICP)等对陕西省不同产地的雄黄进行化学成分、晶体结构、物理性质、成因、产状等的综合分析。

(4)雄黄矿物药的炮制方法研究:应用水飞法炮制,观察炮制前后矿物学特征变化,如除去其中As₂O₃部分等。

(5)药理对比、分析:进行陕西省内不同雄黄矿物药产地、炮制前后等的药理对比分析。

2.2 关键技术。前期需要进行走访陕西省不同中药市场进行调研并深入不同雄黄矿物药产地进行野外地质勘查;室内实验室测试主要通过目前矿物学测试的先进方法,电子探针、X射线衍射(XRD)、扫描电镜(SEM)、热重—差热分析(TG-DTA)、等离子发射光谱(ICP)等对陕西省不同产地的雄黄进行化学成分、晶体结构、物理性质、成因、产状等的综合分析;水飞法炮制测试不同产地的雄黄,并对比陕西省不同产地及炮制前后雄黄矿物药的药理学特征。

3 技术方案

3.1 调研。包括市场调研和野外地质勘查技术。市场调查主要针对陕西省不同中药市场进行雄黄矿物药资源的销售情况;野外地质勘查主要指陕西省不同雄黄矿物药产地的地层特征勘查、记录及分析;同时采集样品以备后期测试不同产地雄黄矿物药的矿物学特征及药理对比。

3.2 室内进行雄黄矿物学特征研究。通过电子探针、X射线衍射(XRD)、扫描电镜(SEM)、热重—差热分析(TG-DTA)、等离子发射光谱(ICP)等对陕西省不同产地的雄黄进行化学成分(主量元素、微量元素)、晶体结构、物理性质、成因、产状等的综合分析。

3.3 雄黄矿物药的炮制方法研究。应用水飞法炮制,观察炮制前后矿物学特征变化,如除去其中As₂O₃部分等。

4 项目的研究基础 (下转第190页)

陕西省凤县铅硐山矿物药礬石矿物学 鉴定及分析*

张丽倩¹,刘养杰^{1,2}

(1.陕西国际商贸学院,陕西 咸阳 712046;

2.西北大学,陕西 西安 710069)

[摘要] 目的:应用不同鉴定技术鉴定及分析陕西省凤县铅硐山矿物药礬石的矿物学成分。方法:利用主要化学成分分析、微量元素光谱半定量、红外光谱、X射线衍射、X射线粉晶数据等测试技术对矿物药礬石进行鉴定。结果:主要化学分析(重量百分比)为Fe 36.63%, As 32.01%, S 31.75%;微量元素主要为Zn、Pb、Ag、Co、Nb、Cu、Ni等,杂质含量微弱,符合药材要求;红外光谱分析表明,礬石成分纯净,几乎百分百为毒砂;X射线衍射曲线表明,主要衍射线均为2.674,2.433,主要矿物为毒砂;X射线粉晶分析结果基本一致,成分纯净。结论:陕西省凤县铅硐山矿物药礬石实则为矿物学中的毒砂。

[关键词] 矿物药礬石;陕西;凤县;铅硐山;矿物学鉴定;分析

[中图分类号] R284 [文献标识码] A [文章编号] 1672-951X(2018)16-0044-03

The Mineralogical Identification and Analysis of Mineral Medicine
in Qiandongshan of Feng County Shaanxi Province

ZHANG Li-qian¹, LIU Yang-jie^{1,2}

(1.Shaanxi Institute of International Trade and Commerce of Geosciences, Xianyang Shaanxi 712046, China;

2.Shaanxi Northwestern University, Xi'an Shaanxi 710069, China)

[Abstract] Objective: To test different identification technology and identification of poisonous Stone mineral medicine to determine the mineralogical composition. Methods: The main chemical composition analysis, trace element spectrum semi quantitative, infrared spectroscopy, X-ray diffraction, X-ray powder diffraction data of different test technology for mineral medicine. Stone was identified. Results: The main chemical analysis (weight percentage) for Fe 36.63%, As 32.01%, S 31.75%, trace elements are mainly Zn, Pb, Ag, Co, Nb, Cu, Ni etc., the impurity content is weak, with medicinal requirements; infrared spectral analysis showed that the composition of pure stone, almost 100% of arsenopyrite; X-ray the diffraction curve shows that the main diffraction were 2.674 and 2.433, the main mineral is arsenopyrite; X-ray powder analysis results are basically consistent, pure elements. Conclusion: The stone is a solid mineral drug, the mineralogy of arsenopyrite.

[Keywords] mineralogical stone; Shaanxi; Feng county; Qiandongshan; mineralogical identification; analysis.

礬石,又称苍石、白礬石,为陕西省矿物药资源种类之一。从矿物学归属上,大多学者将其归属于硫化物类,但在历代本草记载中^[1-4]尚有歧义,《证类本草》和《本草纲目》所载经文内容略异^[5],一种认为礬石即矿物学中的毒砂,化学成分为FeAsS,也有一种说法认为礬石是天然外生地质作用下形成的砷类矿物的沉淀,主要是由于毒砂形成之后受到地表氧化

作用,产出白色的氧化膜,化学成分为As₂O₃,俗称白礬石,实际在矿物学中两者成因具有紧密联系。传统说法也存在将礬石作为“五毒之药”组成之一^[6]。前人对其药理研究成果颇丰,我国首先应用砷剂治疗龋齿,且到目前为止,口腔科方面用砷剂失活牙髓,还被以苏联为首的许多国家在应用着^[7];早在汉代就有“匈奴使用毒药”,将“礬石、桂子、附子、干姜各二

*基金项目:陕西省教育厅2017年度专项科学计划(17JK0945);陕西省雄黄矿物药资源的开发与研究;校级重点科研项目:雄黄矿物药资源的开发与研究(SMXY201606)

两,上四味末之,蜜丸如梧子”用于治疗寒症等^[7-8]。但由于其中含有砷,在汉以前主要以其毒鼠^[9-10],而在中药或中成药的使用过程中也需特别注意。

笔者走访了陕西省西安市几个规模较大的中药市场,经初步调研发现,多数销售者认为在售碧石为由毒砂提炼之后,经炮制形成的砒石。李时珍^[11-12]曾云“砒,性猛如貔,故名。唯出信州,故人称之为信石,而又隐信字为人言”。而信石依据颜色及其它特征可分为两种,一种典型特征为红色晕彩效应,称红信石,又称红砒,形态以块状集合体为主,颜色为白色略带黄色调,不透明-微透明,丝绢光泽,有毒;一种为无色至白色,白信石,又称白砒,形态以块状集合体为主,透明度低,但相对红信石偏高,半透明-微透明-不透明,具较强的玻璃光泽或丝绢光泽,脆性高,毒性相对更高。

目前市场上在售的碧石仍存在一些不确定因素,主要是成分、矿物学鉴定特征及地质学成因等,因此,笔者取样于陕西省碧石矿物药代表产地之一—凤县铅硐山,进行了矿物学肉眼鉴定、主要化学成分及微量元素光谱半定量分析、红外光谱、X射线衍射及X射线粉晶等测试,从矿物学角度确定了碧石的成分。

1 样品来源

陕西省矿物药碧石产地凤县铅硐山,经西北大学刘养杰教授进行肉眼鉴定。

2 矿物学肉眼鉴定特征

碧石在放大镜($\times 10$)下肉眼鉴定特征,单晶体多为柱状、短柱状、棒状或针状,延长方向为c轴或少量为b轴,集合体为粒状集合体或致密块状集合体,粒径多为0.1~1 mm,晶面可见平行条纹,部分可见十字双晶或星状三连晶。颜色为锡白色、铁灰色,部分因表面氧化而呈浅黄锖色,条痕为灰色-黑色,略带紫色或褐色调,不透明,金属光泽,莫氏硬度5.5~6,解理{101}中等-不完全,{010}不完全,常见参差状断口,比重5.9~6.29,性脆,有臭味,灼烧后具有磁性^[13]。(见图1)



图1 放大镜下碧石特征($\times 10$)

反目镜下鉴定特征为白色-乳黄色的反射色,反射率为50%左右,双反射清晰,多色性为白色-粉红黄色,内反射无,显示较强的非均质特征,偏光色为深蓝-红棕色。(见图2)



图2 反目镜下碧石特征

3 光谱半定量分析

光谱半定量分析方法是利用原子发射光谱进行近似定

量,具有简单、快捷的特点,因此,在矿物药的成分测试中得到了较为普遍的应用^[14-16]。

理论上,碧石主要化学成分为FeAsS,计算可得重量百分比值为Fe 34.30%, As 46.01%, S 19.69%。实际前人研究发现,不同产地的碧石化学成分略有差异,主要原因因为类质同象或机械混入物^[17]。经测试,陕西省凤县铅硐山碧石主量元素成分(重量百分比)为Fe 36.63%, As 32.01%, S 31.75%, 微量元素主要为Zn、Pb、Ag、Co、Nb、Cu、Ni等。(见表1)

表1 陕西省凤县铅硐山碧石微量元素光谱半定量分析结果(%)

元素	Cu	Zn	Pb	Sn	Ni	Mo	V	Co	Ag	Nb	Yb
数据	0.0015	3	1.1	0.0002	0.001	0.0001	0.0015	0.0005	0.005	0.002	0.0007

微量元素测试分析结果显示,与碧石主要成分中Fe易发生类质同象的元素Ni、Co含量明显高于其它元素,而易产生机械混入物的Cu、Zn、Pb、Ag也含量较高。这与凤县铅硐山特殊的地质条件有关。

铅硐山地区富集铅锌矿床,其中碧石呈浸染状产于中泥盆统古道岭组的白云岩和石英岩中,与黄铁矿、黄铜矿、石英、铁白云石、磁黄铁矿等矿物共生或伴生。因此,在矿物药采集过程中极易将这些矿物中富集的Zn、Pb等混入而造成杂质。

4 其它测试分析

由于矿物药的研究涉及矿物学、中医学、化学等多学科交叉,因此,矿物类中药在中药鉴定研究中仍处于薄弱环节。传统的性状鉴别方法难以满足矿物类中药鉴别的需要,因此,需要用有效的现代技术手段对矿物药进行系统的鉴别研究^[18]。各类分析技术手段在地矿、环保、地球物理等领域获得广泛应用,为矿物药分析提供了可供借鉴的经验^[19]。在矿物学肉眼鉴定之外,笔者采用了红外光谱、X射线衍射、X射线粉晶衍射3种技术,对陕西省凤县铅硐山地区所产矿物药碧石进行分析测试,以期准确测定矿物成分。

4.1 红外光谱分析 红外光谱分析在中药质量控制中的重要作用^[20],实验证明不同品种的矿物中药,其红外图谱具有不同特征的吸收峰及谱带,应用红外光谱法可鉴别不同品种的矿物药及矿物药炮制品,还可鉴别矿物药的真伪、优劣,此方法简单快速准确,有很好的应用价值^[21]。

测试仪器为傅立叶变换红外光谱仪,以中红外波段(200~1600 cm⁻¹)对陕西省凤县铅硐山地区所产矿物药碧石进行分析测试。样品制备过程主要为用玛瑙研钵对碧石矿物药样品进行研磨,研磨过200目筛,精密称定1 mg溴化钾优级纯,研磨过200目筛,干燥,精密称定100 mg,取精密称定后的碧石1 mg,与精密称定后的溴化钾100 mg研匀,压制成透明的薄片待用。红外光谱测试发现光谱图较标准,显示碧石矿物成分几乎全部为毒砂,含量接近100%,微量元素含量几乎可忽略不计。(见图3)

4.2 X射线衍射测试 X衍射技术是研究物质物相和晶体结构的一种新方法,根据中药化学成分与其X射线衍射Fourier图谱的一一对应关系,可实现对中药的鉴定^[22]。笔者在阅读前人相关文献过程中发现,X射线衍射技术不仅可用于各植物类、动物类、矿物类中药的鉴定^[23],还可用于中药和中成药的鉴定^[24],从而对中药及中成药的质量控制领域有着广泛的应用,由于其准确、简便、可靠而得到相关学者的青睐。

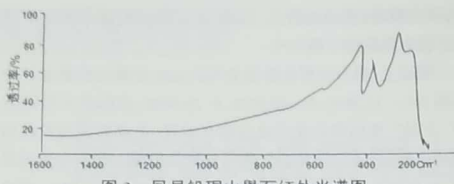


图3 凤县铅硐山碧石红外光谱图

仪器采用DX-2500X射线衍射仪;首先将样品粉碎,过100目筛,压制为可供X射线衍射实验用的薄片样品。实验条件采用定性扫描方式,工作电压:40 kV,工作电流:40 mA,扫描范围(2θ):5°~60°,扫描速度:8°/min,步长:0.02°,预置时间:0.2 s。X射线衍射曲线横坐标表示扫描范围2θ,纵坐标表示衍射强度I_r,结果主要衍射线均为2.674、2.433,次级衍射线为3.650、1.943、1.813、1.631、1.319,显示与红外光谱测试结果一致,主要矿物为毒砂。(见图4)

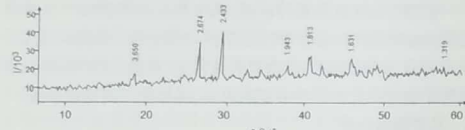


图4 凤县铅硐山碧石X射线衍射曲线

4.3 X射线粉晶衍射分析 X射线粉晶衍射分析一般与其它测试手段结合进行矿物分析、鉴定^[2],对研磨成粉末的多晶样品进行X射线衍射分析。为了进一步测试碧石矿物学纯净程度,笔者又对样品进行了X射线粉晶衍射分析,样品研磨成200目以下的粉末0.2 g,手摸无颗粒感,用玻璃板压实、压平于样品板凹槽,呈10 mm的方块,厚度约5 mm,与样品板平面保持一致。结果显示与前几种测试一致,几乎全部为纯净的毒砂矿物。(见表2)

表2 凤县铅硐山碧石X射线粉晶数据

X射线强度	晶面间距(Å)	X射线强度	晶面间距(Å)	X射线强度	晶面间距(Å)
4	3.62	8	1.817	2	1.275
1	3.31	2	1.750	5	1.220
1	3.11	2	1.685	1	1.190
2	2.93	6	1.630	2	1.165
2	2.82	2	1.610	1	1.130
9	2.67	2	1.548	4	1.109
1	2.54	2	1.525	3	1.070
10	2.44	1	1.480	2	1.051
10	2.41	1	1.427	3	1.043
2	2.19	1	1.400	1	1.030
2	2.10	2	1.380	1	1.020
2	2.00	6	1.347	4	1.006
1	1.945	2	1.298		

5 结 论

利用主要化学成分分析、微量元素光谱半定量、红外光谱、X射线衍射、X射线粉晶数据等不同测试技术对矿物药碧石进行鉴定,主要化学分析(重量百分比)为Fe 36.63%,As 32.01%,S 31.75%,微量元素主要为Zn、Pb、Ag、Co、Nb、Cu、Ni等,杂质含量微弱,符合药材要求;红外光谱分析表明碧石成

分纯净,几乎百分百为毒砂;X射线衍射曲线表明主要衍射线均为2.674、2.433,主要矿物为毒砂;X射线粉晶分析结果基本一致,成分纯净。结合前人及笔者测试综合发现,矿物药碧石实则为矿物学中的毒砂。

参考文献

- 王筠默.《神农本草经》中的碧石考释[C].全国药学史本草学术会议,2007.
- 赵学敏.本草纲目拾遗[M].北京:人民卫生出版社,1983.
- 陈贵廷.本草纲目通释[M].北京:北京学苑出版社,1992.
- 黄泰康.现代本草纲目[M].北京:中国医药科技出版社,2001.
- 张振平.《周礼》中的“祝药刷杀之齐”与“祝当为注”[J].山东中医药大学报,1983,7(4):52~53.
- 周大成.我国首先应用砷剂治疗牙齿的历史[J].中医杂志,1955(12):58.
- 吴莎日娜,巴根那,白梅荣,等.蒙药及其复方的基础研究进展[J].北方药学,2010,7(3):24~28.
- 李今庸.读《神农本草经》札记[J].中医药通报,2013,12(6):10~13.
- 李月.中国古代毒鼠药研究[D].南宁:广西民族大学,2014.
- 黄喻情.含砷矿物药的毒性和使用注意[J].养生保健指南,2017(16):267.
- 谢建军,李钟文,盛展能.砒石与石药用变迁之我见[J].中药材,1987(1):50~52.
- 郭欣林.形形色色“矾药”功效各具千秋[J].东方药膳,2013(5):48.
- 潘兆橹.结晶学及矿物学[M].北京:地质出版社,1993.
- 周晶,陈刚,张恢联,等.光谱半定量分析在微量物证检验中的应用[J].刑事技术,2001(4):45.
- 刘养杰.陕西淳化阎家沟“白血脂”矿物药材研究[J].西北大学学报:自然科学版,1994,24(3):257~260.
- 王雪莹,姚修仁,刘墨庄,等.中药姜石成分的研究[J].中国中药杂志,1983,8(4):28.
- 白学让.陕西省药用矿物[M].西安:陕西人民教育出版社,1992.
- 黄必胜,袁明洋,陈科力.X射线衍射技术在矿物类中药鉴定中的研究进展[J].中国现代中药,2013,15(11):917~921.
- 林瑞超.矿物药检测技术与质量控制[M].北京:科学出版社,2013.
- 闫蔚,王淑美,梁生旺.矿物药的红外光谱分析研究[C].中华中医药学会第八次中药分析学术交流会,2015.
- 曹先兰,李维贤,李菲等.矿物中药鉴定的新方法—红外光谱法的应用[J].中成药,1990,12(10):11~13.
- 裴汉幸.X衍射技术在中药鉴定中的应用新进展[J].中国药业,2005,14(7):89~91.
- 黄燕,姜国青.X射线衍射法在中药鉴定中的应用[J].山东中医杂志,2004,23(4):232.
- 林瑶,路峰,李芬香,等.X射线粉晶衍射法在岩矿鉴定中的应用[J].科技视界,2016(17):230~231.

(收稿日期:2017-07-18 编辑:刘颖)

关于张丽倩等同志的
《陕西省旬阳县公馆地区朱砂矿物药的矿物学鉴定及成分
对比研究》等学术论文
被采纳的证明

陕西国际商贸学院张丽倩、刘养杰等同志撰写的《陕西省旬阳县公馆地区朱砂矿物药的矿物学鉴定及成分对比研究》《陕西省蒲城县伏头地区自然铜矿物药的矿物学鉴定及成分对比研究》《陕西省凤县铅硐山矿物药礫石矿物学鉴定及分析》《两种不同来源的矿物药石膏矿物学分析及鉴定》《陕西省雄黄矿物药资源开发可行性分析》《4种陕西省单矿物类中药资源及功效》等矿物药论文，提交到桓台城区橘源堂中医诊所（市级非物质文化遗产重点保护示范基地）等单位后，受到了单位的采用，并进行矿物药的药理探究与治疗实施，同时指导了郑雯乐等同学实施了陕西省大学生创新创业项目“矿物药智能珠宝”，尝试将各种具有不同功效的矿物药应用于珠宝首饰等保健产品中。

实践证明，陕西国际商贸学院张丽倩等同志关于矿物药的学术论文对于省内外中药行业的发展起到了一定的理论参考价值和实践作用。

特此证明。

公章

日期：2019年10月17日



正式审批材料

陕西省教育厅专项科研计划项目结题证书

(编号: 陕教科结字第 17190230 号)

陕西国际商贸学院:

你校报来的省教育厅科研计划项目: 陕西省雄黄矿物药资源的开发与
研究

结题材料收悉。经审查, 符合《陕西省教育厅科研计划项目管理办法》有关结题
的要求, 同意结题, 特发此证。

项目 编 号: 17JK0945

项目 起 止 时 间: 2017-01-01 至 2019-01-01

项 目 负 责 人: 张丽倩

项 目 组 成 员: 刘养杰, 周蕊, 韦乐乐, 张辛未, 杨蓉, 胡海燕

项 目 合 作 单 位:

批 准 经 费: 2.0 万元



说明 1、本证书由省教育厅科学技术处统一印制, 加盖“陕西省教育厅科研计划项目结题专用章”后生
效。
2、每个项目结题证书一式三份, 省教育厅、学校、课题组各一份。

关于张丽倩等同志的
《陕西省旬阳县公馆地区朱砂矿物药的矿物学鉴定及成分
对比研究》等学术论文
被采纳的证明

陕西国际商贸学院张丽倩、刘养杰等同志撰写的《陕西省旬阳县公馆地区朱砂矿物药的矿物学鉴定及成分对比研究》《陕西省蒲城县伏头地区自然铜矿物药的矿物学鉴定及成分对比研究》《陕西省凤县铅硐山矿物药礫石矿物学鉴定及分析》《两种不同来源的矿物药石膏矿物学分析及鉴定》《陕西省雄黄矿物药资源开发可行性分析》《4种陕西省单矿物类中药资源及功效》等矿物药论文，提交到淄博橘源血管病研究所（市级非物质文化遗产重点保护示范基地）等单位后，受到了单位的采用，并进行矿物药的药理探究与治疗实施，同时指导了郑雯乐等同学实施了陕西省大学生创新创业项目“矿物药智能珠宝”，尝试将各种具有不同功效的矿物药应用于珠宝首饰等保健产品中。

实践证明，陕西国际商贸学院张丽倩等同志关于矿物药的学术论文对于省内外中药行业的发展起到了一定的理论参考价值和实践作用。

特此证明。



正式审批材料

2018 “微软”创新杯

大学生创新创业大赛

商业策划书

所 属 学 校 陕西国际商贸学院

参 赛 项 目 名 称 矿物药智能珠宝

指 导 教 师 张丽倩

项 目 负 责 人 郑雯乐

负 责 人 电 话 17719679249

第一章 执行总结

1.1 项目背景

随着高新科技的不断发展，可穿戴的智能装备也逐渐进入了消费者视野之中，人们在意穿着打扮，更在意健康。智能手环并不稀奇，但是具有珠宝、中药和智能结合起来的宝贝一定能吸引人的眼球。

另一方面，珠宝行业作为我国改革开放的新兴行业，今年的发展也是不容乐观。变则通，通则兴。珠宝行业与可穿戴智能装备的联姻是两大行业的改革性创举。

1.2 项目规划

本项目工作主要分为以下三部

前期，各种原材的准备。对于珠宝样式的设计、具有保健、治疗功能的矿物药首饰原材料的收集。

中期，对于产品的宣传，设计理念的推广，已期吸引更多的投资方。

后期，对于产品售卖的，以及对于产品实时反馈跟踪，以及对售后的规划。

1.3 市场分析

随着改革开放进一步深化，我国居民对于健康养生的需求，对与高档耐用的宝石玉石的需求都将空前增大。其次市场已有的的智能可穿戴装备都已趋于雷同化，单调化。珠宝行业市场中一是急缺创意产品，另外就是具有保健、治疗功能的珠宝产品，随时能观测身体情况的珠宝首饰更是少见。

1.4 行业竞争分析

首先，项目的新颖性。随着互联网加的不断深入，各行各业都再与互联网积极的联姻，可穿戴智能装备已然成为了各方积极抢占的新兴市场，但从已有市场来看目前的可穿戴智能装备仅局限于手环，手表等装备。其美观性，耐用性远不及珠宝首饰。其次珠宝玉石的天然理疗功效也是我们该系列的另一大卖点，矿物药也蕴含了深厚的传统中医药文化。

另一方面，智能手环并不等同于我们的产品，我们要在智能手环基础上研发更综合的功能。

1.5 财务分析

前期对于芯片供应的洽谈、珠宝原材料的取材，中期对于产品的宣传包装，

后期对于珠宝学生加工的雇佣费用。

1.6 风险分析

财务风险: 在产品线建立初期，由于一切都是从零开始，难免会遇到资金周转不灵的情况，从而引发经营危机。一方面我们要积极开展业务，获得收入，提高资金周转率。另一方面我们会尽可能的节约成本，减少不必要消费。面临流动资金不足的困难局面，造成经营困难，引发各类危机。一方面，我们会做好财务计划，减少坏账、呆账，提高资金周转率。另一方面，我们会提升服务质量，做充分的市场推广，增加收入，争取利润最大化。

客户风险: 智能珠宝的理疗功效是否能达到客所期望值，产品的使用寿命都是我们潜在的致使客户流失的风险因素。

经营风险: 在经过短期的竞争空白期后，我们如何应对极大的竞争压力，如何提前抢占市场，使消费者在短时间内信任我们。是我们将面临的不可忽视的经营风险。

第二章 项目简介

2.1 项目概述

订制珠宝与智能健康相结合，在衬托出佩戴者优雅高贵的同时点缀出更科技化人性化的光辉。集矿物药的保健、治疗功能、珠宝的奢华感、天然矿物晶体的创意设计、智能检测健康情况为一体，再添加智能时代的科技感。将现有珠宝（戒指，项链等）进行精加工内置智能芯片，连接手机 APP，实现珠宝与人的深度交互，由佩戴者的心率，脉搏运动轨迹，消耗能量等测量手段提醒佩戴者保持身体健康。

2.2 项目服务及业务简介

服务对象主要定位中高等收入人群。

力求在满足消费者审美需要增进更多智能元素，创新出珠宝人性科技健康元素。使珠宝不仅仅有美观作用，更有健康的疗效。

在珠宝学院的基础上可以完成珠宝首饰的镶嵌及加工，芯片及 App 的开发则与现在市面上的检测公司合作用已经成熟的技术将二者合二为一。

售卖则会通过线上线下两期宣传，共同售卖

2.3 发展规划

运用网络自媒体等互联网技术进行宣传，其次，通过与顾客交流进行私人定制，严格按照顾客的意愿进行加工，确保审美效果的独一无二，而且需要与开发芯片公司精诚合作，对顾客保障产品质量及功能寿命，还要适当透明加工流程以优势价格赢得顾客，最后要有良好的售后服务。

第三章 市场与竞争分析

3.1 市场现状

当前，我国国民身体素质不高、生活压力大，人们基本都处于亚健康状态，因此保健及健康监测类商品受到了人们的热捧，而且由于我国经济的迅速发展到本世纪中叶，我国将进入中等发达国家行列。人们越来越重视养生，养生类产品也较为火爆，市场需求巨大。但是，此类绝大多数产品只以保健或养生监测为主题，忽视顾客的审美需求，也就是说保健监测类产品与审美需求完全脱节，而宝石拥有耐久、美观等优点人们普遍喜爱佩戴，所以市场需要将两者进行有机结合，以适应更多的受众群体。

3.2 市场前景

我国国民身体素质仍呈下降趋势，而且中老年人比重不断攀升，据民政部门权威信息显示，到 2020 年，老年人口将达到 2.48 亿，加之我国环境前景并不乐观，所以高血压、脂肪肝等慢性疾病及各种心脑血管疾病会成为困扰大部人群的问题并且随着我国经济的迅速发展，到本世纪中叶，我国将进入中等发达国家行列。国民生活水平不断提高，在物质较为丰富的情况下人们越来越重视自己的生活方式是否健康，也更追求生活品质、追求美的享受，所以该产品集保健监测和审美功能于一身，因而有巨大前景。

3.3 目标市场

目标市场定位在中高等收入人群。

3.4 市场营销策略

通过网络自媒体等互联网技术进行宣传，其次，通过与顾客交流进行私人定制，严格按照顾客的意愿进行加工，确保审美效果的独一无二，而且需要与开发芯片公司精诚合作，对顾客保障产品质量及功能寿命，还要适当透明加工流程以优势价格赢得顾客，最后要有良好的售后服务。

3.1 竞争分析

服务优势：高科技互联、以使用者需求为导向的设计，力求做到审美效果的独一无二，给顾客高级的审美享受

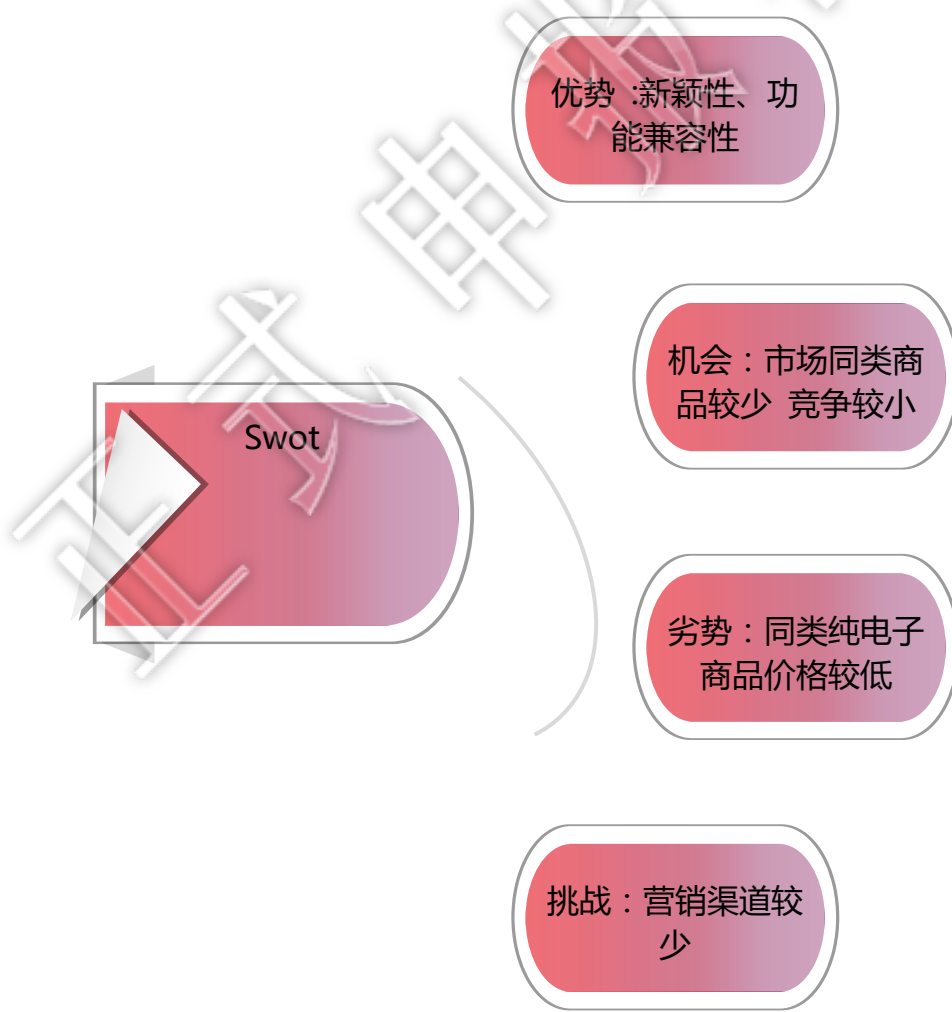
功能兼容优势：通过宝石与芯片的有机结合 将审美需求与健康监控相结合 做到比同类型商品的多元化功能性优势既给顾客提供健康监测又有审美价值。

价格优势：发挥我校宝玉石专业优势，通过自主选材及加工以降低成本，发挥价格优势。

第四章 运营分析

4.1 生产组织

4.2 质量控制



产品效果保证，有限起到检测作用，质量坚固，不宜损坏。

4.3 组织管理

总经理——财务部——业务部——技术部

4.4 人事管理

郑雯乐（负责人），女，籍贯山东省淄博市，珠宝学院首饰设计与工艺专业。在校期间一直是学生干部，积极参加各类演讲比赛均获佳绩，做过珠宝的市场调研。联系电话 17719679249

苏成猛（主要参与人），男，籍贯河北省秦皇岛市，文化与艺术学院汉语言文学专业在读学生，品性良好，勤奋好学，积极参与各种活动，对市场营销有深刻认识且具备一定经验。联系电话 18233505602

王祺（主要参与人），男，籍贯山西省大同市，珠宝学院学生。平日与学生老师关系融洽，善于思考。在校期间多次获评校级荣誉。善于天马行空的思考。对于新鲜事物有极大的热情。联系电话：15035200939

李嘉豪（主要参与人），男，籍贯陕西省西安市，商学院互联网金融专业。平日与学生老师关系融洽，善于思考。平日积极参加学校各类活动，是个完美主义者，力求每一件事做到更好。联系电话
17629083772

第五章 财务分析

5.1 投融资分析

考虑充分发挥珠宝学院宝石研究成果及现在智能健康检测技术

5.2 财务预算及财务分析

费用名称：	所需费用：	备注：
智能芯片	1000 元	商家自带 App
中端具有保健疗效宝石	1000 元	如石榴石，玛瑙
宣传费用	1000 元/年	

第六章 风险分析

6.1 财务风险

创业初期缺乏全盘成本意识及对成本的分析与控制能力，从而导致产品或服务成本过高，带来成本风险。同时，创业初期企业的财务活动主要表现为资金

金的大量付出，现金回收的流量很小。创业初期的企业从产品服务的开发、整体设计与规划、生产、市场开拓等全部生产经营过程，都需要支付大量成本付出；且企业初期产品、服务尚处于开发推广阶段，不能立即被消费者认可，市场占有率小，企业的无法迅速获得现金流的回收，如果不能及时注入补充资金，很可能面临破产倒闭的境地。一方面我们要积极开展业务，获得收入，提高资金周转率。另一方面我们会尽可能的节约成本，减少不必要消费。面临流动资金不足的困难局面，造成经营困难，引发各类危机。一方面，我们会做好财务计划，减少坏账、呆账，提高资金周转率。另一方面，我们会提升服务质量，做充分的市场推广，增加收入，争取利润最大化。

6.2 技术风险

技术风险是由于技术开发失败的可能性、生产工艺开发失败的可能性以及技术效果的不确定性而带来的风险。技术是公司创业初期的核心动力，尤其是对一家高科技型中小企业而言，技术研发是否成功并持续跟进，往往直接决定了企业能否继续发展甚至生存。加上企业前期获得的资金有限，往往只能集中力量将资金投入一个研发项目，一旦研发失败或技术停滞便可能全盘皆输。所以同于财务风险解决，做好市场推广，增加收入，保持技术研发的资金支持和人才吸引。定期吸纳贤士，稳定现有人才，保证研发的持续性。

6.3 市场风险

与传统企业相比，高科技中小型企业面临的市场风险主要体现以下几个方面：

①产品的市场接收程度的不确定性；产品销售渠道的不确定性；产品价格的不确定性。
②本项目为新概念项目，虽然目前来看产品在市场上有很好的预期，但基于产品的材质和成本，可能普通消费者会因产品价格而对消费做出考虑。
③产品的测血压、测心率等功效市面上普通的智能手表（环）也有此功能，所以对本产品有一定程度的替代性，消费者从经济的角度上考虑，不会废掉原有产品另外花钱购买新产品。
④消费者和厂家信息不对称，对新产品（技术）存在认知障碍，不足以判断新产品的所有效用。
⑤新产品的更新换代可能会短于传统智能手表（环），消费者担心更新产品推出时会使现有产品贬值，推迟产品购买时间。
⑥消费者处于对新产品的副作用和缺陷的预防心理会表现出观望态度。对此我们前期要做好宣传和调研工作，在包装说明上注明产品的所有功效，并且在宣传中注

重本产品与一般智能手表（环）的区别，如侧重宣传宝石的功效。还要向消费者说明本产品无一切副作用，保证产品顺利进入市场。在产品定价方面，要根据大众消费水平，将产品定位为中端消费产品。对于产品的更新换代，可向消费者推出一种换代保险，在更新产品时消费者可凭保险单和上一代产品对换代产品进行折扣。以此来打消消费者对产品更新换代快的顾虑。

第七章 团队介绍

郑雯乐（负责人），女，籍贯山东省淄博市，珠宝学院首饰设计与工艺专业。在校期间一直是学生干部，积极参加各类演讲比赛均获佳绩，做过珠宝的市场调研。联系电话 17719679249

苏成猛（主要参与人），男，籍贯河北省秦皇岛市，文化与艺术学院汉语言文学专业在读学生，品性良好，勤奋好学，积极参与各种活动，对市场营销有深刻认识且具备一定经验。联系电话 18233505602

王祺（主要参与人），男，籍贯山西省大同市，珠宝学院学生。平日与学生老师关系融洽，善于思考。在校期间多次获评校级荣誉。善于天马行空的思考。对于新鲜事物有极大的热情。联系电话：15035200939

李嘉豪（主要参与人），男，籍贯陕西省西安市，商学院互联网金融专业。平日与学生老师关系融洽，善于思考。平日积极参加学校各类活动，是个完美主义者，力求每一件事做到更好。联系电话 17629083772

六、附件材料

要求：

1. 各成果类型

A. 基础研究、应用基础研究：（1）主要论文、著作（限 15 篇，仅附首页）；
（2）被他人引用情况检索证明；（3）科学评价证明。

B. 技术开发、发明、推广：（1）技术评价证明；（2）应用证明；（3）相关技术资料。

C. 软科学：（1）技术评价证明；（2）应用证明；（3）相关技术资料。

注：科学评价证明包括：他人在学术刊物或公开场合发表的对本成果重要科学发现点（观点、结论）的学术性评价意见，或者验收、评审、鉴定等第三方评价结论。

技术评价证明包括：评审、检测、验收、鉴定、专利证书等。

相关技术资料包括：研究报告、技术总结报告、调查、咨询报告、查新报告、发表著作、论文等。

2. 涉及各级政府资助完成的项目，需提交计划项目下达部门同意结题、验收的证明。

3. 附件最多不得超过 60 页。